

AD-A057 420

NAVAL RESEARCH LAB WASHINGTON D C
GULF STREAM GROUND TRUTH PROJECT: RESULTS OF NRL AIRBORNE SENSO--ETC(U).
JUN 78 C R MCCLAIN, D T CHEN, D L HAMMOND

F/G 8/3

UNCLASSIFIED

NRL-MR-3779

NL

1 of 2
AD A057420



AD NU. —
DDC FILE COPY

AD A 057420

Final copy

MR 100-100

23

211P

F 02-003

WF 52 553000

DDC



18 08 09 035
254 RPD

LEVEL II

SECURITY CLASSIFICATION OF THIS PAGE (When Data Entered)

REPORT DOCUMENTATION PAGE		READ INSTRUCTIONS BEFORE COMPLETING FORM								
1. REPORT NUMBER NRL Memorandum Report 3779	2. GOVT ACCESSION NO.	3. RECIPIENT'S CATALOG NUMBER								
4. TITLE (and Subtitle) GULF STREAM GROUND TRUTH PROJECT: RESULTS OF NRL AIRBORNE SENSORS		5. TYPE OF REPORT & PERIOD COVERED Final report on one phase of task.								
7. AUTHOR(s) C. R. McClain, D. T. Chen and D. L. Hammond		6. PERFORMING ORG. REPORT NUMBER								
9. PERFORMING ORGANIZATION NAME AND ADDRESS Naval Research Laboratory Washington, D. C. 20375		10. PROGRAM ELEMENT, PROJECT, TASK AREA & WORK UNIT NUMBERS NRL Problem G01-10, 62759N Project WF 52-553-000 (Continues)								
11. CONTROLLING OFFICE NAME AND ADDRESS Naval Air Systems Command, Washington, D.C. 20361 and NASA Wallops Flight Center, Wallops Island, Virginia 22337		12. REPORT DATE June 1978								
14. MONITORING AGENCY NAME & ADDRESS (if different from Controlling Office)		13. NUMBER OF PAGES 100								
		15. SECURITY CLASS. (of this report) UNCLASSIFIED								
		15a. DECLASSIFICATION/DOWNGRADING SCHEDULE								
16. DISTRIBUTION STATEMENT (of this Report) Approved for public release; distribution unlimited.										
17. DISTRIBUTION STATEMENT (of the abstract entered in Block 20, if different from Report)										
18. SUPPLEMENTARY NOTES										
19. KEY WORDS (Continue on reverse side if necessary and identify by block number) <table> <tr> <td>Ocean wave spectra</td> <td>Gulf Stream</td> </tr> <tr> <td>Laser profilometer</td> <td>Significant wave height</td> </tr> <tr> <td>Wind-wave radar</td> <td>Spectral aliasing</td> </tr> <tr> <td>Precision radiation thermometer</td> <td>Angular spreading</td> </tr> </table>			Ocean wave spectra	Gulf Stream	Laser profilometer	Significant wave height	Wind-wave radar	Spectral aliasing	Precision radiation thermometer	Angular spreading
Ocean wave spectra	Gulf Stream									
Laser profilometer	Significant wave height									
Wind-wave radar	Spectral aliasing									
Precision radiation thermometer	Angular spreading									
20. ABSTRACT (Continue on reverse side if necessary and identify by block number) <p>Results of ocean surface measurements by NRL active and passive sensors are summarized. The data set was collected during three flights over the Gulf Stream in the spring of 1976 and coincided with <u>in situ</u> measurements taken from an oceanographic research vessel. The sensors were the NRL high flight radar, NRL wind-wave radar, a laser profilometer and a precision radiation thermometer. The quantities derived include sea state, ocean wave frequency spectra, surface wind speed and sea surface temperature. The remote determinations are found to agree very well with other data</p>										

DD FORM 1473 EDITION OF 1 NOV 65 IS OBSOLETE
1 JAN 73 S/N 0102-014-6601

SECURITY CLASSIFICATION OF THIS PAGE (When Data Entered)

10. Program Element, Project, Task Area & Work Unit Numbers (Continued)

NRL Problem G01-05C
 NASA P-62257(G)

20. Abstract (Continued)

sources. In addition, experimental and theoretical results regarding the effects of ocean wave angular spreading on airborne profilometer determinations of wave frequency spectra are included as well as a detailed description of the data analysis algorithm. The spectral distortion is not severe for track angles within 15 degrees of the wind vector. These indicate that airborne profilometer data is still useful for wind-wave generation studies as long as close attention is given to the track angle relative to the dominate surface wave direction. Also, the proposition of using spectra from various track angles to infer the angular spreading function does not appear promising because the spectra do not show a substantial enough variation with the angular spreading function.

ACCESSION NO.	
RTD	White Button <input checked="" type="checkbox"/>
DSG	Soft Button <input type="checkbox"/>
DEPARTMENT	
NOTIFICATION	
BY.....	
DISTRIBUTION/AVAILABILITY CODES	
QTY.	AVAIL AND/OR SPECIAL
A	

CONTENTS

I. INTRODUCTION	1
II. EXPERIMENT PLAN	2
III. INSTRUMENTATION	4
IV. ENVIRONMENTAL DATA	10
V. DATA PROCESSING	21
VI. PRESENTATION AND DISCUSSION OF RESULTS	29
VII. SUMMARY	49
ACKNOWLEDGMENTS	51
REFERENCES	52
APPENDIX A	A-1
APPENDIX B	B-1
APPENDIX C	C-1
APPENDIX D	D-1
APPENDIX E	E-1
APPENDIX F	F-1

D D C
REF ID: A
AUG 15 1978
D
RECORDED
D

GULF STREAM GROUND TRUTH PROJECT: RESULTS OF THE NRL AIRBORNE SENSORS

I. INTRODUCTION

During late May and early June of 1976, NASA Wallops Flight Center (WFC) conducted a concerted study of the Gulf Stream. The experiment combined in situ measurement of hydrographic and atmospheric parameters with those made by a large variety of airborne remote sensors. The sea truth was furnished by the R.V. Advance II (North Carolina State University). NASA Wallop's C-54 aircraft was instrumented with its AAFe SEASAT-A altimeter, NASA Langley Research Center's AAFe scatterometer (RADSCAT), Naval Research Laboratory's (NRL's) high flight radar, wind-wave radar, a laser profilometer, and a precision radiation thermometer (PRT-5).

The project area was situated due east of WFC in the vicinity of the Gulf Stream. This location was selected for the expressed purposes of (1) testing the satellite altimeter's ability to detect geostrophic current systems, (2) comparing the surface temperature signature to the actual current location, and (3) checking the airborne altimeter's sensitivity to rapid changes in sea state, such spatial inhomogeneities in sea state should exist there because of strong wave-current interactions (Chen and Bey, 1977). Results relevant to (1) have indicated a positive capability which have been reported by Leitao, et al. (1977). In addition to these goals, the experiment afforded an excellent opportunity to resolve some fundamental questions about a profilometer's ability to obtain correct

Note: Manuscript submitted April 26, 1978.

wave-frequency spectra as well as information on the wave field's directional properties. NRL was also responsible for the analysis of the precision radiation temperature data. The results presented herein are only those derived by the NRL-sponsored sensors and appropriate comparisons are made with those of other devices.

II. EXPERIMENT PLAN

Because the aircraft housed several instruments, each with its own particular requirements, a rather complicated flight plan was devised by the participants. Figure II-1 is a depiction of the general scheme and the sensors to be operated at each altitude. A 3048 m altitude was selected because it is the ceiling for flights without supplemental oxygen and it is necessary to fly as high as possible for the operation of altimeters using waveform analysis as is shown by Walsh (1977). Star patterns of different geometries were incorporated at the 1524 m and 305 m levels. At 1524 m, the RADSCAT was flown upwind, downwind and at 45° to the wind. Figure II-2 shows the proposed pattern at 305 m where the NRL wind-wave radar and the laser profilometer were operated. Two sets of such patterns were included, one on each side of the Gulf Stream front with continuous data to be collected by all designated sensors during the 3048 m transit.

Three missions (5/27, 6/2, 6/4) were completed during a two week period. The position of the frontal system was supplied prior to each flight by the Advance II, which continuously maintained stations along the track between the coordinates (36°28'N, 72°30"W) and (37°28.5'N, 72°30'W) during this time interval. Earlier flights included an initial systems check-out and later another (5/26) that was scrubbed due to a malfunction in the Inertial Navigation System (INS).

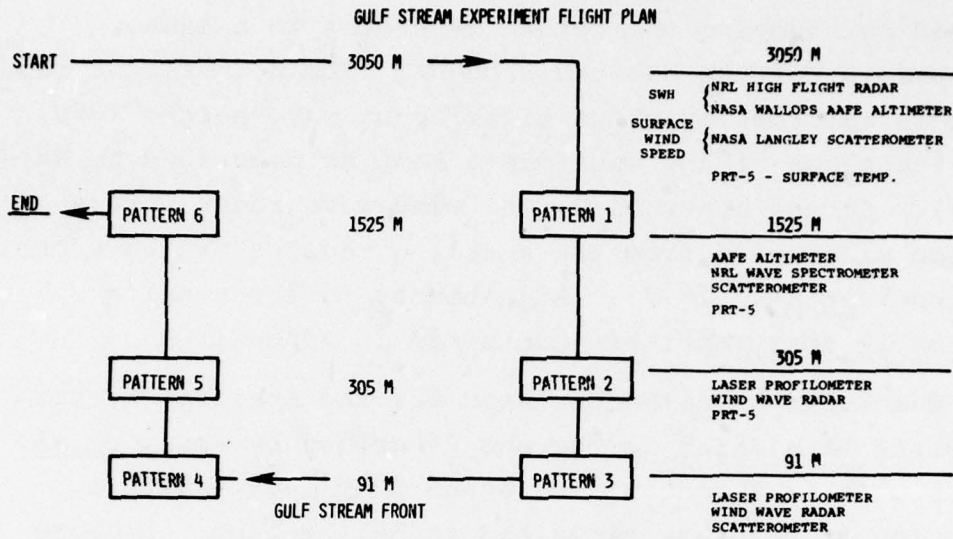


Fig. II-1 — General flight scheme

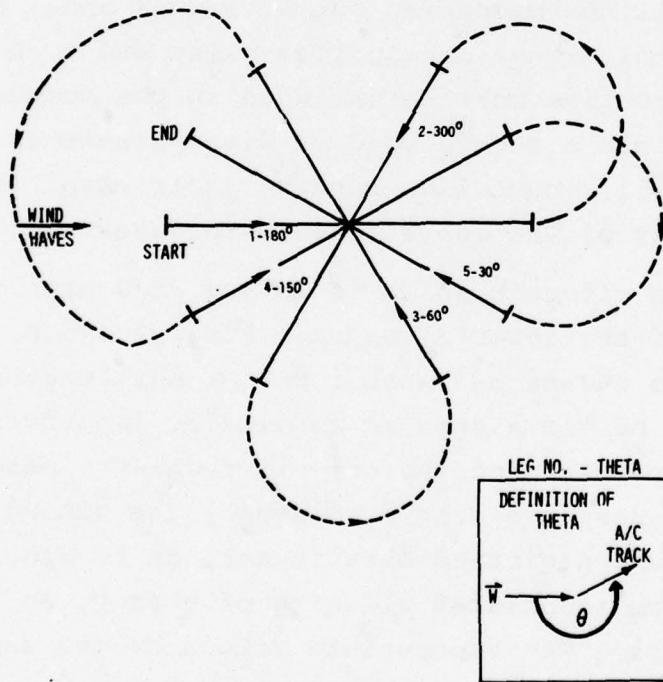


Fig. II-2 — Star pattern at 305 meters

III. INSTRUMENTATION

NRL's microwave devices mentioned above are nadir-looking short pulse radars, the results from which are derived by studying the return waveforms in a manner appropriate for the desired product. The high-flight radar provides information about significant wave height (SWH) from the slope of the waveform's ramp as described by Walsh (1974). On the other hand, the wind-wave radar infers surface wind speed from the trailing edge of the waveform (Hammond, et al., 1977). Adjustments to the results printed in that paper are contained in Appendix A.

The laser profilometer used was the Spectra-Physics Geodolite 3A similar to the one described by Ross, et al. (1970). It is a continuous output (CW) device with a selection of response times and range settings. Because range is measured by comparing the phase shift between the returning amplitude-modulated output signal and a similar reference signal, range ambiguities exist and a phase shift detection subroutine must be included in the computer software to yield a record void of discontinuities. These are rather easily identified because their magnitude is similar to that of the range scale being used.

Since the aircraft (A/C) is moving at a high velocity, the effects of the laser's response time should be investigated so as to understand what apparent wavelengths being profiled will be diminished in amplitude. Appendix B includes a derivation of the cut-off frequency based on the definition of response time provided by the operation manual. Because digitized data is subject to Nyquist folding and the associated aliasing of energy, an additional calculation using the appropriate values of the sampling frequency (f_s) and cut-off frequency (f_c) is included. Additionally, the folding frequency (45 Hz) is high enough

in this instance to ensure that little energy would be found in the corresponding portion of the wave spectra.

The laser was calibrated prior to the experiment and was found to be working properly on all range settings (10 ft., 20 ft., 40 ft., and 100 ft.). Table 1 gives the conversion coefficients for these ranges subject to the output voltage options (± 1.4 V, 0-10V). It should be noted that the analog-to-digital converter used on board the aircraft had a ± 1.0 V maximum input and voltage dividers were inserted wherever necessary to accommodate this restriction and these modify the laser calibration constants. Figure III-2 shows the entire recording system.

Figure III-1 indicates that pitch, roll, and vertical acceleration were monitored. These quantities were supplied by the Inertia Navigation System (INS), but only vertical acceleration was utilized in the data analysis. Our flights occurred during periods of relatively quiescent atmospheric conditions, therefore we did not feel that pitch or roll would significantly affect the profilometer ranging. A simple calculation provides an estimate of the ranging error (Δz) induced by these two motions.

$$\Delta z = z(\sec \phi - 1), \quad (1)$$

where z is the A/C altitude and ϕ is the value of the pitch or roll angle. Equation (1) refers to a plane surface. Closer examination reveals that any attempt to correct these errors based on (1) may not improve the result. The beam's horizontal excursion (Δx) from nadir is given by

$$(2), \quad (2)$$

$$\Delta x = z \tan \phi .$$

For example, if $\phi = 3^\circ$ and $z = 305$ m, Δx would equal 16 m, a distance sufficiently far away from nadir to make a range correction for a random ocean surface rather questionable.

Table 1 - Laser Conversion Factors

RANGE (FT)	LASER PEAK-TO-PEAK OUTPUT (V)	CONVERSION FACTOR (FT/mv) - (m/mv)	MODIFIED FACTOR (FT/mv) - (m/mv)
10	+1.4 0-10	0.00357 - 0.00109 0.001 - 0.000305	0.005 - 0.00152
20	+1.4 0-10	0.00714 - 0.00218 0.002 - 0.000610	0.010 - 0.00305
40	+1.4 0-10	0.0143 - 0.00436 0.004 - 0.00122	0.020 - 0.00610
100	+1.4 0-10	0.0357 - 0.0109 0.010 - 0.00305	0.050 - 0.0152

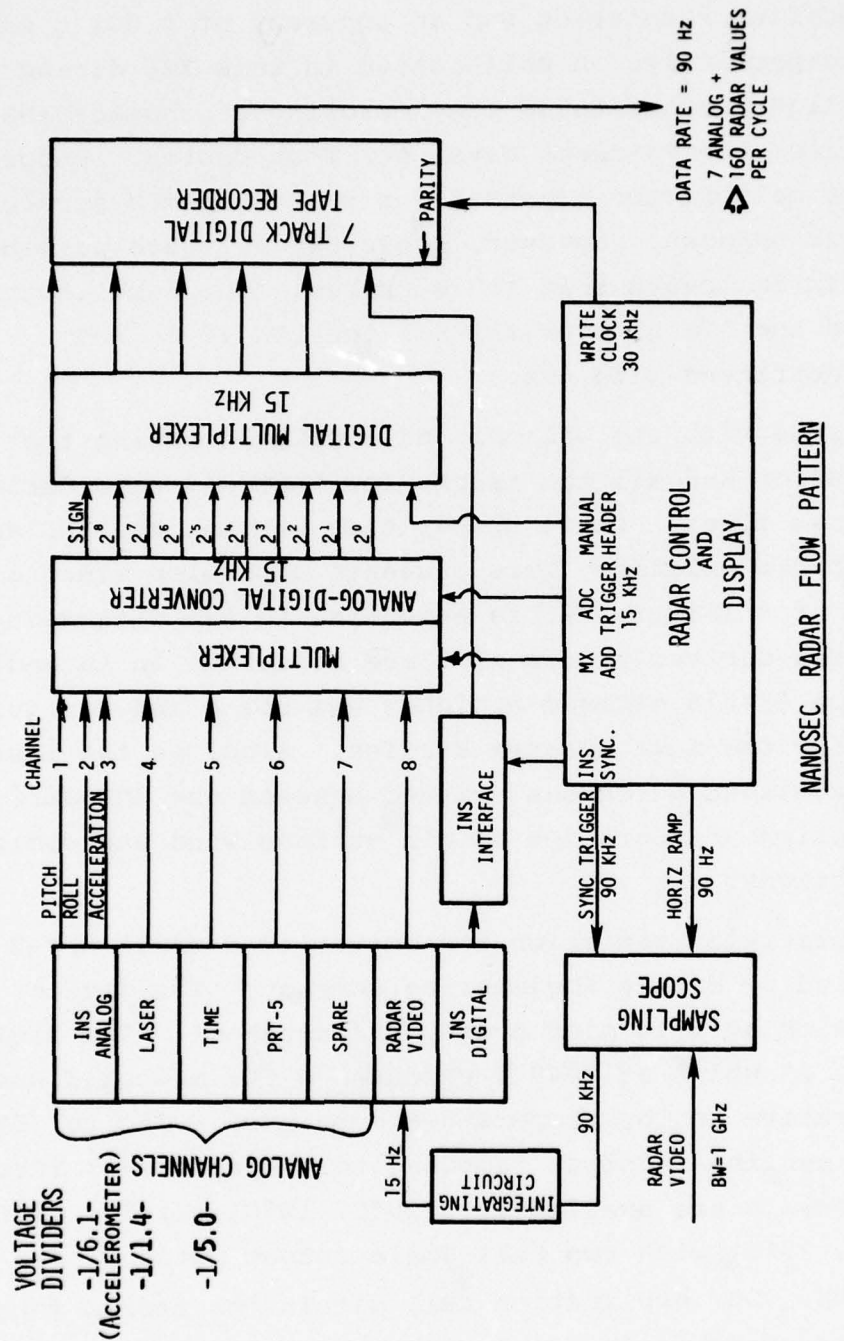


Fig. III-1 — Data recording system

Thus, one has little recourse but to accept this limitation on the profilometer's accuracy.

The accelerometer in the Wallops INS (a Bendix LTN 51) has a specified resolution and an accuracy of 0.001 g and 0.01 g, respectively. A malfunction in this INS during the 5/26/76 flight necessitated the borrowing of another INS (LTN 72) from the Patuxent Naval Air Test Center. Unfortunately the calibration constant for that system's accelerometer was unknown. However, conversations with personnel from Bendix indicated that it is probably the same instrument as in the LTN 51 even though the LTN 72 is not normally outfitted with one.

Problems with the Wallops INS continued during the 6/2/76 mission and all the tracks for that day were derived from LORAN-A fixes. Large disparities between the INS and LORAN-A tracks existed. This presents a problem since a knowledge of θ (Figure II-2) is essential to the data reduction. Loran-derived values of θ are contained in Appendix C. Data on 6/4/76 offered a higher sea state and was quite adequate for the wave spectra studies. Also, on the last flight, excellent agreement existed between the INS-derived wind direction and both the ship's surface wind and dominant wave directions.

The precision radiation thermometer is a model PRT-5 manufactured by Barnes Engineering Company. The device operates with an 8-14 micron window (infrared). The field of view is 2° which at 3048 m produces a 106 m spot diameter. It is operative in the temperature domain of -20°C to 75°C , but has a nonlinear output response to temperature. Three range intervals are available, (-20°C , 15°C), (10°C , 45°C) and (40°C , 75°C) with two full scale output options, 0-1 V and 0-50 MV. Our application fell within the medium range. Examination of Table 2 indicates that the output is

Table 2 — PRT—5 Calibration

TEMPERATURE ($^{\circ}$ C)	% FULL SCALE OUTPUT
10	0.000
11	2.430
12	4.886
13	7.366
14	9.871
15	12.401
16	14.956
17	17.535
18	20.140
19	22.770
20	25.425
21	28.105
22	30.810
23	33.540
24	36.295
25	39.075
26	41.881
27	44.712
28	47.568
29	50.449
30	53.356
31	56.288
32	59.245
33	62.228
34	65.236
35	68.269
36	71.328
37	74.412
38	77.522
39	80.656
40	83.817
41	87.003
42	90.214
43	93.450
44	96.712
45	100.000

INTERVAL
USED IN
EQUATION 3

particularly nonlinear near the high temperature end of that range. The data in Table 2 was taken from the operation manual. For this reason a temperature subrange (15°C , 27°C), was selected based on Figures IV-1 and IV-2 and a calibration constant was calculated to be $0.371^{\circ}\text{C}/\%$ full scale over that interval. The 0-1 V output was used during the Gulf Stream flights and since the recording system registers MV values, the equation for temperature ($^{\circ}\text{C}$) becomes

$$T = 15^{\circ} + (X - 124.0) (0.0371), \quad (3)$$

where X is the value recorded.

Operation in cold environments (below -20°C) may cause the apparatus to provide false values. A precision thermistor Bolometer mounted in a tightly controlled reference temperature cavity is used in stabilizing the system. If the cavity temperature is allowed to drop below the design value, incorrect readings will result. Also the wind chill factor can elevate the minimum ambient operating temperature.

IV. ENVIRONMENTAL DATA

When attempting to draw conclusions pertaining to ocean wave development, environmental history is of primary importance. A large number of factors are involved in the physics of this phenomenon and the technique used here requires additional information. Consequently, we have placed much emphasis on the collection of these physical parameters and were assisted in doing so by several different agencies. The data gathered included surface weather charts from the National Weather Service (NWS), Gulf Stream frontal analysis from the Naval Oceanographic Office (NOO), SWH analysis from Fleet Numerical Weather Central (FNWC) and additional supporting data taken on the Advance II. Of fundamental importance are the surface wind speed, direction, duration

and fetch, air-sea temperature difference, estimated SWH and the direction of the dominant wave component. Other factors such as the curvature of the wind field also enter into SWH analyses. Since we did have at least two sources of SWH, the ship and FNWC, no attempt to implement a wave height analyses scheme based on the above mentioned data was made for the area concerned. Nonetheless, that additional data is included in the figures discussed below.

The frontal analysis charts indicate that the flight patterns were flown directly over the Gulf Stream and that the location of the current was stationary in the test area during the project period. The experiment area is indicated by the two ship survey lines, the first of which was completed prior to the flights. The in situ measurements plotted along the ship's track are in excellent agreement with the NOO data derived from satellite IR determinations (see Figures IV-1 and IV-2).

May 27: (Figures IV-3a to 3d)

The general weather situation at the beginning of the day (0000 GMT) was as follows: the experiment area was under the influence of a weak high pressure cell (1022 mb) which was the eastern portion of a high pressure ridge extending from the Great Lakes region southeastward through the mid-Atlantic states. The resulting isobaric pattern was in a NE-SW orientation over the area of interest. An atmospheric surface wave formed at that time approximately 1055 km due east of the area along a stationary front which extended southwestward through central Florida. During the next 24 hours, this wave developed into a weak low pressure system, intensified, and moved rapidly towards the northeast away from the test area. As this low migrated into the North Atlantic, the high pressure ridge extended further seaward from the Virginia and Carolina coasts causing the geostrophic

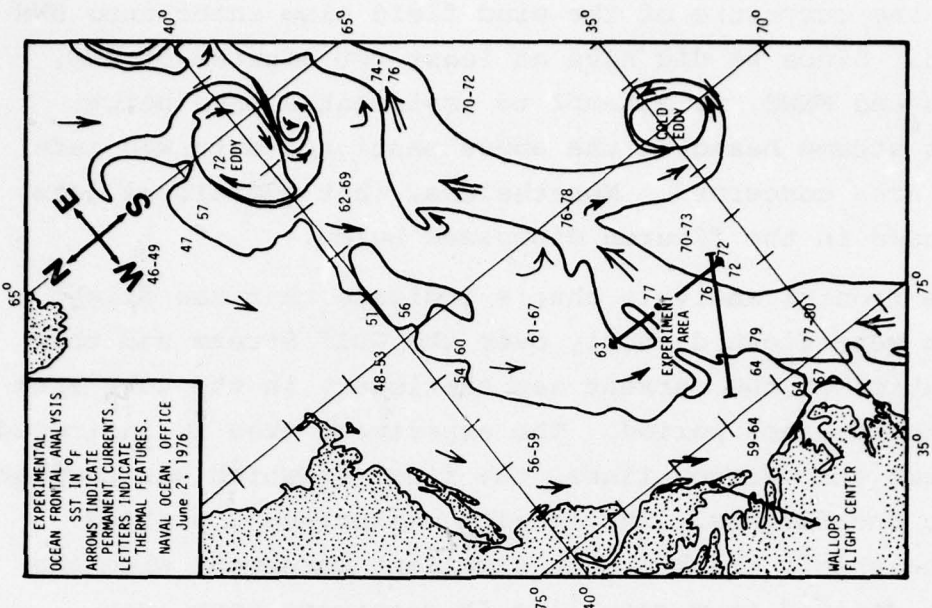


Fig. IV-2 – NOO Gulf Stream frontal analysis,
6/2/76

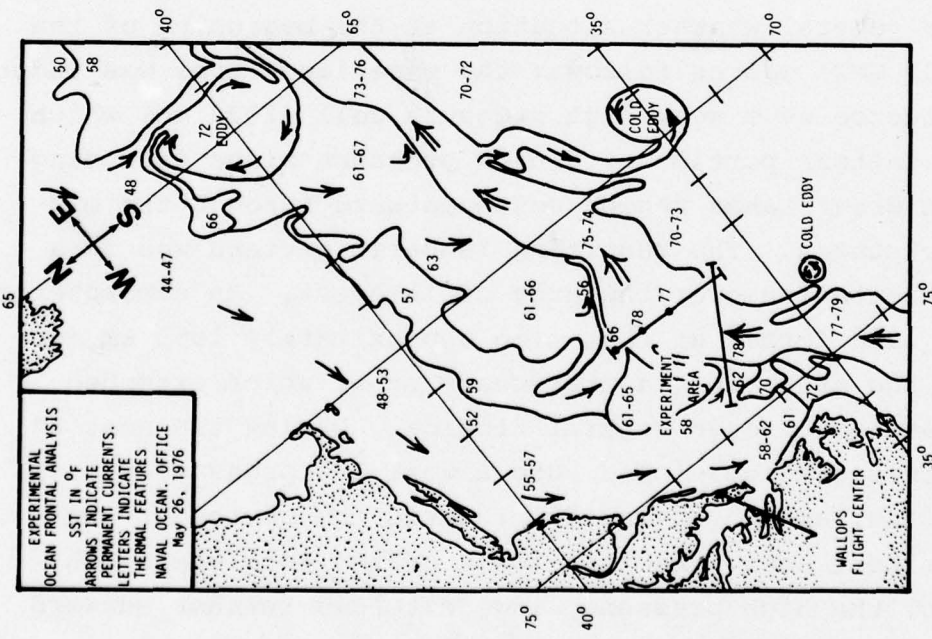
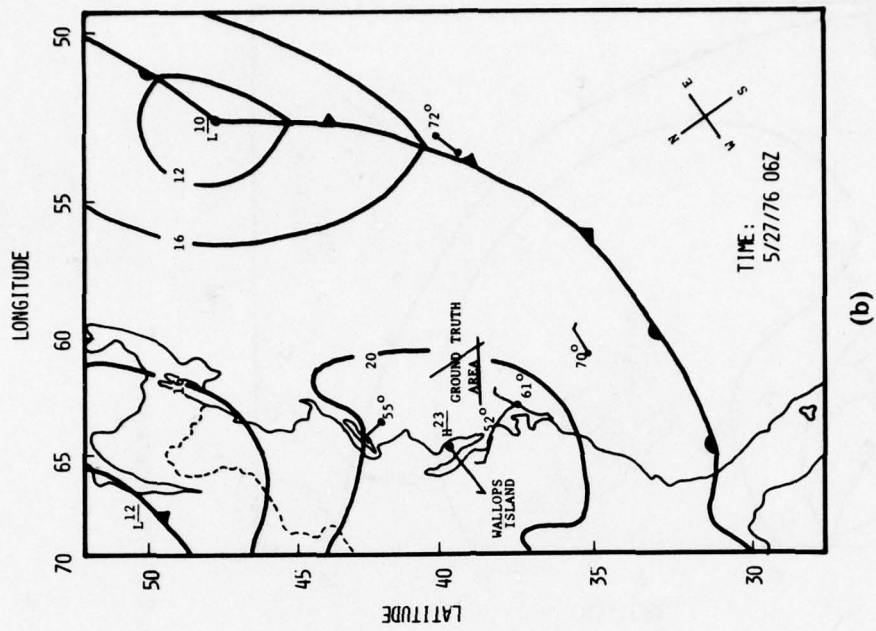


Fig. IV-1 – NOO Gulf Stream frontal analysis,
5/27/76



(b)

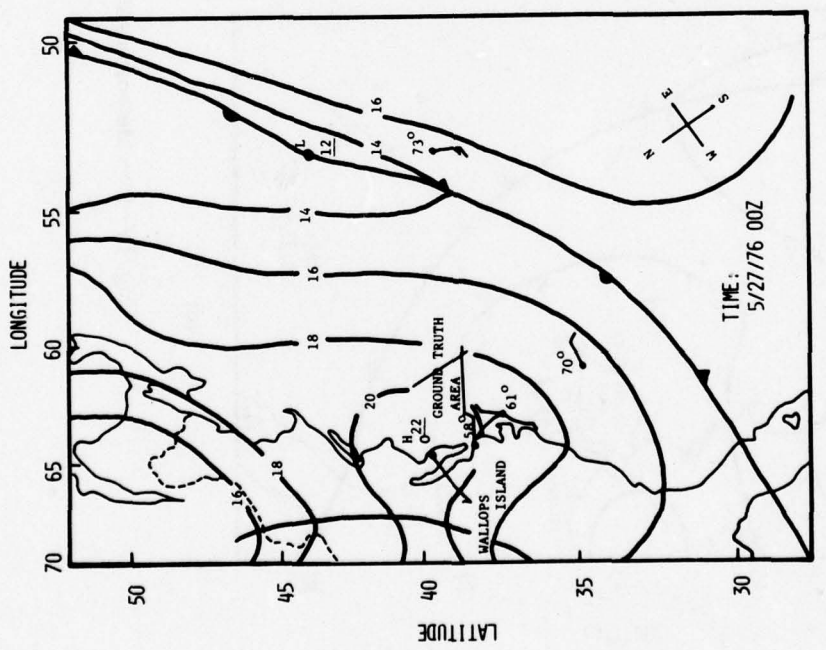


Fig. IV-3 — Meteorological data on 5/27/76 (Continues)

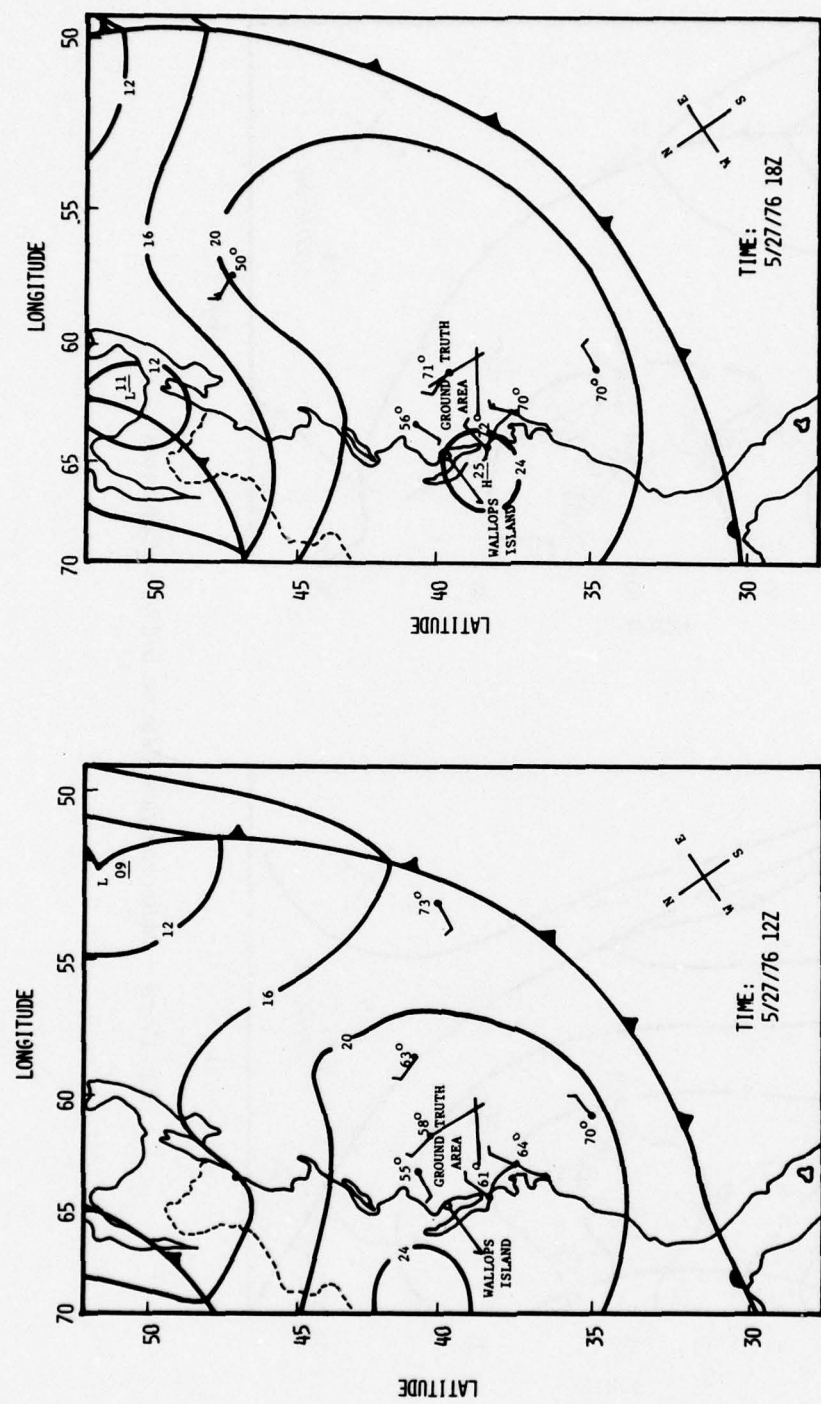


Fig. IV-3 — Meteorological data on 5/27/76 (Continued)

flow over the test area to rotate to a more N to NNE direction by 2400 GMT. With the weather following such a pattern, fetch and duration estimation is rather subjective. Indeed, swell propagating at a large angle to the wind direction (ship report) that afternoon definitely confused the issue of spectral development and therefore spectral analysis was not routinely made.

June 2: (Figures IV-4a to 4d)

Initially, a southbound cold front extended in an east-west direction just north of the 40° parallel. Also, a surface wave which had formed 30 hours earlier and had been located along a stationary front (over central Missouri) was now centered over western Virginia. It resided along the northern extension of the stationary front approximately 110 km south of the advancing cold front. At this time, the test area was experiencing a southwesterly flow and was situated beneath the western portion of a high pressure system centered over the north Atlantic (31.5° N, 47° W). About 1200 GMT the cold front overtook the stationary front to the south and became stationary itself. It now extended southwestward through central Maryland and Virginia approximately 280 km north of the experiment area. Thus, a southwestward flow continued over the project regions until the cold front shifted southward past the region of interest sometime between 0000 GMT and 0600 GMT the next day. The result of these atmospheric motions lead to generally steady winds with a long fetch oriented towards the NE. Therefore, by the afternoon of June 2, the seas were undoubtedly full-developed as defined by Pierson and Moskowitz (1964). Ship reports gave the dominant wave heading to be consistently 40 degrees.

June 4: (Figures IV-5a to 5d)

After the above-mentioned front had passed, the area remained under the influence of a high pressure ridge

(b)

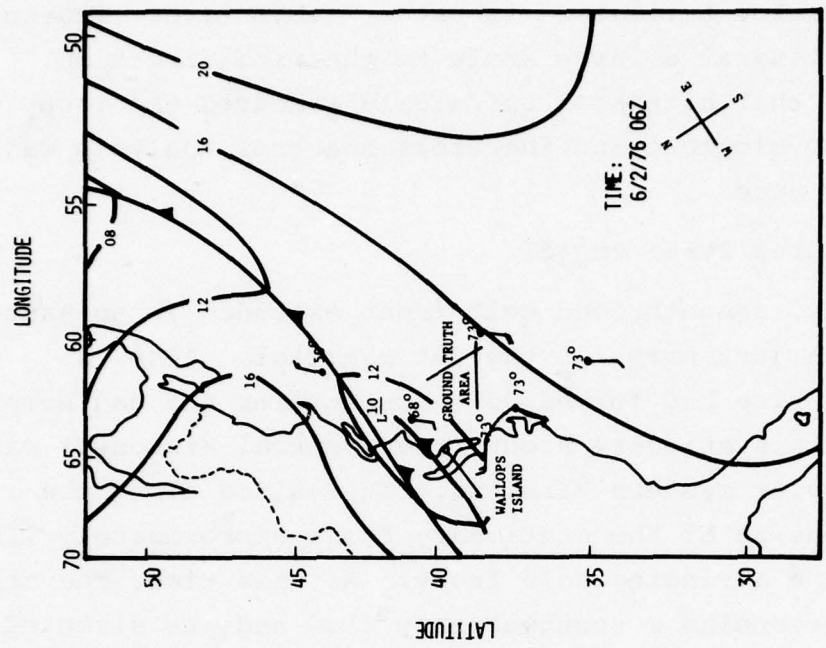
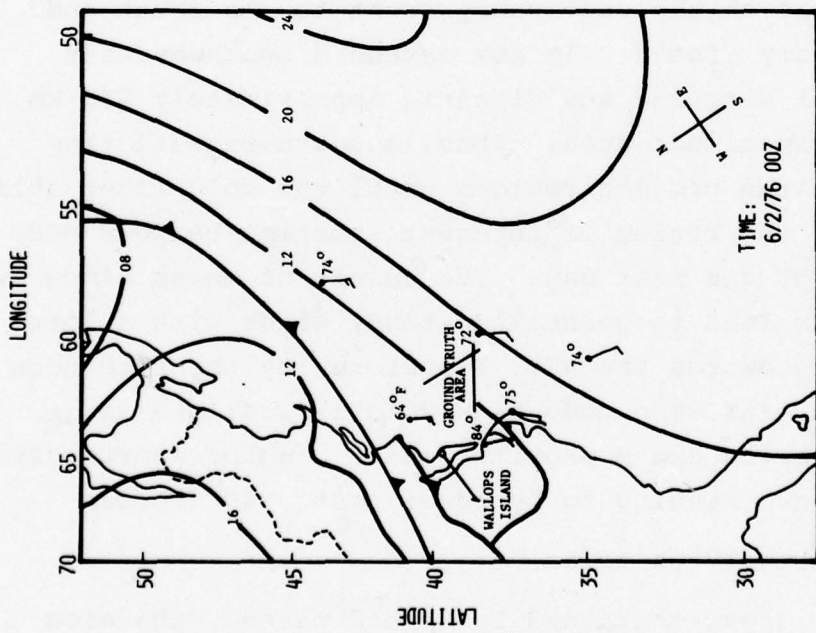


Fig. IV-4 — Meteorological data on 6/2/76 (Continues)
(a) 6/2/76 00Z

(a)



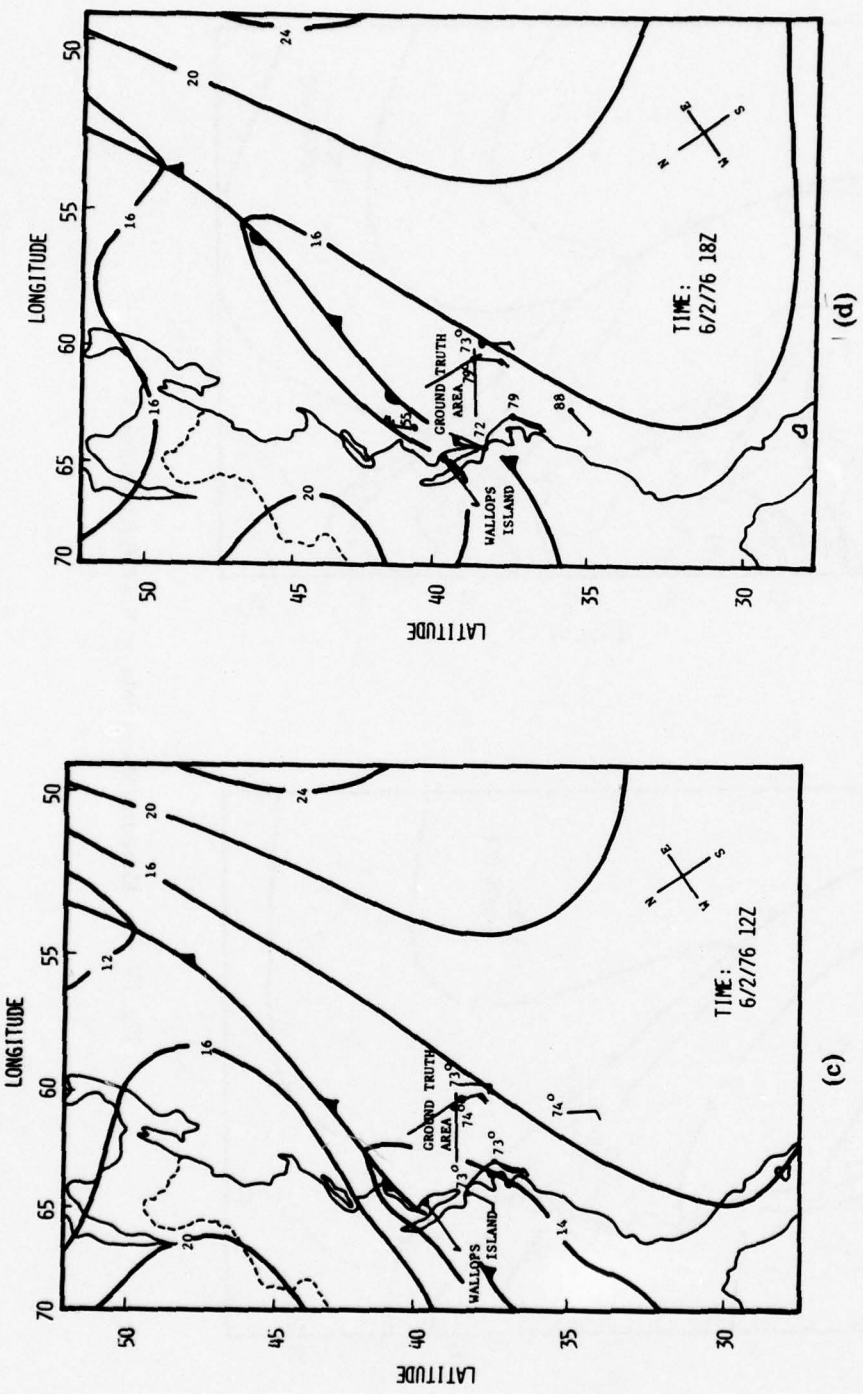
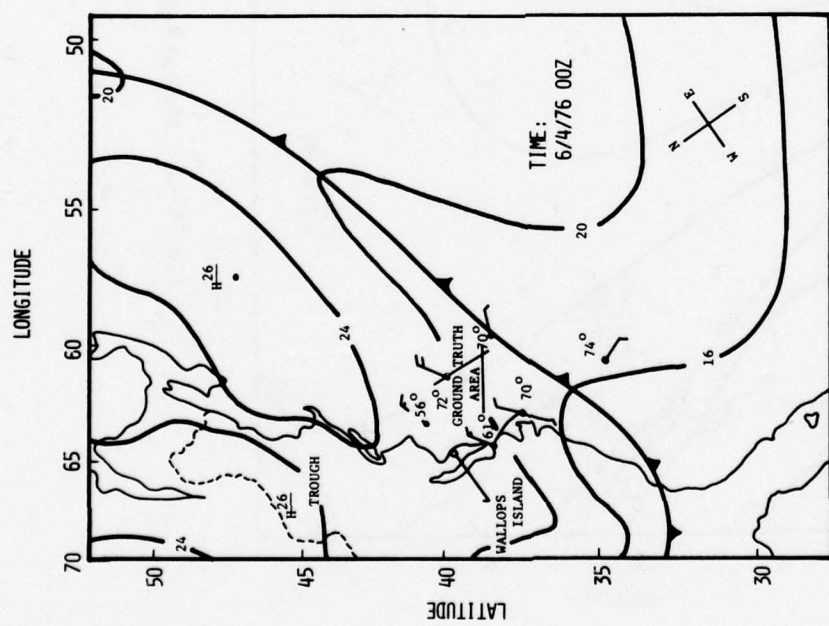
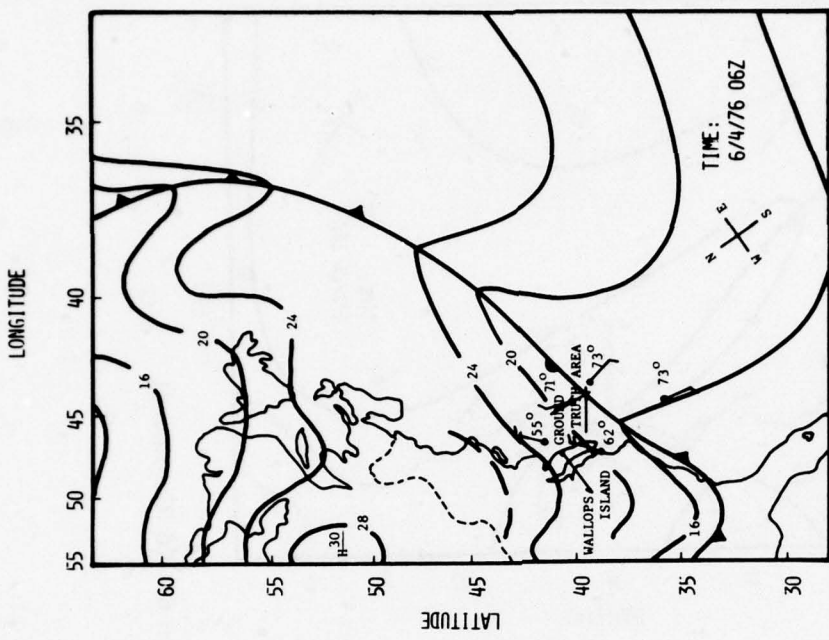


Fig. IV-4 — Meteorological data on 6/2/76 (Continued)

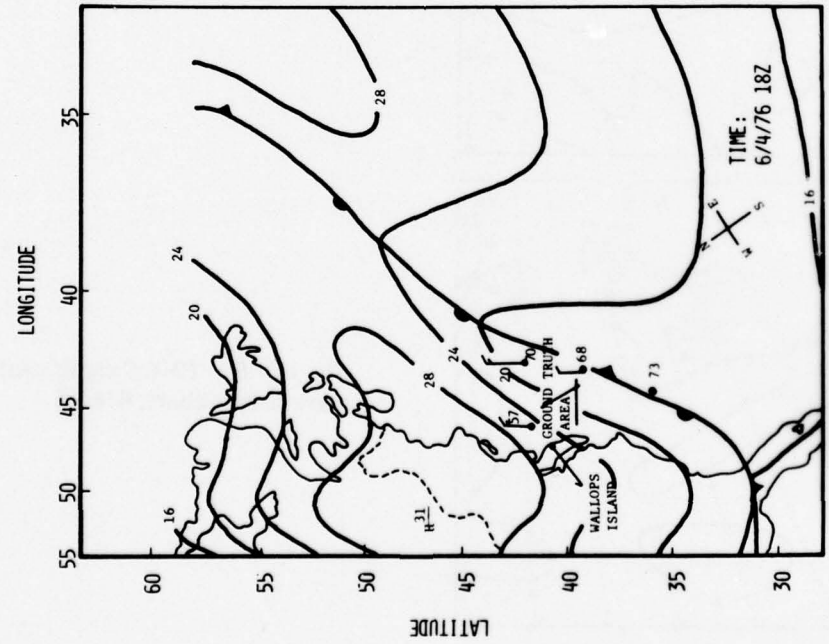


(a)

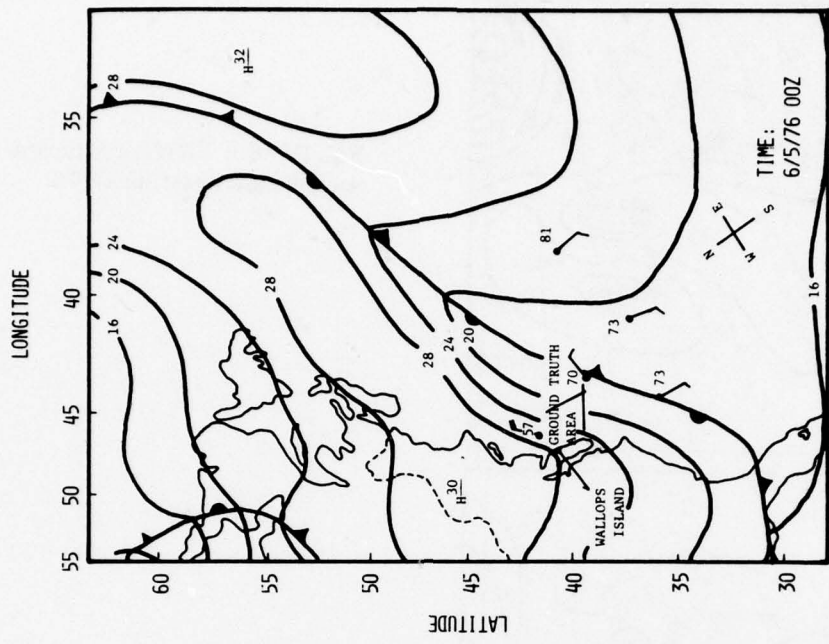


(b)

Fig. IV-5 — Meteorological data on 6/4/76 (Continues)



(c)



(d)

Fig. IV-5 — Meteorological data on 6/4/76 (Continued)

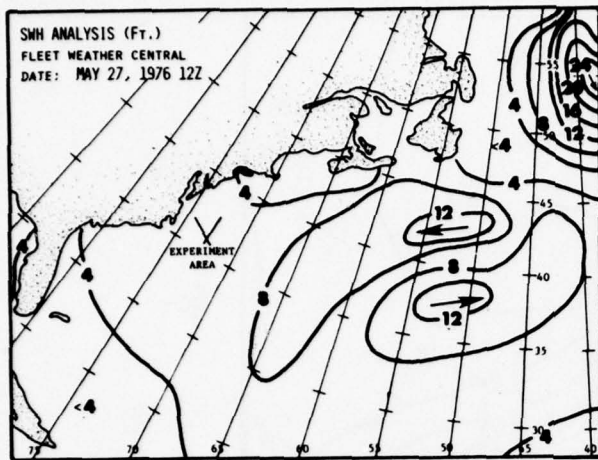


Fig. IV-6 — FNWC significant wave height chart, 5/27/76

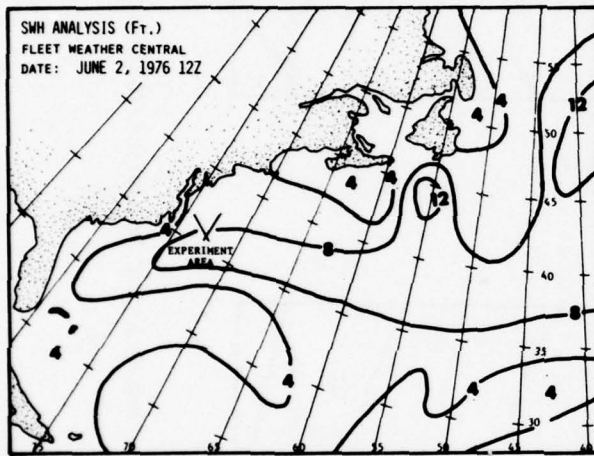


Fig. IV-7 — FNWC significant wave height chart, 6/2/76

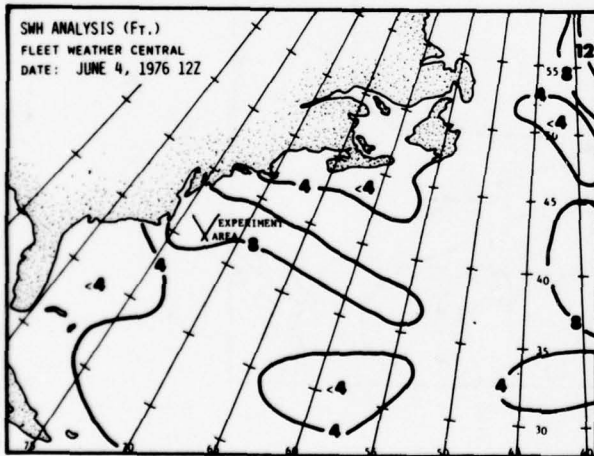


Fig. IV-8 — FNWC significant wave height chart, 6/4/76

extending in a E-W direction over the Great Lakes. The associated southwesterly flow continued through June 4. The highest SWH during the project occurred on this day, however, the low wind speeds indicate that this sea state is due mostly to swell generated earlier that morning. Rain and clouds did hamper the laser's operation but not seriously and the wind-wave radar's waveguide was flooded prohibiting its operation. The ship reported the dominant wave direction to be constant at all stations with a heading of 225°. No weather chart for 1200 GMT was available.

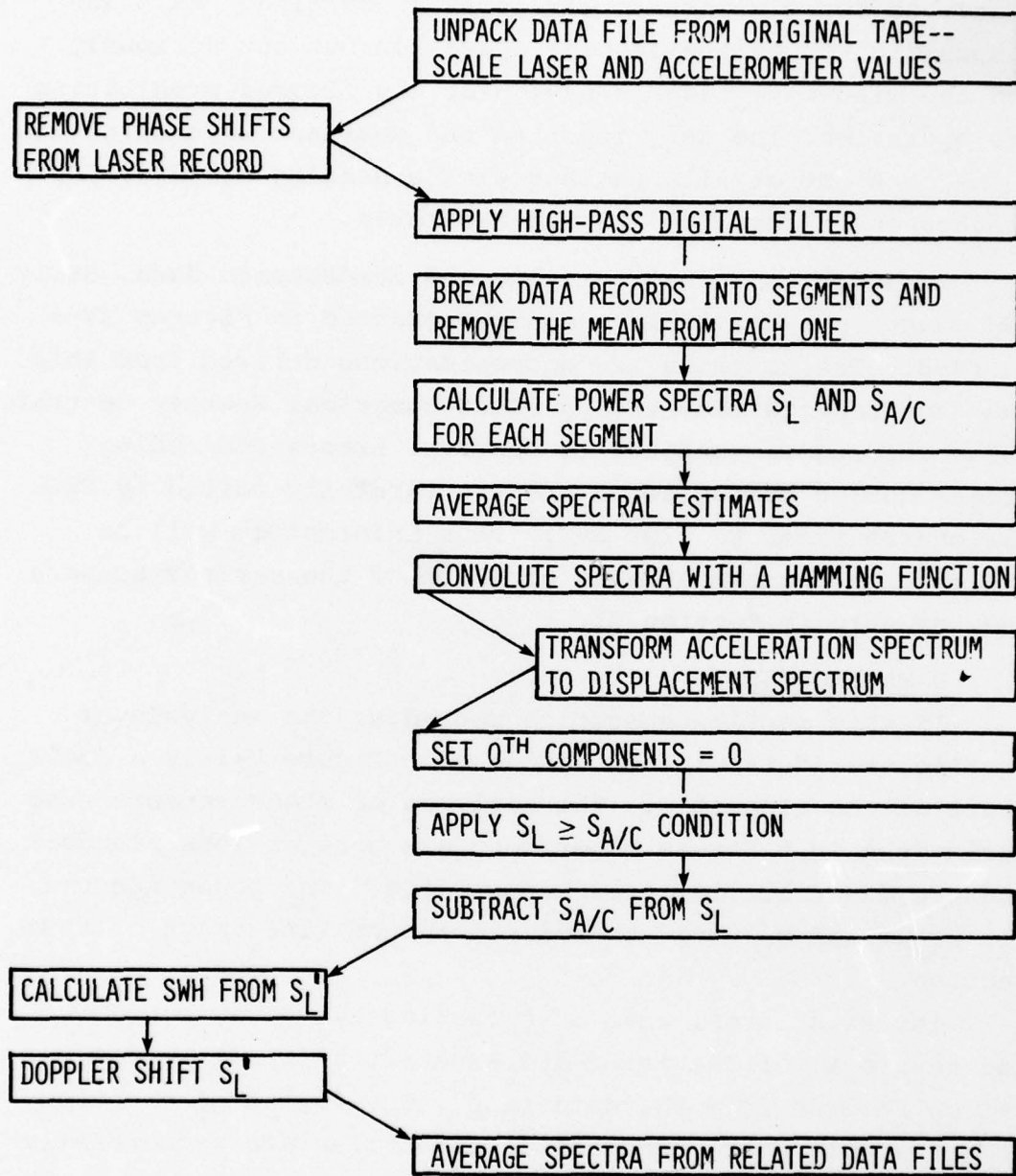
In addition to hydrographic and atmospheric data, daily SWH charts are available and are presented in Figures IV-6 to IV-8. The contours are approximations derived from ship and buoy reports received by Fleet Numerical Weather Central. These reports are subject to observer errors and coding errors during transmission and are carefully edited by FWC. All charts refer to 1200 GMT. This information will be included in the comparisons of SWH from the various sensors and the ship in Section VI.

V. DATA PROCESSING

In this section specifics regarding the analysis of profilometer data will be discussed. Figure V-1 is a flow chart of the algorithm. The analyses of other sensors used during the Gulf Stream Experiment are more or less standard and are described in other manuscripts. The power spectra S_L' , $S_{A/C}'$, and S_L'' will be defined in the later part of this section.

The first step, that of unpacking the data, concerns the retrieval of the laser and aircraft vertical acceleration records from the data tape. The format of the tape is not simple since a number of quantities are sequentially recorded and a masking technique is necessary for picking out particular data sets. The manner in which the data was recorded is as follows. The basic data block is called a file. At the beginning of each file is a header which

DATA ANALYSIS FLOW CHART - AIRSPEC 5*



(* SEE APPENDIX F)

Fig. V-1

contains the file number, date, time, altitude, and radar sampling scope settings. Each file contains 32 records which in turn contains one INS latitude and longitude fix. A record also contains 256 sweeps. A sweep is composed of one sample from each of seven analog input channels and 160 samples from the radar sampling scope which define the recorded radar return waveform. The sweep rate is approximately 90 Hz which implies a sample interval of 1/90 seconds. The analog channels (see Figure III-1) are INS aircraft pitch, INS aircraft roll, INS aircraft vertical acceleration, laser profilometer, time of day, PRT-5 and a spare. The eighth input is the radar. The pulse rate of the radar is 90 KHz, but the system is designed with an integrating circuit which averages about 6 return pulses before the signal is feed into the analog-to-digital converter which is triggered at 15 KHz. The magic number of 167 samples per sweep is derived by the division, 15 KHz/90Hz. Therefore, the recorded radar pulse is comprised of a sample from each of 160 consecutive waveforms from the A/D converter. Each file contains $8192 = 2^{13}$ sweeps and an seven-track tape can hold seven files. After unpacking, the values of each quantity are transformed from millivolts to physical units using the appropriate calibration constants.

After the laser phase shifts have been removed, both the accelerometer and the laser records are high-pass filtered. The purpose is two fold. First, any spectral analysis should include a "prewhitening" of the data to remove segments of components whose periods are longer than the data segment and also to decrease the sidelobes of the transform that are introduced by analyzing data intervals of finite length. The second reason is to remove aircraft motion contamination which will be discussed later.

The numerical filter applied was the so-called "Martin Filter" (Martin, 1957). It is a symmetric, non-recursive

filter which features a sine termination to the gain function and a correction which insures unity gain at $\tau = f_c/f_s = 0$ (f_c = cut-off frequency, f_s = sample frequency). The sine termination is introduced to avoid large oscillations in the gain function due to a sharp cut-off (Gibbs phenomenon). Since the filter is a low-pass filter, the high-pass filter weights, w_H , are derived from the low-pass weights, w_L .

$$w_H(n) = \begin{cases} 1 - w_L(0) \\ w_H(-n) = -w_L(n) \end{cases} \quad n = (1, N) \quad (4)$$

There are $2N+1$ weights in the filter. As with any filter, once N exceeds some value, it becomes more efficient to apply the filter in the frequency domain rather than the time domain. The other two parameters required to generate the weights are f_c and the "slope of weights", h , which originates in the sine termination scheme.

The domain of τ is $(0, 0.5)$. With the value of f_s and the size of the data block used, the value of τ is very small and this can cause problems with the filter gain function. Several factors determine how the filter is to be designed. To begin, the flight patterns for the laser included five legs and during each leg three files of data were taken. In order to have an acceptable confidence interval, a compromise had to be reached between the length and the number of data segments to be analyzed and averaged. Since the filter removes $2N$ points from each file and because the FFT requires 2^P points, the selection was 22.8 second data blocks = 1/4 file or 2^{11} points per analysis. Therefore, three analyses per file could be made, and nine spectral estimates per leg could be averaged. The 22.8 second interval was chosen because it was felt that a

representative sample of the surface would be obtained over a distance equal to $22.8 \text{ S} \times 55 \text{ m/s} \approx 1250 \text{ m}$. The 55 m/s figure is the lowest ground speed of the aircraft. Thus, a prewhitening filter would require $f_c \approx 1/20 \text{ s}^{-1}$, (Davis, 1974). Since $f_s = 90 \text{ Hz}$, $\tau = 5.6 \times 10^{-4}$. No filter with $N \leq 1024$ points could be obtained for such a τ that had an actual cut-off anywhere near 20 seconds. The alternatives are to increase f_c , decrease f_s , or both.

At this point, aircraft motion plays a part in filter design. Originally, the accelerometer was to be used as the primary method for aircraft motion removal. However, most aircraft energy has periodicities above 10 seconds and would be concentrated in the lower harmonics of our transform. These are the least accurately estimated. The error in these harmonics is increased when the power spectrum of the acceleration record is transformed to one of aircraft displacement. This transformation is accomplished by dividing each component by ω^4 , ω is the circular frequency. Therefore, a higher cut-off frequency than 0.05 s^{-1} was advisable. It should also be remembered that the accelerometer was not of the highest quality in the first place.

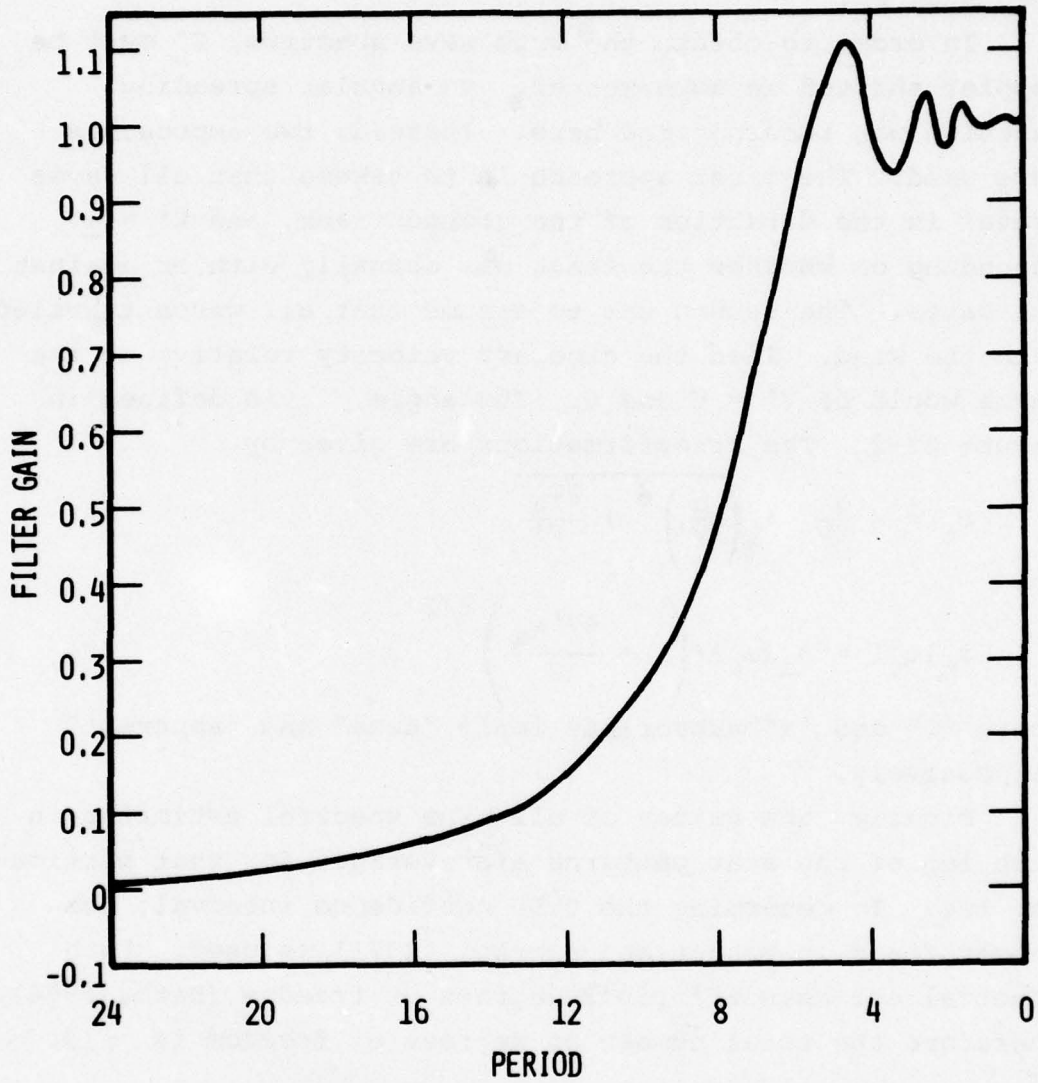
Why not reduce f_s by digitizing at a lower rate? Many laser-profilometer derived ocean wave spectra available in the literature curiously deviate from what is expected theoretically and from other empirical methods (Parsons and Goodman, 1975). Therefore, we opted for the highest sampling resolution available which was $f_s = 90 \text{ Hz}$ rather than going to a larger spacing. At 100 m/s aircraft speed, a sample every meter would be obtained.

With these considerations, a trial and error approach was made to find the best filter. The compromise was between the 10% attenuation point, the shape of the filter ramp, and the size of the sidelobes. Figure V-2 shows the

filter gain function. The 10% attenuation point is at approximately 6 s. The filter parameters are $\tau = 0.0012346$, $h = 0.0001$, and $N = 512$. This filter requires a great deal of time to convolute with a data file. Actually, the reduction of f_s by a third or a fourth would sharpen up the filter response greatly, and would make the filter more sensitive to the value of f_c selected.

After the Fast Fourier Transform (FFT) and application of the Hamming convolution to each spectrum, the above mentioned transformation is carried out on the acceleration spectrum to produce the aircraft displacement spectra, $S_{A/C}$. Through the same FFT and Hamming function the power spectra, S_L , derived from the laser profilometer measurements are also evaluated. It should be noted that strong objections may be raised about applying a spectral window in the frequency domain instead of the time domain (see Davis, 1974). In this instance, the filter applied to the data was probably adequate for reducing the sidelobes. The problem is further alleviated by the fact that the wave spectra are not characterized by sharp peaks but are rather smooth with gradual slopes. Since the means were removed from each data segment prior to the FFT, no energy should reside in the zeroth harmonic. However, because of the problems with the filter ramp and the relatively large spacing between adjacent harmonics in this portion of the spectrum, the zeroth harmonic usually did have a finite value after the Hamming function convolution. It was arbitrarily set to zero.

Another condition was implemented as well. No component of $S_{A/C}$ should exceed S_L . Ideally S_L should always be equal to or greater than $S_{A/C}$ because it is the sum of two uncorrelated motions. If $S_{A/C}$ did exceed S_L , they were considered equal and due to the aircraft and S_L was set equal to zero. All other components of $S_{A/C}$ were subtracted from those of S_L and residual spectrum is defined as S_L' . The significant



RESPONSE FUNCTION OF HIGH-PASS DIGITAL FILTER

Fig. V-2

wave height, SWH, was calculated from the result given in Neumann and Pierson (1966).

$$H_{1/3} = 4\sqrt{\sigma^2} \quad (5)$$

where σ^2 is the total variance or power in the residual spectrum, S_L' .

In order to obtain the true wave spectrum, S_L' must be doppler shifted in some manner. No angular spreading function was incorporated here. Instead, two approaches were used. The first approach is to assume that all waves travel in the direction of the ground track, and $V' = \pm V$ depending on whether the track was actually with or against the waves. The second was to assume that all waves traveled with the wind. Then the aircraft velocity relative to the waves would be $V' = V \cos \theta$. The angle, θ , is defined in Figure II-2. The transformations are given by

$$\omega_t = -\frac{g}{2V'} + \sqrt{\left(\frac{g}{2V'}\right)^2 + \frac{g\omega_a}{V'}} \quad (6)$$

and

$$\phi_t(\omega_t) = \phi_a(\omega_a) \cdot \left(1 + \frac{4V'\omega_a}{g}\right)^{1/2}, \quad (7)$$

where "t" and "a" subscripts imply "true" and "apparent" respectively.

Finally, the values of all nine spectral estimates in each leg of the star patterns are averaged for that particular leg. To determine the 0.90 confidence interval, the result found in Bendat and Piersol (1971) is used. Each spectral estimate affords 2 degrees of freedom (Bath, 1974). Therefore the total number of degrees of freedom is ≈ 18 .

$$\frac{n}{2} \leq \frac{G(f)}{G(f)} < \frac{n}{2} \chi_{n, (1-\frac{\alpha}{2})}^2, \quad (8)$$

where n = number of degrees of freedom, α is a parameter

determining the confidence interval desired, $(1-\alpha)$, $G(f)$ is the estimated spectrum, $\hat{G}(f)$ is the true spectrum, and χ^2 is the chi-square function. Equation (8) yields (0.62, 1.9) for the 90% interval.

VI. PRESNTATION AND DISCUSSION OF RESULTS

A. Wind and $H_{1/3}$

Table 3 contains all of the results for wind and significant wave height. As for the wind-wave radar, due to the malfunction of a transmitting cable on 5/27/76 and clogged horn by rain on 6/4/76 only the data taken on 6/2/76 was consistently good during the 305 m patterns. For this reason, only one data point was obtained. It should be noted that the algorithms for the wind-wave radar relates the wind speed to a 12.5 m reference level, while the ship's anemometer is positioned 24.5 m above mean sea level. The elevation corresponding to the NWS values is not known to us. The aircraft speeds are given for the 3048 m transects in order that the distance between measurements can be calculated. The actual positions and orientations of the patterns and legs are shown in Figures VI-1 to VI-4b. All of the 3050 m tracks proceed in a southerly direction and therefore SWH values near the end of the track relate more closely to Pattern 2. Initial values from the high flight radar (3050 m) were obtained in locations closer to Pattern 5 although a time lag of 3 to 4 hours may exist between those measurements. The laser results do show some spatial inhomogeneities between legs, ie. Pattern 2 on 5/27/76. The laser data is most consistent on 6/2/76. Unfortunately, there were no satellite overflights coincident to these measurements.

B. Ocean Wave Spectra

The data selected for spectral analysis was the data obtained on 6/4/76. Figures VI-5a to VI-14b are spectra from the two star patterns flown that day. Each figure contains two plots, the ocean wave spectrum and the aircraft

Table 3 — Wind and SWH Results

WIND (m/s) Time=15:16	DATE PATTERN-LEG	NRL RADAR	LASER PROFILOMETER	SHIP REPORT	NWS/FWC	COMMENTS
	6/2/76	8		8.7	5-10	
H _{1/3} (m)	5/27/76					
13:21	3048m	2.45				
13:25	3048m	2.60				
13:27	3048m	2.00				
13:31	3048m	1.94				
15:06	2-1		1.23			
	2-2		1.35			
15:24	2-3		1.80			
	2-4		1.26			
15:42	2-5		2.06			
	6/2/76					
13:18	3048m	1.65				
13:23	3048	1.70				
13:25	3048m	1.92				
14:56	2-1		1.88			
	2-2		1.72			
15:16	2-3		2.12			
	2-4		1.78			
15:39	2-5		1.83			
	3-UW		1.90			
	5-1		1.98			
16:46	5-2		1.96			
	5-3		1.99			
17:05	5-4		1.90			
	5-5		1.89			
	6/4/76					
13:18	3048m	3.27				
	3048m	3.26				
	3048m	3.25				
	3048m	3.29				
15:02	2/1		2.77			
	2/2		2.94			
15:28	2/3		2.84			
	2/5		2.64			
15:51	2/4		2.36			
	3-UW		2.83			
	3-DW		3.27			
16:48	4-UW		3.33			
	4-DW		3.72			
	5-1		3.34			
17:14	5-5		3.32			
	5-2		2.67			
	5-3		2.72			
17:32	5-4		3.60			

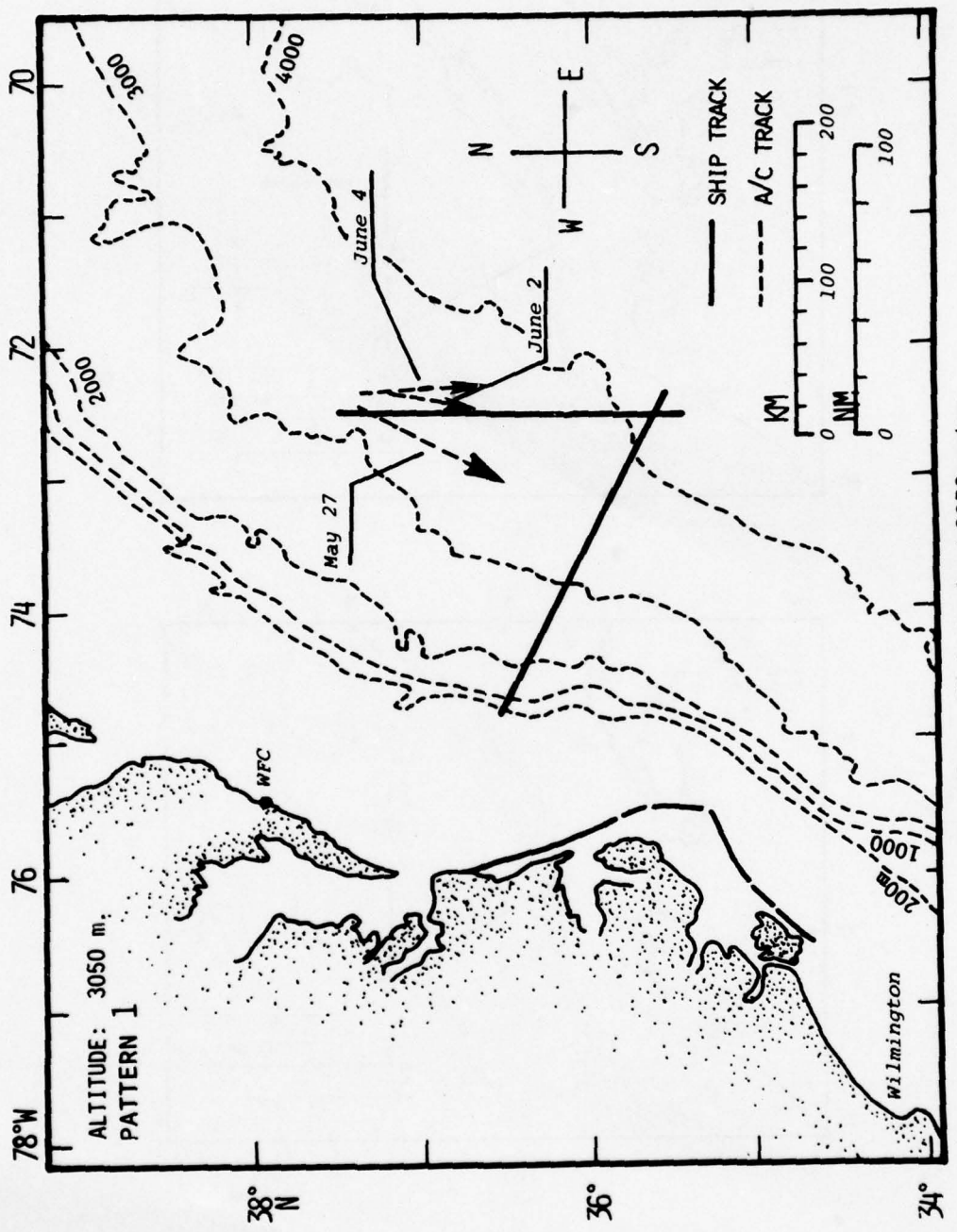
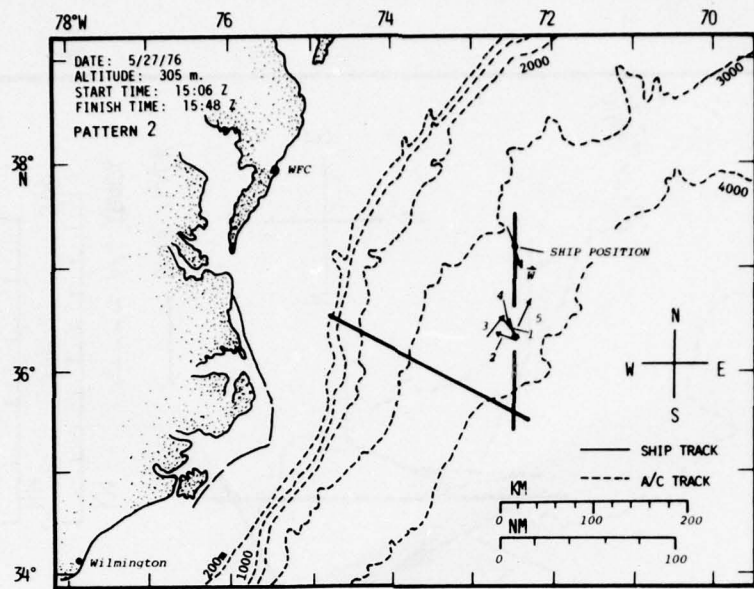
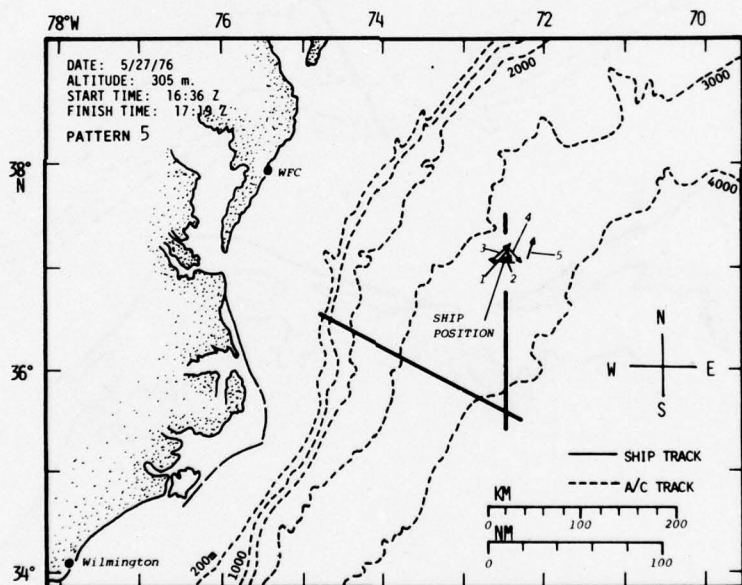


Fig. VI-1 — Flight tracks at 3050 meters

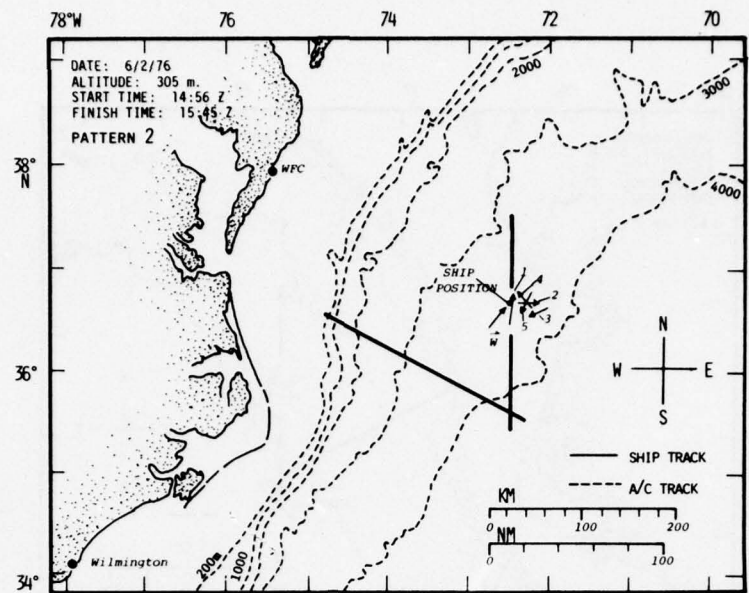


(a)

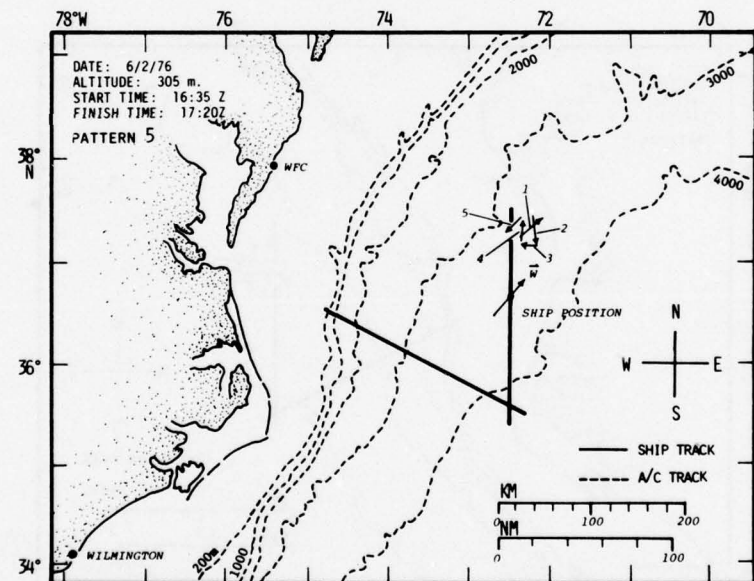


(b)

Fig. VI-2 — Star patterns on 5/27/76

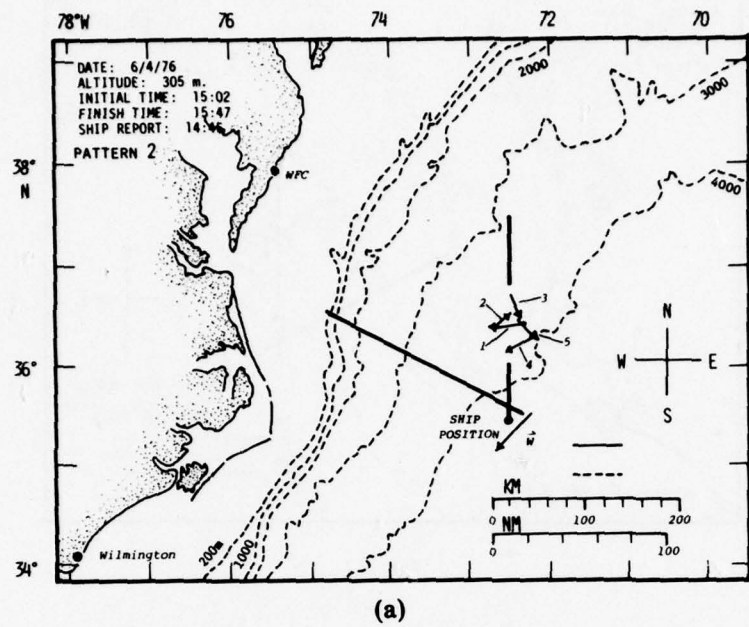


(a)

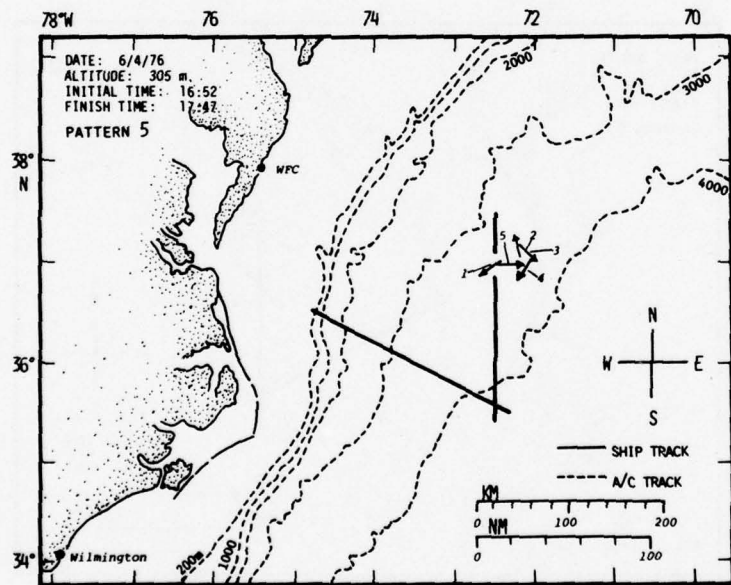


(b)

Fig. VI-3 — Star patterns on 6/2/76



(a)



(b)

Fig. VI-4 — Star patterns on 6/4/76

displacement spectrum. The convention for "TAPE" printed on each plot is data tape number--pattern number (Figure II-1)--leg number. The plots are arranged in the order of increasing aircraft track deviation from the wave direction. The plots are log-log covering five orders of magnitude on the ordinate and three on the abscissa. The plots of the aircraft motion power spectral density demonstrates what was discussed in Section V regarding the problems of estimating that parameter using short data lengths (≈ 22.5 s). Since the energy resides in a frequency interval where spectral resolution is relatively coarse and where the transformation from acceleration to displacement is particularly sensitive, the proper elimination of the side lobes introduced by the discrete finite Fourier transform is difficult. For this reason, those curves do not break downward on the low frequency end. This problem might have been avoided had the spectral window been applied in the time domain before the mean was removed. Also, components with amplitudes too low are not plotted. When comparing the standard deviation of the aircraft motion to the significant wave height (both values supplied on each plot), large differences in the first is often seen between data segments even though $H_{1/3}$ estimates usually show little variation. This fact indicates that the algorithm handles this rather perplexing situation reasonably well. Its performance would certainly improve if the data set could allow for longer data segments and a sharper filter gain cutoff as argued in Section V. Figure VI-15 is provided in order to demonstrate the effect of erroneous estimation of aircraft motion on the SWH. Appendix D gives the derivation and definitions for this plot.

For each leg, two spectra are shown. The "a" designation corresponds to a doppler shift which assumes that the waves are traveling in a direction parallel to the

flight track, i.e. $\theta = 0^\circ, 180^\circ$. The "b" relates to the assumption that the waves propagate parallel to the wind direction. The direction of the dominant wave component as given by the ship report was perfectly downwind on that day. However, if the Pierson-Moskowitz model is used to relate SWH to wind speed,

$$H_{1/3} = 0.0212 U_{19.5}^2 \quad (9)$$

the wind speed during the time of flight is insufficient to generate the seas that were encountered. Indeed, the winds had gradually subsided from higher values (ship report: 10-12 m/s winds, 4-6 m seas) early that morning. Therefore, the seas were not in a purely generation phase. Nonetheless, the spectra from upwind and downwind tracks do conform to a 5:1 slope as expected.

Included are two additional spectra (Figures VI-16, 17) taken from upwind and downwind flights near Newfoundland during February-March, 1976. The seas were much higher and offered a good test of the algorithm's performance because of high wind speeds experienced by the aircraft (up to 40 knots). As can be seen, the 5:1 slope is maintained. Also, when these are compared with the Gulf Stream spectra (lower sea state) from similar tracks, the plots align perfectly showing that the high frequency components do saturate and are maintained as $H_{1/3}$ increases. Spectral growth does proceed in the manner predicted by Phillips and aptly depicted in Kitaigorodskii (1973). It should be noted that line-profiled data taken from a directionally dispersive system will produce power spectra that are distorted to some degree. The more directional the wave field is, the smaller the distortion (see Appendix E). The spectra shown here tend to exhibit the least distortion

Fig. VI-5a

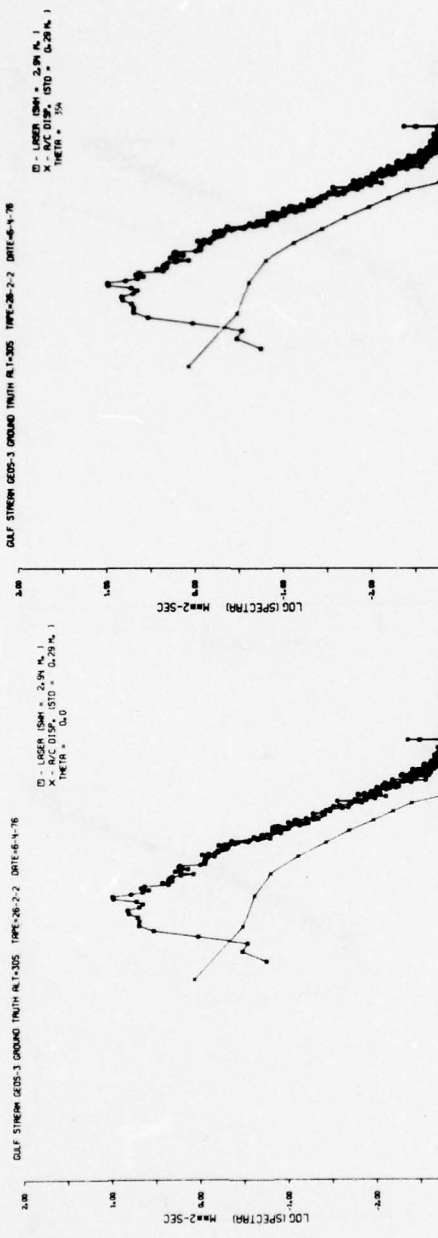


Fig. VI-5b

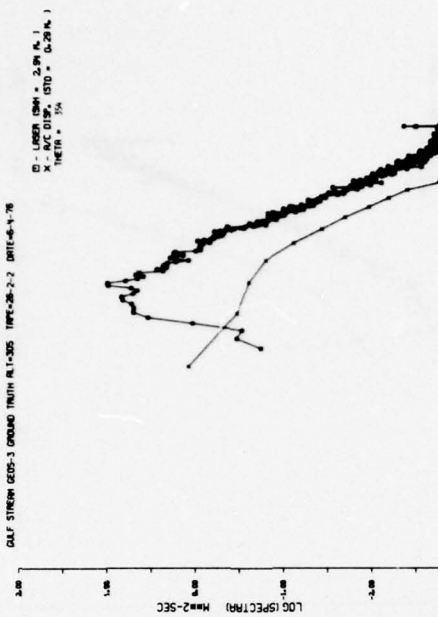


Fig. VI-6a

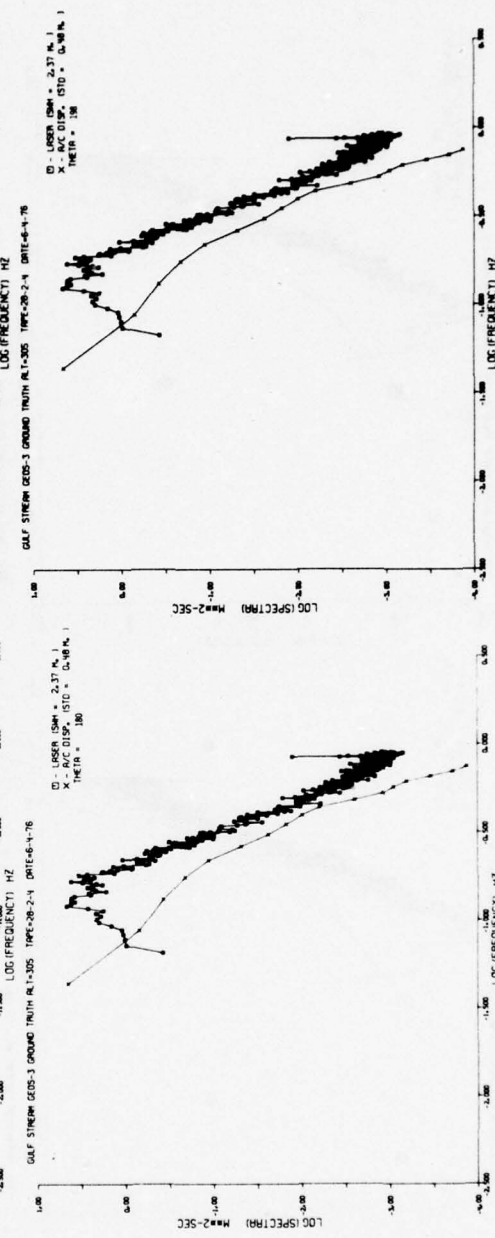


Fig. VI-6b

Fig. VI-7a

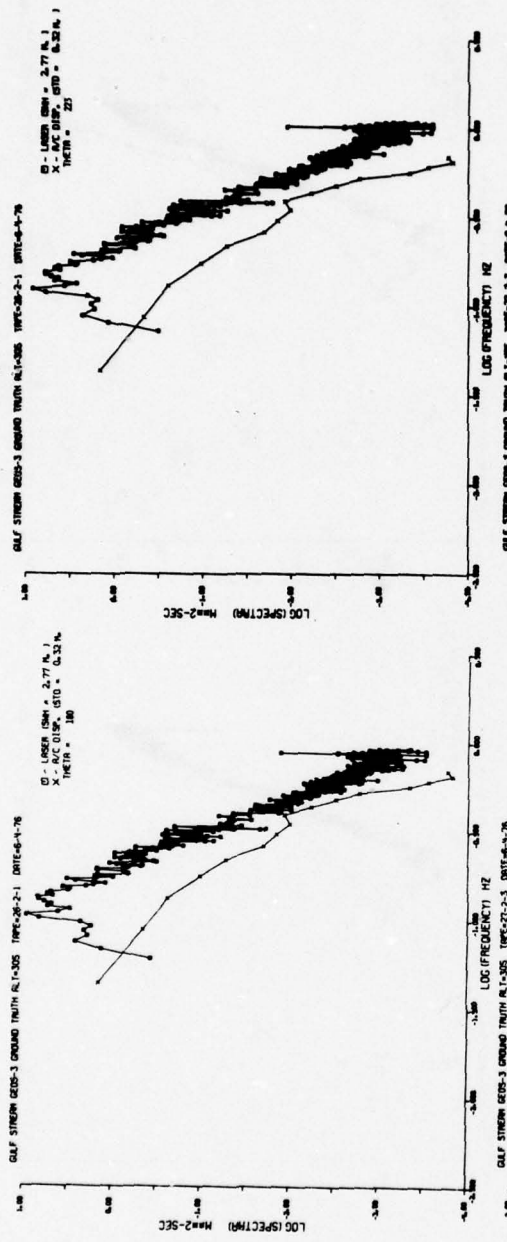


Fig. VI-7b

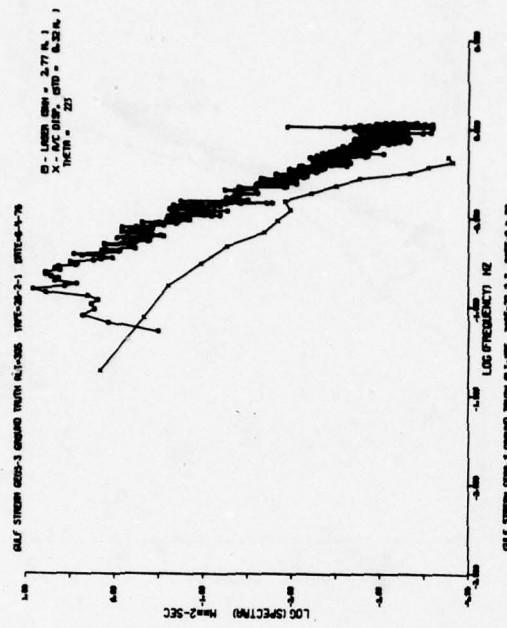


Fig. VI-8a

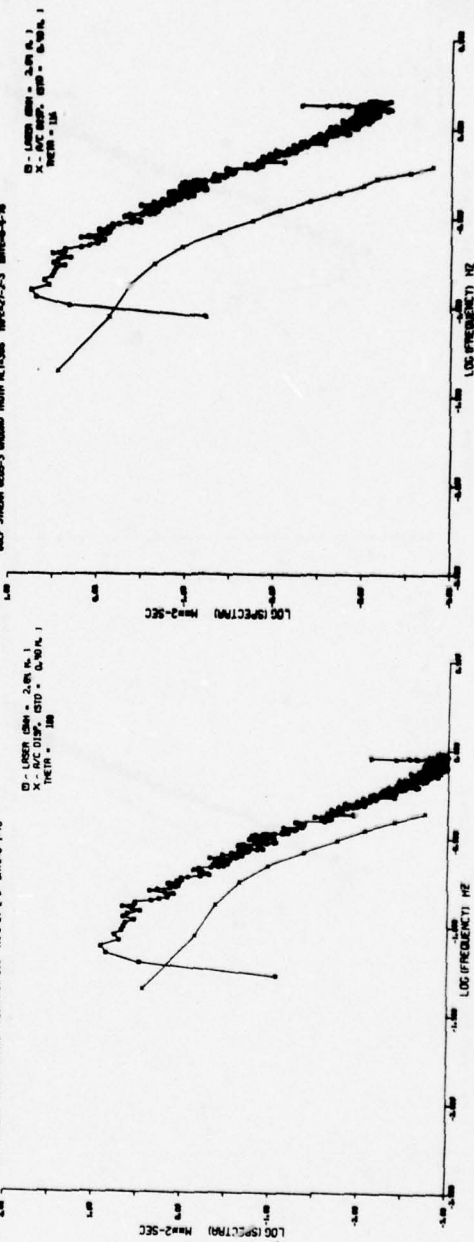


Fig. VI-8b

Fig. VI-9a

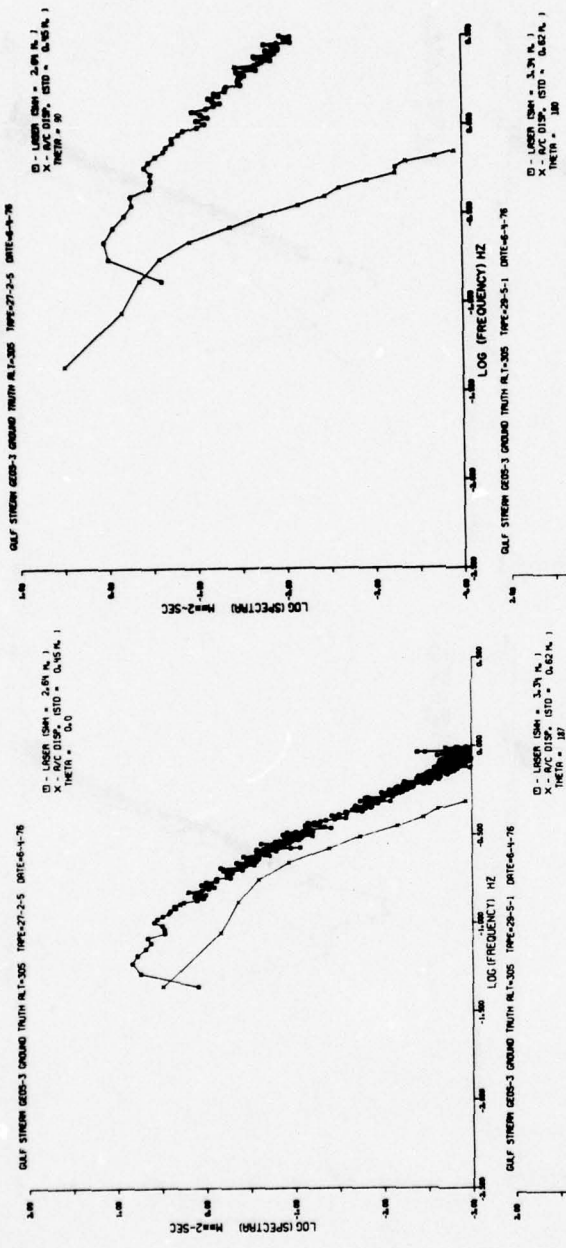


Fig. VI-9b

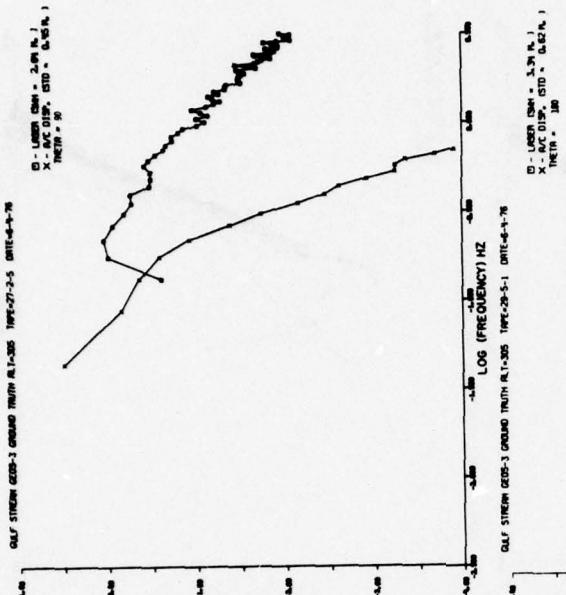


Fig. VI-10a

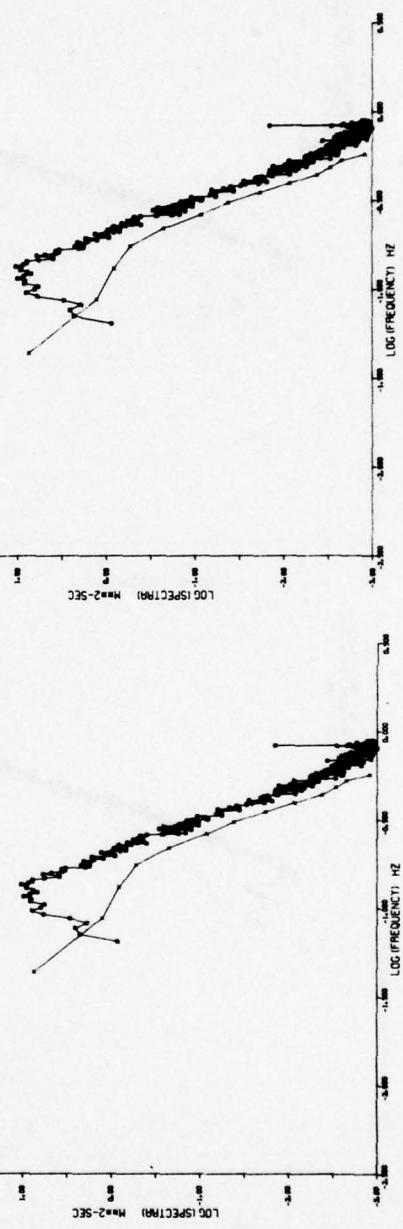


Fig. VI-10b

Fig. VI-11a

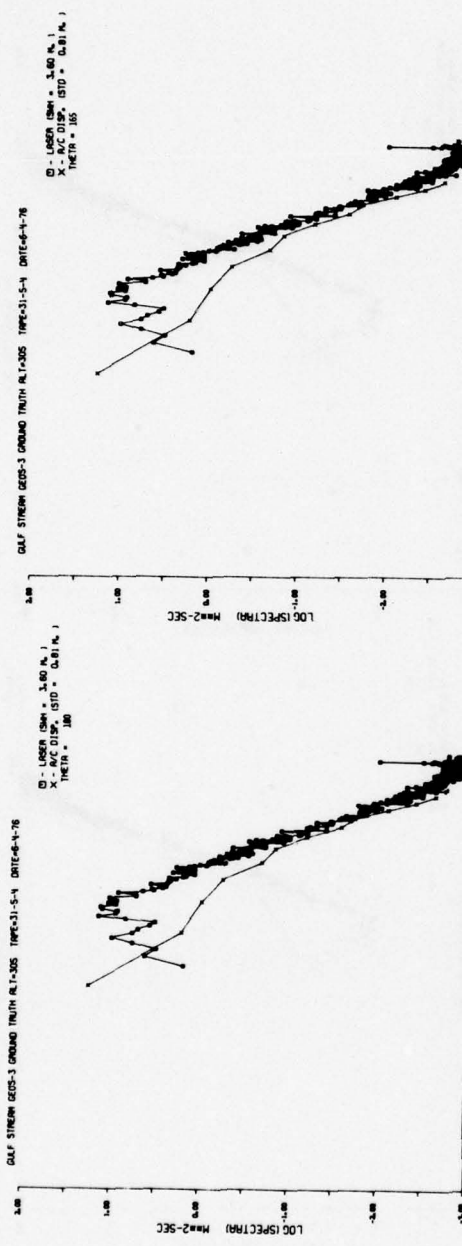


Fig. VI-11b

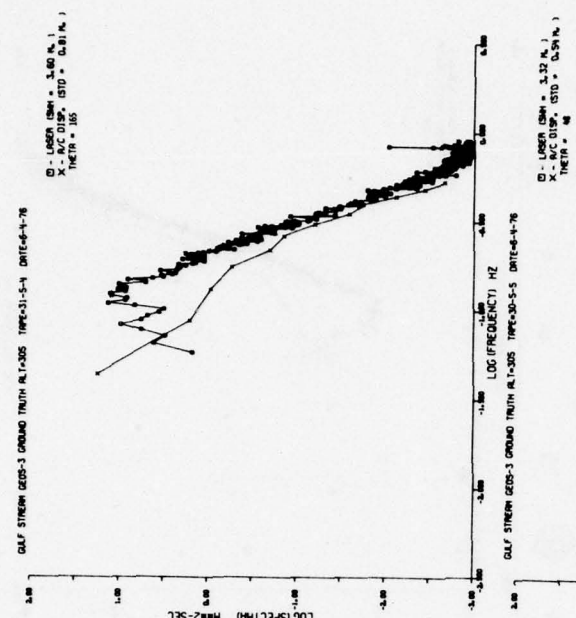


Fig. VI-12a

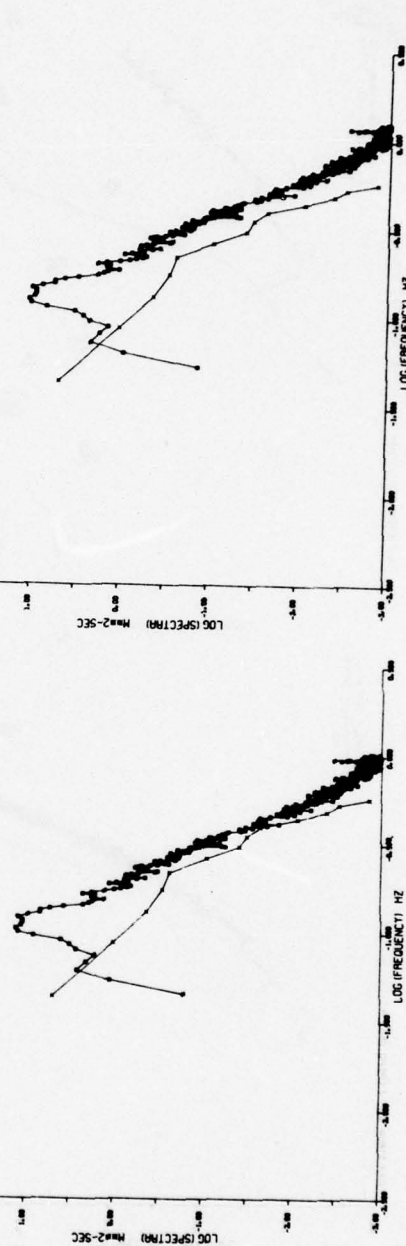


Fig. VI-12b

Fig. VI-13a

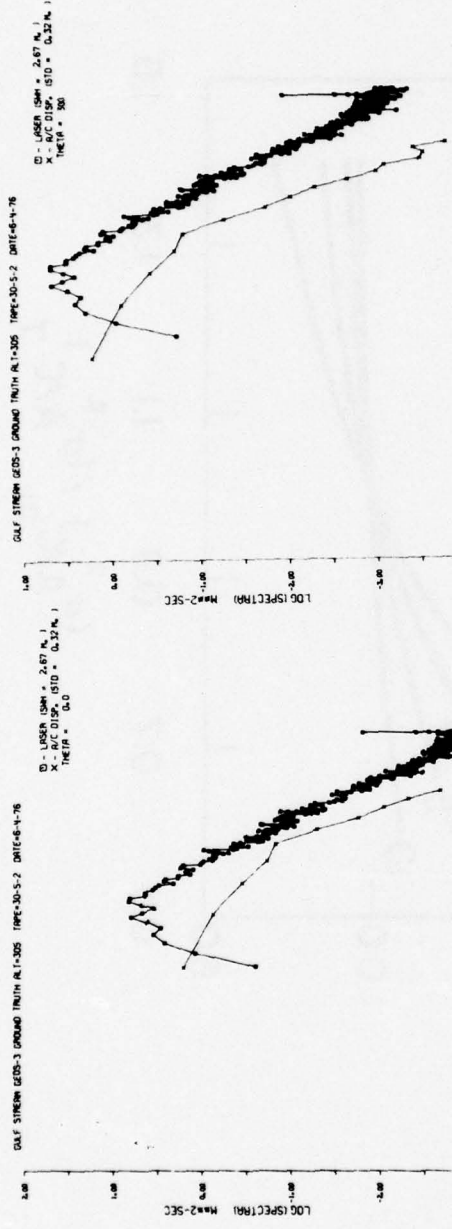


Fig. VI-13b

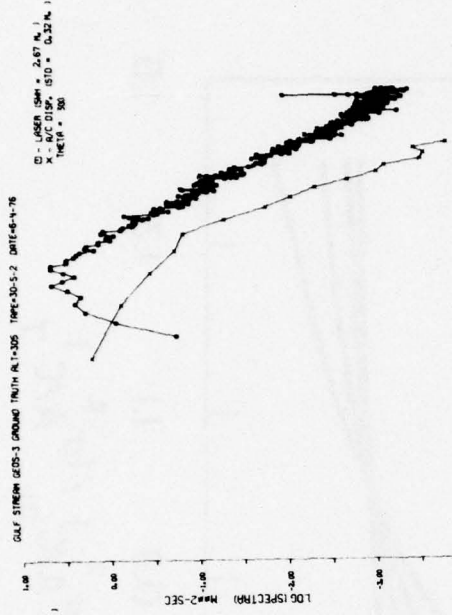


Fig. VI-14a

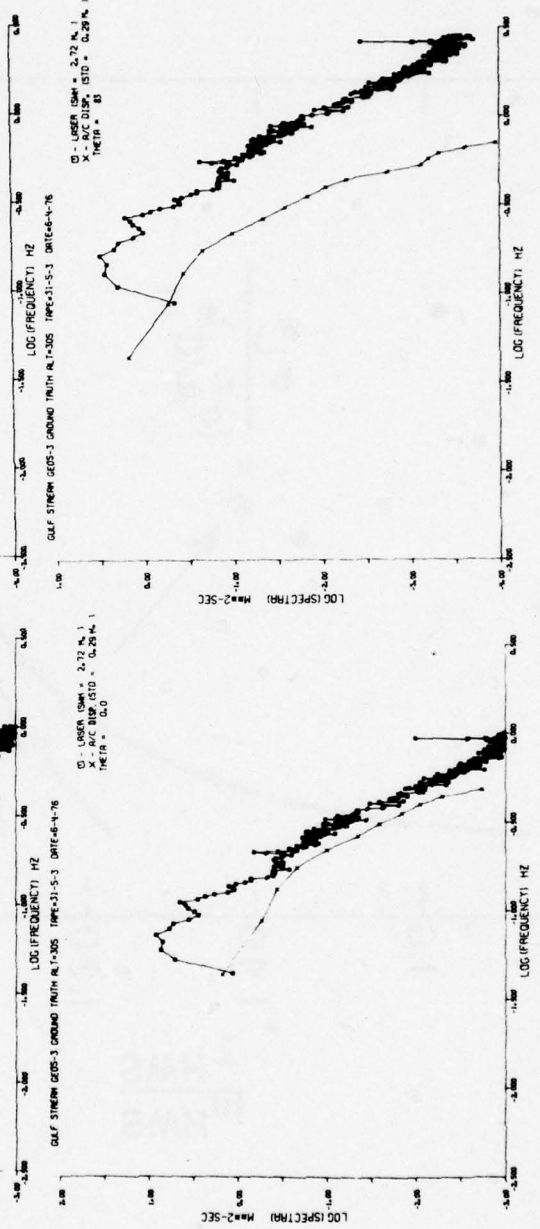


Fig. VI-14b

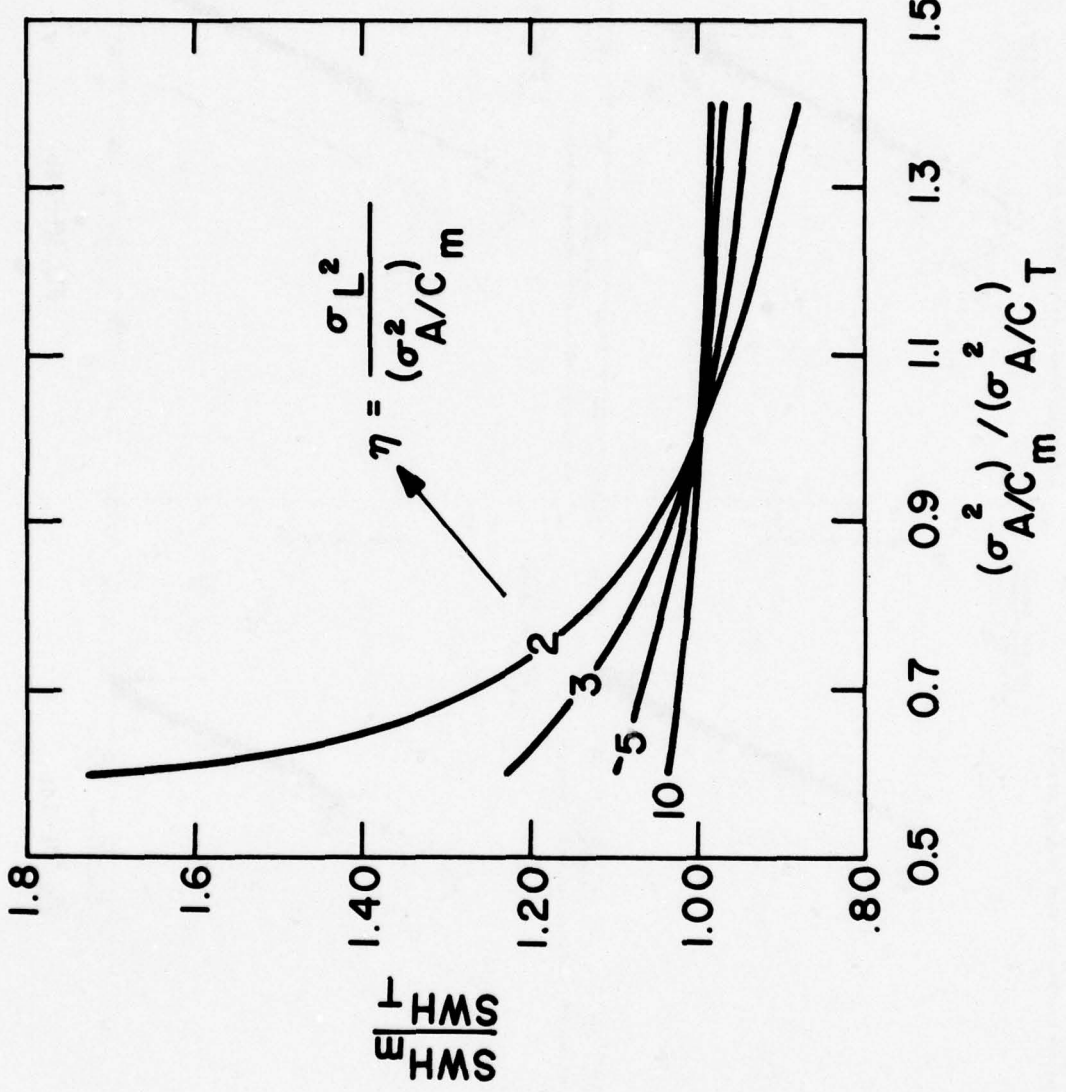


Fig. VI-15 — Effect of erroneous estimation of aircraft motion on $H_{1/3}$

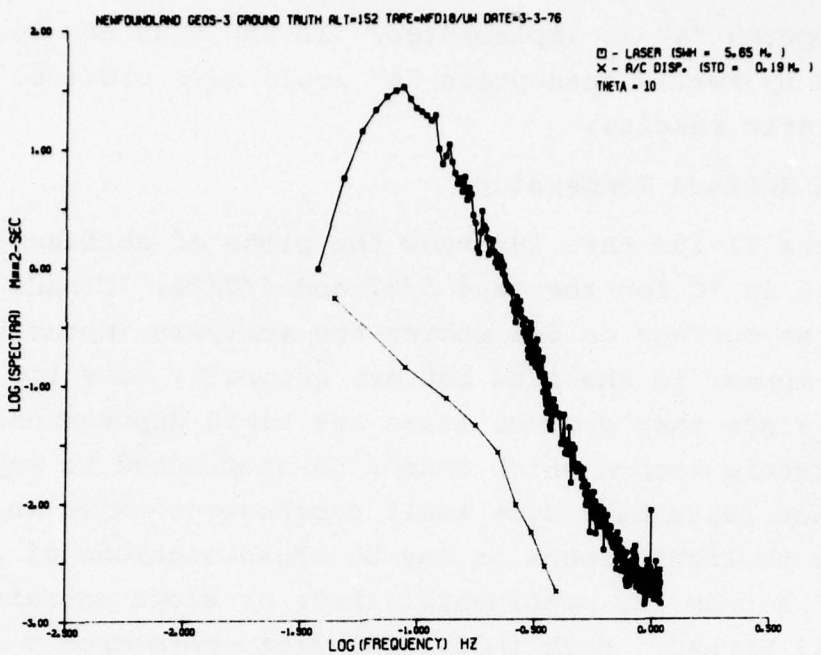


Fig. VI-16 — Wave spectra from Newfoundland GEOS-3 underflight, 3/3/76

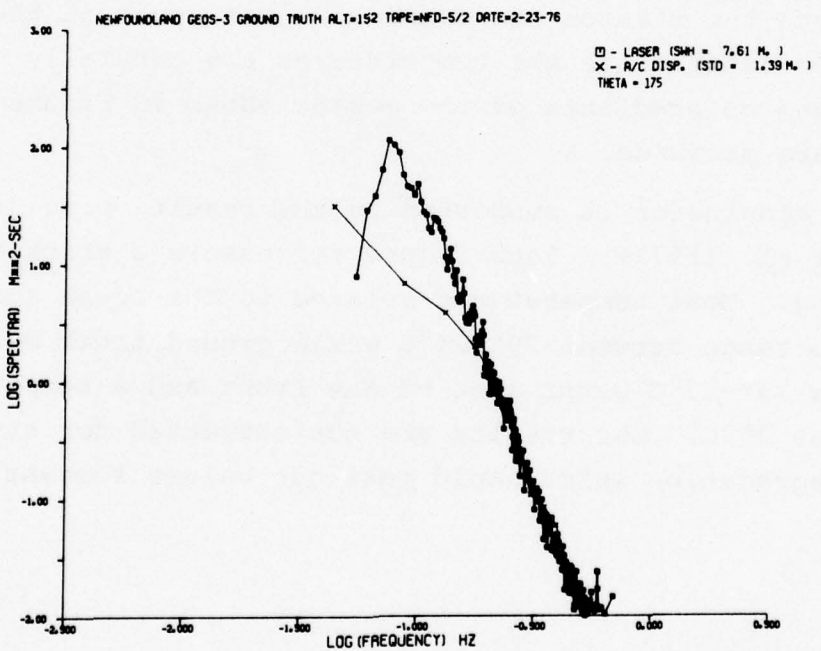


Fig. VI-17 — Wave spectra from Newfoundland GEOS-3 underflight 2/23/76

when assumption "a" is implemented. If the seas had been dominated by swell, assumption "b" would have provided the most realistic results.

C. Ocean Surface Temperature

Figures VI-18a thru 19f show the plots of surface temperature in °C for the days 5/27 and 6/2/76. Clouds obscured the surface on 6/4 making the analysis impossible. Clouds do appear in the data but are generally easy to recognize since they produce large and rapid depressions in the temperature record which cannot be attributed to any real surface features. Some small depressions exist which may be due to light clouds or may be cross-sections of cold water bodies from the continental shelf or slope entrained by the Gulf Stream. Each individual plot represents a data file, seven of which were taken each day along the 3050 m track. Only the first six files are presented. Apparently on both days the mission was commenced just south of the Gulf Stream front since the temperatures are generally constant and no gradients of the scales shown in Figures IV-1 and 2 were measured.

This conclusion is supported by the results provided by Curtin, et al. (1978). Each figure represents a track only 7-8 km long. Most temperatures related to the ocean surface lie in the range between 20°-24°C while ground truth measurements show 16°-17°C water west of the front and a temperature maxima near 25°C. Our results are not corrected for atmospheric degradation which would make our values somewhat low.

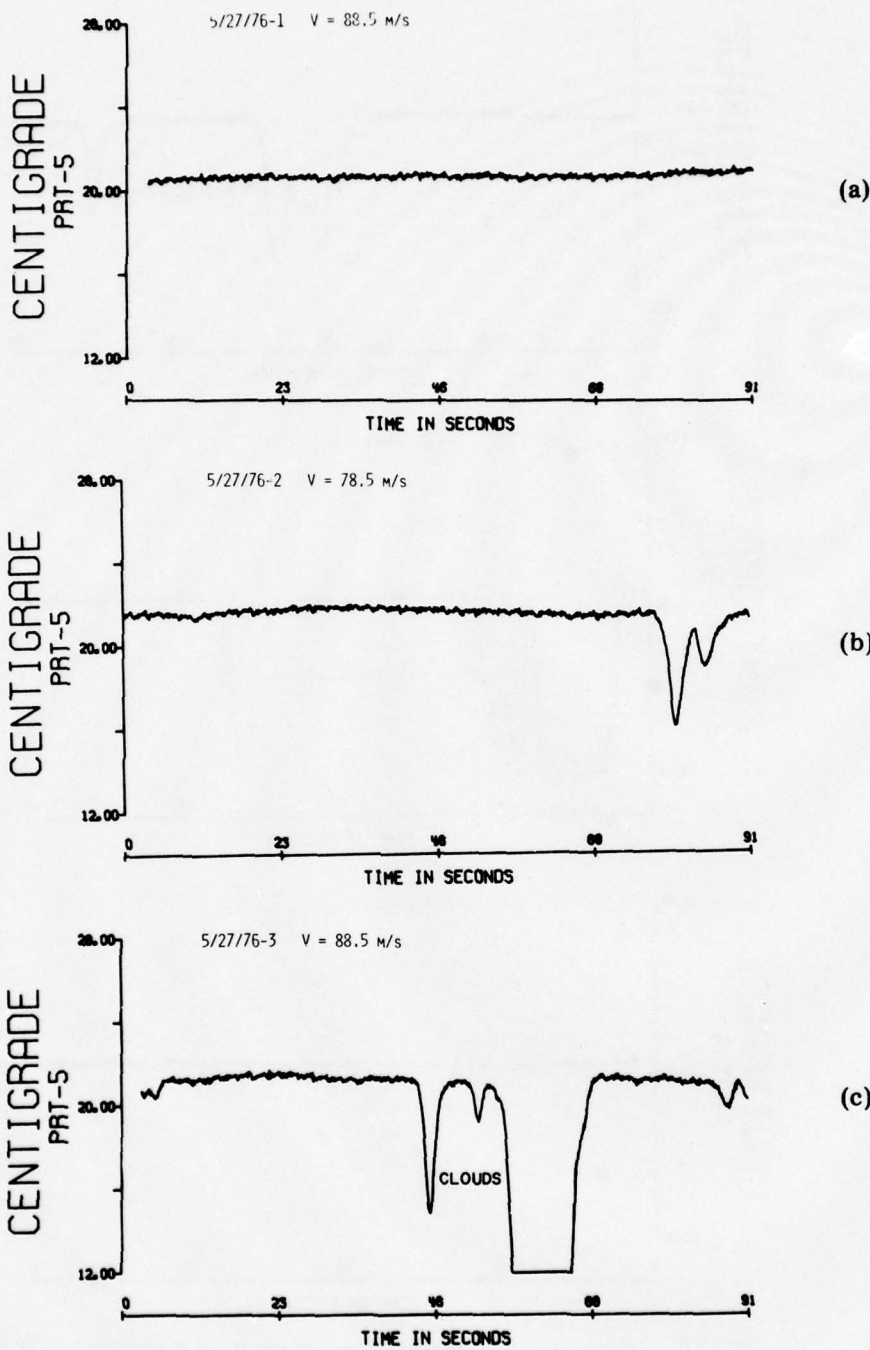


Fig. VI-18 — Ocean surface temperature from PRT-5 at 3050 meter altitude, 5/27/76 (Continues)

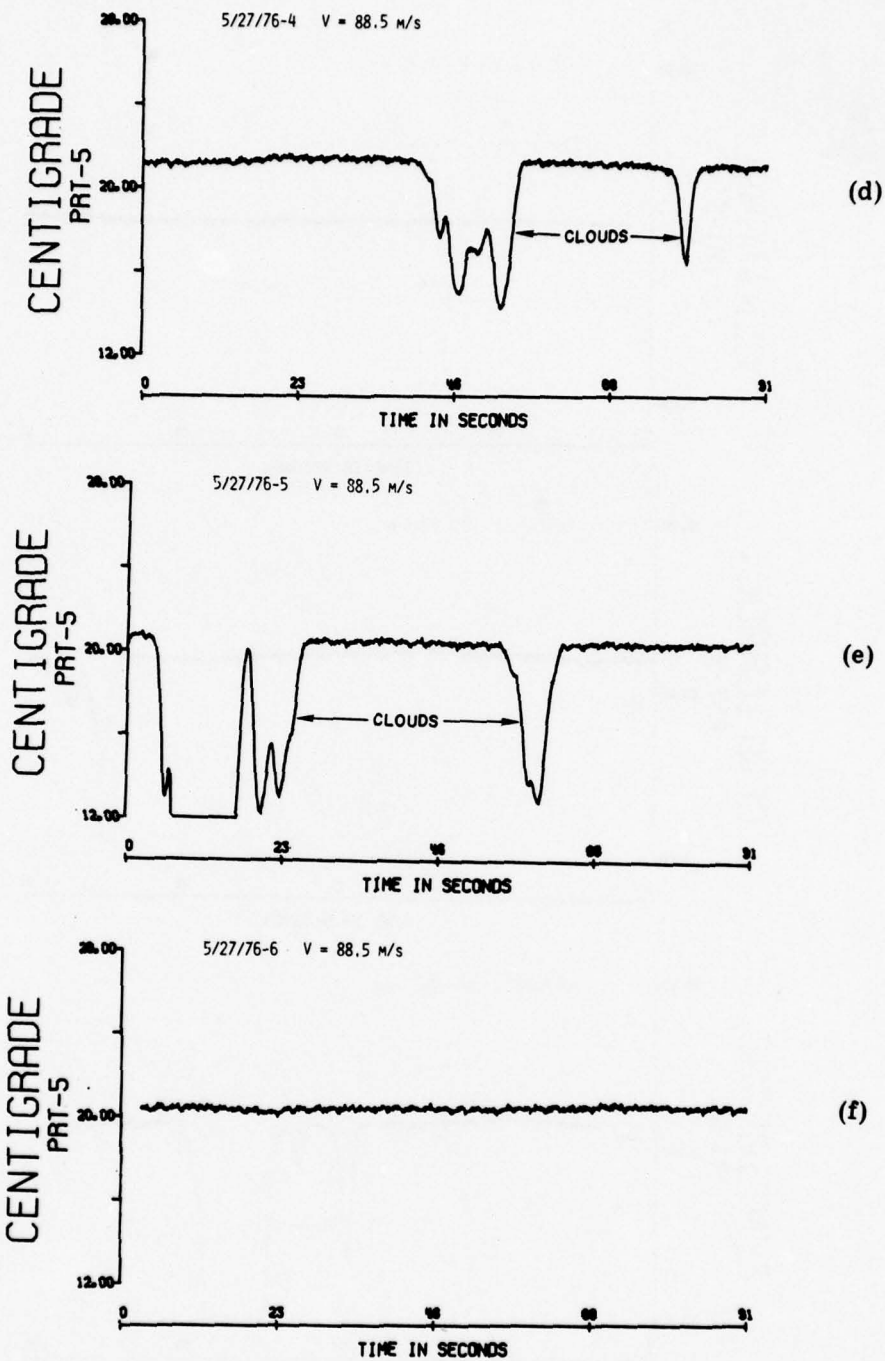


Fig. VI-18 — Ocean surface temperature from PRT-5 at 3050 meter altitude, 5/27/76 (Continued)

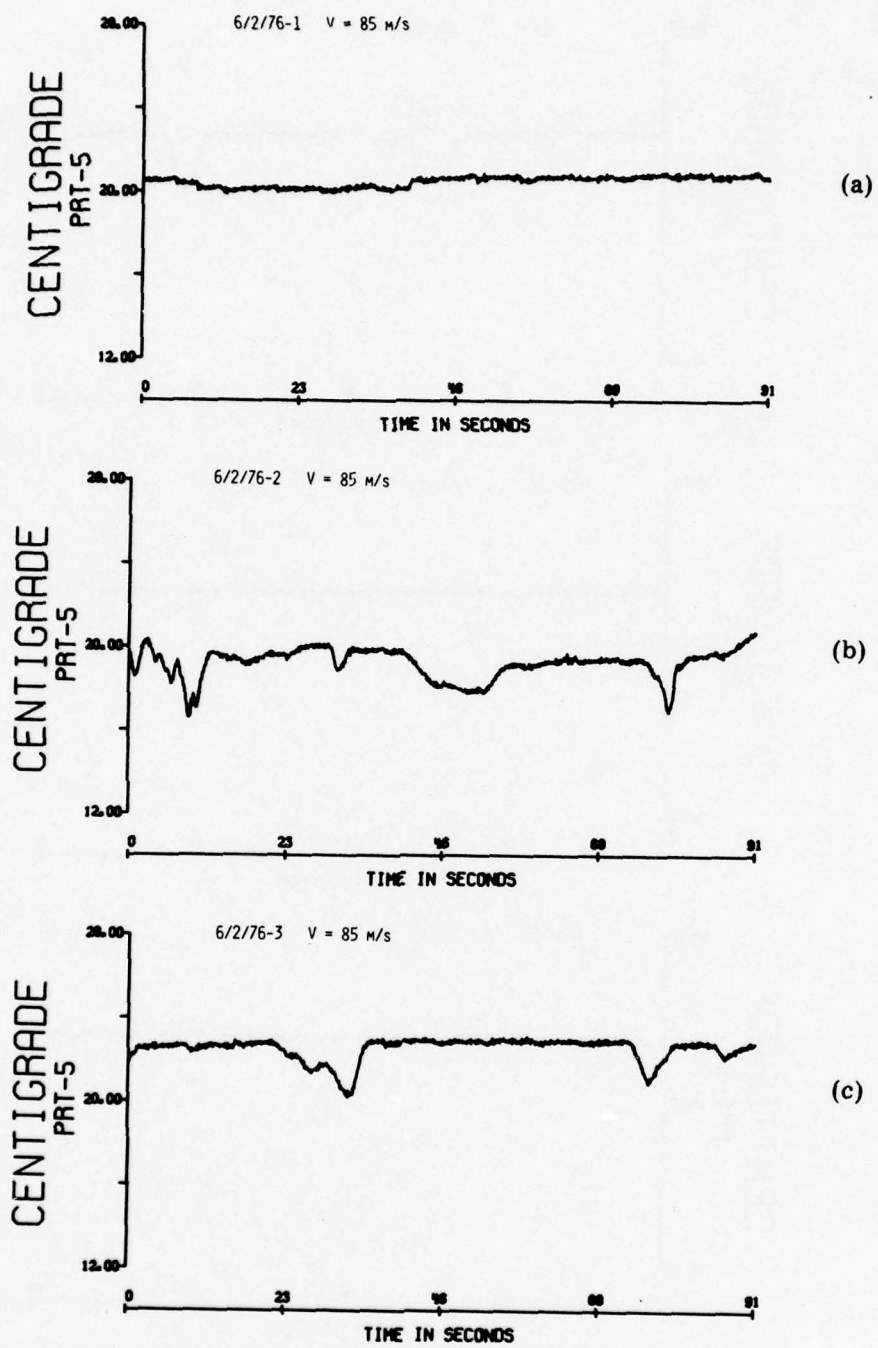


Fig. VI-19 — Ocean surface temperature from PRT-5 at 3050 meter altitude, 6/2/76 (Continues)

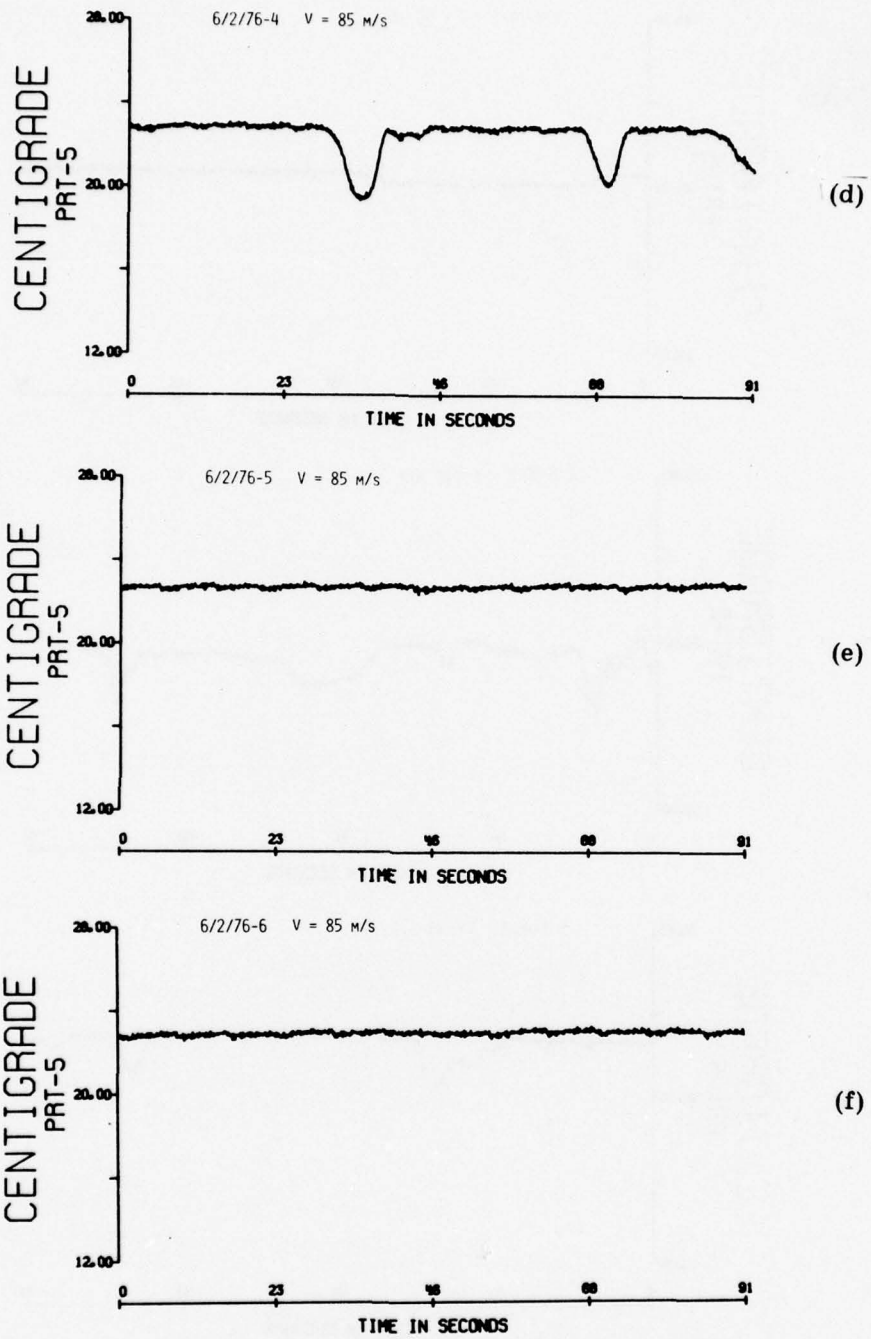


Fig. VI-19 — Ocean surface temperature from PRT-5 at 3050 meter altitude, 6/2/76 (Continued)

VII. SUMMARY

The results of this experiment show that the active microwave sensors (high-flight radar, wind-wave radar) provide consistent and accurate estimates of significant wave height and surface wind speed, respectively. It should be emphasized that the atmospheric conditions existing during this project were relatively calm with wind speed below 12 m/s and the sea states not higher than 4 meters. Measurements of significant wave height by the laser profilometer, in general, correlate quite well with those from the high-flight radar although comparisons between simultaneous laser and radar measurements are not possible since they operate at different altitudes. The laser estimates of SWH from individual legs of the star-patterns flown indicate that considerable spatial variability in sea state can exist at least for low sea state conditions.

Satisfactory removal of aircraft motion from the profilometer data was a major effort in this study. The approach was to filter the laser record so as to remove the low frequency components which were not coincident with the ocean surface signal, then incorporate the aircraft's vertical acceleration information for the removal of high frequency contamination that did overlie the true signal obtained in the profilometer record. Examination of individual spectral estimates of the filtered accelerometer data exhibited large fluctuations in this quantity, yet the resultant significant wave height estimates remained stable. In addition, two results of profilometer data collected from another ground truth mission (Newfoundland) are provided to further establish confidence in the algorithm's performance on data sets having much more severe aircraft motion contamination and higher sea states. The results are very satisfactory. An alternative approach to aircraft motion removal is to take longer data segments which would allow an adequate estimation

of the entire aircraft motion spectrum and subtract this from the spectrum provided by the profilometer. This approach would eliminate the necessity of applying a numerical filter, but would require much longer tracks.

The effects of angular dispersion on profilometer-derived ocean wave spectra can also introduce serious problems since the flight track may not be parallel to the direction of a wave component's propagation. Experimental results show that the previous practice of assuming that all waves propagate parallel to the wind can cause more extreme spectral distortion than simply assuming that all waves travel in a direction coincident with the flight track. This is especially true when the angle between the track and the wind exceeds 30 degrees. However, this observation would not be true if the wave field were highly direction^{al}, then the previous assumption would be more appropriate. To clarify this issue, a mathematical simulation has been included which models the spectrum derived from a line-profile sample of a directional wave field. Several mathematical forms for the directional wave spectra were used and track angles of 0, 15, 30, 45, and 60 degrees to the wind were considered. The result indicates that spectral aliasing is not serious for wind-driven seas if the flight track is within 15 degrees of the wind direction. Otherwise, the distortion become more prevalent as that angle increases. This distortion may indicate a possible technique for determining the functional form of the angular spreading function. By taking airborne profilometer data at various angles to the wind simultaneously with a stationary wave profiler, various angle spreading functions could be applied to the airborne profile-derived spectra so as to shift it back upon the spectra from the stationary sensor.

Finally, the passive airborne temperature sensor, the PRT-5, produced very realistic values of the sea surface

temperature even though atmospheric corrections were not employed. The temperature range from PRT-5 lies within the domain of values supplied by in-situ measurements.

ACKNOWLEDGEMENTS

The authors wish to thank the members of the Advanced Space Sensing Applications Branch of NRL for their assistance in the completion of this study and flight crew of the NASA Wallops C-54 used in this experiment whose cooperation was invaluable. Particular mention should be made of Jim Kenney (NRL) who operated the laser profilometer and was responsible for replacing the faulty INS and also of Dr. Steven Long (NASA-WFC) who operated the PRT-5. We are indebted to Dr. Thomas Davis (NOO) for many timely recommendations regarding the spectral analysis, Pete Mitchell (NRL) who assisted in the meteorological analysis, and Dr. Norden Huang (NASA-WFC) for his help in preparing the manuscript. The support of Fleet Numerical Weather Central, the Naval Oceanographic Office, the National Weather Service, and North Carolina State University is greatly appreciated.

The principal author, C. McClain, was a NRC-NRL research associate during 1976 and 1977 and a special expression of gratitude is due to Benjamin Yaplee and Dr. Vincent Noble for making this position possible.

This work was sponsored by NASA Wallops Flight Center Contract No. P-62257(G) and NAVAIR Task No. A370/370C/058B/WF52-553000 to the Naval Research Laboratory.

REFERENCES

- Bath, M. (1974) Spectral Analysis in Geophysics, Elsevier Scientific Publ. Co., N.Y., 563p.
- Bendat, J.S., A. G. Piersol (1971) Random Data: Analysis and Measurement Procedures, John Wiley and Sons, N.Y., 407p.
- Chen, D.T., P. Bey (1977) Interaction between steady non-uniform two-dimensional currents and directional wind-generated gravity waves with applications for current measurements, NRL Memorandum Report 3508, 30p.
- Curtin, T.B., L. J. Pietrafesa, N.E. Huang (1978) Concurrent satellite and ship observations across the Gulf Stream north of Cape Hatteras, (in press).
- Davis, T.M. (1974) Theory and practice of geophysical survey design, Naval Oceanographic Office Reference Publication 13, 137p.
- Hammond, D.L., R.A. Mennella, E.J. Walsh (1977) Short pulse radar used to measure sea surface wind speed and SWH, IEEE Trans. on Antennas and Propagation AP-25:1, 61-67.
- Kitaigorodskii, S.A. (1973) The Physics of Air-Sea Interaction, Israel Program for Scientific Translations, Ltd., Jerusalem, 237p.
- Krylov, Y.M., S.S. Strekalov, V.F. Tsyplukhin (1966) On the angular energy spectrum of wind waves, Izv., Atm. and Oceanic Phys., 2:7, 729-739. English, 441-446
- Leitao, C.D., N.E. Huang, C.G. Parra (1977) Ocean current surface measurement using dynamic elevations obtained by the GEOS-3 radar altimeter, Proc. of the Conference on Satellite Applications to Marine Technology, New Orleans, November 15-17, 43-49.

- Lonquet-Higgins, M.S. (1962) The directional spectrum of ocean waves, and processes of wave generation, Proc. Roy. Soc., London, A265, 286-315.
- Martin, M.A. (1957) Frequency domain applications in data processing, General Electric Co. Document No. 575D340, 128p.
- Neumann, G., W.J. Pierson, Jr. (1966) Principles of Physical Oceanography, Prentice-Hall, Inc., Englewood Cliffs, N. J., 545p.
- Olver, F.W.J. (1964) Bessel functions of integer order, from Handbook of Mathematical Functions with Formulas, Graphs, and Mathematical Tables (M. Abramowitz and I.A. Stegun, editors), 355-433. Washington: U.S. Govt. Print. Off.
- Ou, S.H., C.L. Bretschneider, F.L. Tang (1974) Relationship between the significant waves and the directional wave spectrum, Proc. Internat. Sym. Ocean Wave Measurement and Analysis, New Orleans, Vol. 1, 728-744.
- Parson, C.L., L. R. Goodman (1975) GEOS-3 Phase B ground truth summary, NASA TM X-69360, 261p.
- Pierson, W.J., Jr., L. Moskowitz (1964) A proposed spectral form for fully developed wind seas based on the similarity theory of S.A. Kitaigorodskii, JGR 69:24, 5181-5190.
- Ross, D.B., V.J. Cardone, J.W. Conaway, Jr. (1970) Laser and microwave observations of sea-surface condition for fetch-limited 17- to 25-m/s winds, IEEE Trans. Geos. Elect., GE-8:4, 326-336.
- Walsh, E.J. (1974) Analysis of experimental NRL radar altimeter data, Radio Sci., 9:8, 711-722.
- Walsh, E.J. (1977) Problems inherent in using aircraft for radio oceanography studies, IEEE Trans. Antennas and Propagation, AP-25:1, 145-149.

APPENDIX A

DETERMINATION OF WIND FROM THE WIND-WAVE RADAR

The results published by Hammond, et al (1977) show how wind speed can be obtained from the return waveform of the nanosecond radar. However, the particular cases derived in that paper relate to the aircraft altitude of 150 m. It was therefore necessary to recalibrate the algorithm for an altitude of 305 m. Figures A-1 and A-2 represent the appropriate curves. Figure A-1 shows the normalized waveforms that correspond to various mean wind speeds 12.5 meters above mean sea level. The wind is related to the slope of the trailing end of the waveform and Figure A-2 plots wind speed vs slope of the trailing end. The device is particularly sensitive at low wind speeds as were experienced during the Gulf Stream flights.

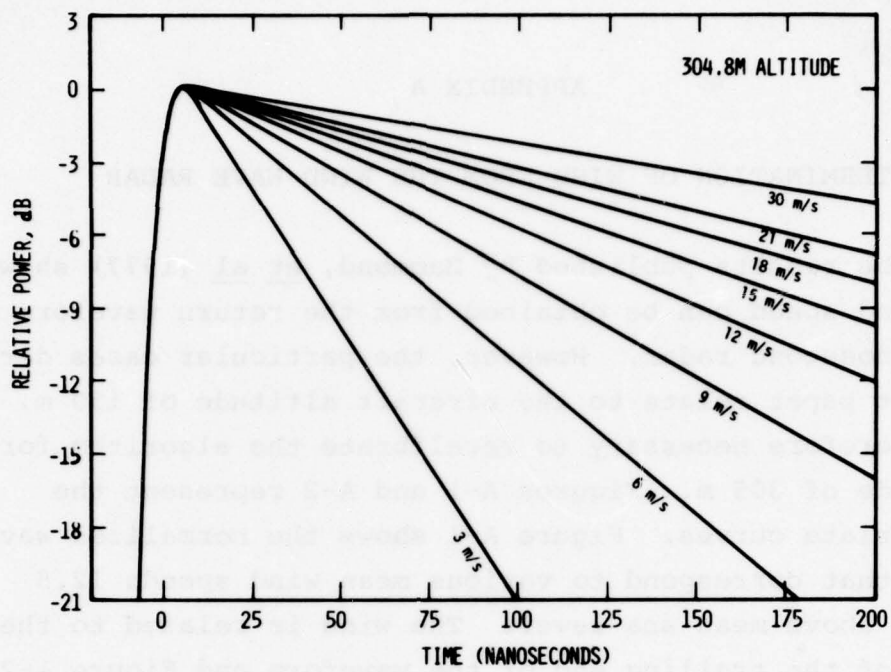


Fig. A-1 — Normalized return waveform vs. surface wind speed

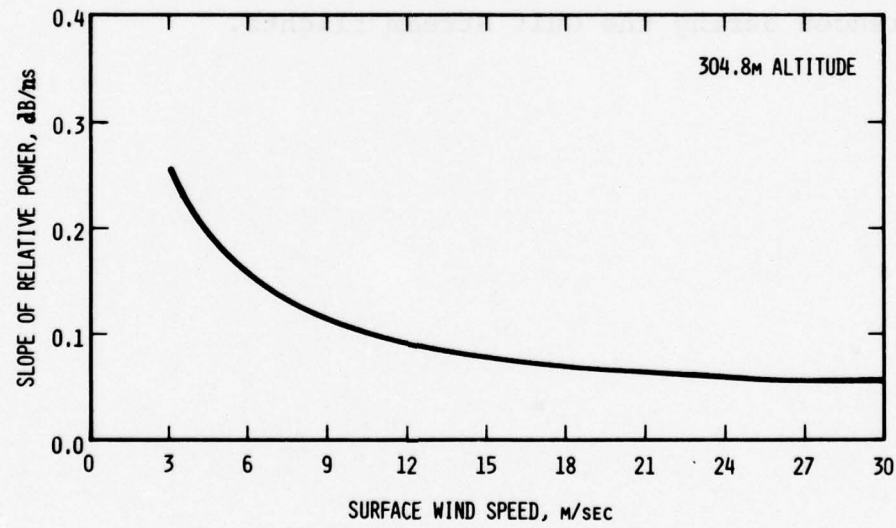


Fig. A-2 — Slope of waveform trailing end vs. wind speed

A-2

APPENDIX B

EFFECT OF LASER RESPONSE TIME

The Spectra-Physics Geodolite 3A has a selection of three response times, 5, 10, and 20 ms. The response time, τ , is defined as the time interval for the range output signal to get to 90 percent completion in response to a step change in range. Thus there is a smoothing effect on the measured profile, the severity of which is determined by the aircraft speed and the response time. During the Gulf Stream experiment, the response time, τ , was 20 ms. If the aircraft speed were 75 m/s, then the smoothing effect covered 1.5 m.

It is desirable to find a cut-off frequency, f_c , so as to determine the power gain at the Nyquist frequency, $f_f = f_s/2$. From the above information, the time constant of the laser circuit may be found.

$$0.9 = 1 - e^{-\alpha\tau} \quad (1)$$

Using $\tau = 0.02$ s, α equals 115. The voltage gain, A , is given by

$$A = [1 + (\omega/\alpha)^2]^{-1/2} \quad (2)$$

where ω is the radian frequency of an input component. The standard definition of f_c corresponds to a voltage gain = 0.707.

$$0.707 = [1 + (2\pi f_c/\alpha)^2]^{-1/2} \quad (3)$$

Immediately one sees that $\alpha = 2\pi f_c$ and $f_c = 18.3$ Hz.
Therefore,

$$A = [1 + (f/f_c)]^{-1/2} \quad (4)$$

The power gain, G , is of interest because distance is directly proportional to the output voltage and power spectra derived from the variance of the distance measurements is the final product. In decibels, the power gain is

$$\begin{aligned} G_{db} &= 10 \cdot \log (A^2) \\ &= -10 \cdot \log \left(1 + \frac{f}{f_c} \right) \end{aligned} \quad (5)$$

If $f_f = 45$ Hz, then

$$G_{db} = -10 \log \left(1 + \frac{45}{18.3} \right) = -8.5 \text{ db}$$

which is the case for the analysis used in this study. The laser does serve as a low-pass filter but 8.5 db decrease is not generally considered sufficient for eliminating spectral aliasing. Fortunately, for our application, no significant energy is found at wavelengths $\approx (75 \text{ m/s}) \cdot (1/45)\text{s} < 2 \text{ m}$. However, if the data is digitized at slower rates, then that wavelength increases. For $f_f = 22.5$ Hz, $G_{db} = -4$ db and the corresponding wavelength would be ≈ 3.3 m. For $f_f = 11.25$ Hz, $G_{db} = -1.4$ db and the wavelength increases to 6.5 m. The maximum amplitude of a 6.5 m wave is approximately 0.5 m, therefore significant error could be introduced during low sea states if the data is digitized too coarsely. All of these factors should be taken into consideration when a profilometer is used.

APPENDIX C

DETERMINATION OF THETA

As discussed in Section VI, the data has been analyzed in two fashions, the analysis using assumption "b" requires the angle between the ground track and some reference direction be known in order to properly doppler shift the wave spectra. This angle, θ , (Figure II-2) can be defined and evaluated in several ways depending on which vector is used as the reference. These choices include the surface wind given by the ship or by weather maps, wind derived from the aircraft INS data and dominant wave direction provided by the ship.

Using the wind direction as a reference direction could prove troublesome since the dominant wave may be swell not correlated to the wind. This can cause a large error in the doppler shift. Since the wind direction can change rapidly in space and time due to the presence of fronts, using the wind to derive θ is not advisable in such situations. The weather patterns during the Gulf Stream experiment included several fronts as discussed in Section IV. Furthermore, use of INS-derived wind would be subject to error if the wind vector rotates with elevation. Despite these objections, wind vectors from the INS data were derived for each leg of each star pattern on the 6/2/76 and 6/4/76 flights. The INS provided the aircraft heading, ground track, true air speed, ground speed and drift angle. The vector analysis was not made on 5/27/76 data because

the aircraft true air speed was not recorded by the INS operator. The best way of utilizing these vectors is to average the individual estimates over the five legs to obtain a mean wind for the star pattern. The individual vectors showed a great deal of scatter, particularly in direction. The data on 6/2/76 produced extremely scattered wind directions where a maximum difference of 138° within one star pattern existed. The INS was not operating properly that day and Loran-A data was collected as an alternative. The individual vectors from the star patterns of 6/4/76 were much more consistent for both star patterns. The mean wind vectors from the two star patterns had the headings 214° and 225° while the ship reported wind and dominant wave direction was 225° . Therefore on 6/4/76, all values of θ were derived using 225° as the reference heading. For the reasons stated above, the dominant wave direction was used in defining θ even when the direction differed from the wind direction as it did on 5/27 ($\approx 40-45^\circ$ misalignment reported by the ship). Also, ground tracks derived from the Loran A information were used on 6/2. Table C-1 presents the final values of θ .

TABLE C-1

VALUES OF THETA

Day	Pattern/ Leg	Ground Track	Dominant Wave Heading	True θ	Design θ
5/27/76	2/1	169.4	225	124.4	180
	2/2	283.7	225	238.7	300
	2/3	41.6	225	356.6	60
	2/4	134.1	225	89.1	150
	2/5	11.2	225	326.2	30
	5/1	161.5	220	116.5	180
	5/2	281.1	220	236.1	300
	5/3	50.6	220	10.6	60
	5/4	141.6	220	101.6	150
	5/5	20.5	220	340.5	30
6/2/76	2/1	0	40	140	180
	2/2	94	40	234	300
	2/3	240	40	20	60
	2/4	338	40	119	150
	2/5	192	40	336	30
	5/1	64	40	204	180
	5/2	210	40	313	300
	5/3	261	40	41	60
	5/4	13	40	153	150
	5/5	258	40	38	30
6/4/76	2/1	268.0	225	223.0	180
	2/2	39.3	225	354.3	300
	2/3	160.8	225	115.8	60
	2/4	242.7	225	197.7	150
	2/5	134.8	225	89.8	30
	5/1	232.0	225	184.0	180
	5/2	345.0	225	300.0	300
	5/3	128.2	225	83.2	60
	5/4	209.5	225	164.5	150
	5/5	93.2	225	48.2	30

APPENDIX D

EFFECT OF ERRONEOUS ESTIMATION OF AIRCRAFT MOTION ON $H_{1/3}$

In this appendix, the derivation of η in Figure VI-21 is given. The subscripts "m" and "T" stand for "measured" and "true" respectively. The symbol, σ^2 , is the variance and the subscript "L" implies "laser and "A/C" relates to the aircraft motion.

$$(H_{1/3})_T = 4 \left[\sigma_L^2 - (\sigma_{A/C}^2)_T \right]^{1/2}$$

$$(H_{1/3})_m = 4 \left[\sigma_L^2 - (\sigma_{A/C}^2)_m \right]^{1/2}$$

$$v = \frac{(H_{1/3})_m}{(H_{1/3})_T} = \left[\frac{\sigma_L^2 - (\sigma_{A/C}^2)_m}{\sigma_L^2 - (\sigma_{A/C}^2)_T} \right]^{1/2}$$

If $\eta = \sigma_L^2 / (\sigma_{A/C}^2)_m$, and $\epsilon = (\sigma_{A/C}^2)_m / (\sigma_{A/C}^2)_T$, then

$$v = \left\{ \frac{\epsilon(\eta-1)}{\epsilon\eta-1} \right\}^{1/2} .$$

Thus the ratio of measured to true SWH is a function of the relative size of the measured aircraft motion to the true aircraft motion and the ratio of the laser measurement to the measured aircraft motion. Figure VI-21 presents the family of curves for $\eta = \text{constant}$.

APPENDIX E

EFFECTS OF WAVE DIRECTIONALITY ON LINE-PROFILE DERIVED SPECTRA

We will simulate analytically the frequency spectrum that would be obtained by using surface elevation data taken by a profilometer moving in a straight line. Angular dispersion in the wavefield will affect our results. The wave number of any wave component will be aliased in the manner indicated in Figure E-1. Please note that the θ defined in Figure E-1 is not related to the θ defined in Figure II-2 of the main text and is used here in order to be consistent with most of the literature describing angular dispersion of ocean waves. To derive a unique quantitative result is not possible since no single form for the directional wave spectrum has been proven to be superior to other proposed expressions found in the literature. Therefore, we will select a model spectrum from the literature that yields qualitative answers to this question.

The directional wave spectrum is generally written as the product of a frequency-dependent angular spreading function, $H(\sigma, \theta)$, and a frequency dependent function.

$$\Phi(\sigma, \theta) = H(\sigma, \theta)\phi'(\sigma) \quad (1)$$

This form has been suggested by many investigators including Lonquet-Higgins (1962) and more recently Ou, et al. (1974), but insufficient data exists to really specify $H(\sigma, \theta)$. More often a simplified version, $h(\theta)$, is used. On

the assumption that wave energy should be distributed symmetrically about the wind vector, $h(\theta)$ is usually chosen to be a cosine function raised to some power or a summation of such terms. Indeed, Krylov, et al. (1966) has indicated $h(\theta) \propto \cos^2 \theta$. Therefore, we will use the following functions:

$$h(\theta) = B(n) \cos^{2n} \theta = \begin{cases} \pi^{-1} \text{ Isotropic} & n=0 \\ (2/\pi) \cos^2 \theta & n=1 \\ (8/3\pi) \cos^4 \theta & n=2 \end{cases} \quad (2)$$

where

$$B(n) = \left(\int_{-\pi/2}^{\pi/2} \cos^{2n} \theta \, d\theta \right)^{-1}.$$

$B(n)$ represents a normalization factor which ensures the conservation of energy.

The equations developed below are general in that θ' (see Figure E-1) may assume any value within the domain $[-\pi/2, \pi/2]$. The relationship between $\phi'(\sigma)$ and the frequency spectrum, $\phi(\sigma)$, is found by integrating $\Phi(\sigma, \theta)$ with respect to θ and $\phi'(\sigma) = \phi(\sigma)/\sigma$. A similar relationship holds in wave-number space, $S'(\mathbf{k}) = S(\mathbf{k})/\mathbf{k}$.

The Pierson-Moskowitz (P-M) spectrum will be used for $\phi(\sigma)$.

$$\phi(\sigma) = \frac{\alpha g^2}{2\sigma^5} \exp \left(-\beta \frac{g}{U \cdot \sigma} \right)^4 \quad (3)$$

where g is the gravitational acceleration, U is the surface wind speed at 19.5 meters and α and β are 4.05×10^{-3} and 0.74 respectively.

Since the aliasing problem deals with spatial rather than temporal frequencies, $\phi(\sigma)$ is transformed to $S(\mathbf{k})$ via

the dispersion relationship, $\sigma^2 = gk$.

$$S(k) = \frac{\alpha}{2k^3} \exp \left(-\beta \frac{g}{U^2 k} \right)^2 \quad (4)$$

The directional wave number spectrum may be written in a form analogous to (1) .

$$\Psi(k, \theta) = \frac{\alpha h(\theta)}{2k^4} \exp \left(-\beta \frac{g}{U^2 k} \right)^2 \quad (5)$$

From Figure E-1, the apparent wave number, k_a , is related to the true wave number by

$$k_a = k \cos \gamma, \quad (6)$$

and therefore,

$$S_a(k_a) = S(k) \sec \gamma. \quad (7)$$

Substituting (2), (6), and (7) into (5),

$$\begin{aligned} \Psi_a(k_a, \theta) &= h(\theta) \cdot S'_a(k_a) \\ &= \frac{A}{k_a^4} \cos^{2n}(\theta' + \gamma) \cos^3 \gamma \exp \left(-\frac{v \cos^2 \gamma}{k_a^2} \right), \end{aligned} \quad (8)$$

where $A = \alpha B(n)/2$ and $v = \beta g^2/U^4$. It should be noted that $\theta' + \gamma = \theta$ for all cases only when γ is defined as the angle measured from the flight track to the wave ray. To obtain the desired result, $S_a(k_a)$, (8) must be integrated over the coordinate plane from $\theta = -\pi/2$ to $\pi/2$. Because $\theta' = \text{constant}$ for a particular track, $d\theta = d\gamma$. Thus,

$$S_a(k_a, \theta') = \int_{-\pi/2}^{+\pi/2} \psi_a(k_a, \theta', \gamma) k_a d\gamma \quad (9)$$

and the apparent wave number spectrum retains an additional dependence on θ' . At this point, specific values of n must be substituted into (8) in order to determine (9). The results involve modified Bessel functions $I_j(\zeta)$ where $\zeta = \beta(g/U^2 k_a)^{1/2}/2$ and the integrals are given by Olver (1964) after having been simplified to the appropriate forms. It should be remembered that these functions are even when j is an even integer and odd when j is odd. The expressions for the apparent wave-number spectra are

$$\begin{aligned} & \frac{\alpha e^{-\zeta}}{4k_a^3} (I_0(\zeta) - I_1(\zeta)) & n=0 \\ S_a(k_a, \theta') = & \frac{\alpha e^{-\zeta}}{8k_a^3} \left[(2 + \cos 2\theta') \cdot I_0(\zeta) - 2(1+\cos 3\theta') \cdot I_1(\zeta) \right. \\ & \left. + \cos 2\theta' \cdot I_2(\zeta) \right] & n=1 \\ & \frac{\alpha e^{-\zeta}}{24k_a^3} \left[2(3 + 2 \cos 2\theta') I_0(\zeta) - (8 \cos 2\theta' \right. \\ & \left. + \cos 4\theta' + 6) \cdot I_1(\zeta) + 2(\cos 4\theta' + 2 \cos 2\theta') \right. \\ & \left. \cdot I_2(\zeta) - \cos 4\theta' \cdot I_3(\zeta) \right] & n=2. \end{aligned} \quad (10)$$

In order to present the results in a form that generally appears in the literature, we have transformed $S_a(k_a, \theta')$ back to the frequency domain and nondimensionalized those expressions in the same manner as Pierson and Moskowitz (1964). The transformation is given by

$$\phi_a(f_a, \theta') \frac{g^3}{U^5} = \frac{4\pi g^3}{U^5} \left(\frac{k_a}{g} \right)^{1/2} \cdot S_a(k_a, \theta') . \quad (11)$$

Figures E-2 thru E-6 show the apparent frequency spectra for various track angles relative to the dominate wave direction. The P-M spectra is plotted as a reference and the isotropic case is included because it is the limiting case as directionality decreases. Several trends can be seen: the spectral peak shifts to lower frequencies for larger values of θ' ; the peak broadens and decreases monotonically as θ' increases; the slope of the high frequency portion of the apparent spectrum does not dramatically deviate from that of the P-M spectrum until large values of θ' are reached; the difference between the $\cos^2\theta$ and $\cos^4\theta$ directionality models is not particularly strong until θ' exceeds 45 degrees. The spectral distortion is not severe for track angles within 15 degrees of the wind vector. These indicate that airborne profilometer data is still useful for wind-wave generation studies as long as close attention is given to the track angle relative to the dominate surface wave direction. Also, the proposition of using spectra from various track angles to infer $h(\theta)$ does not appear promising because the spectra do not show a substantial enough variation with $h(\theta)$.

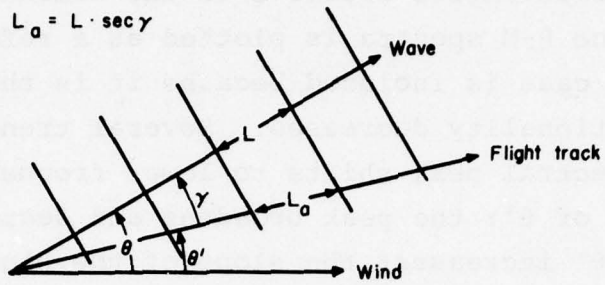


Fig. E-1 — Airborne profilometer measurement of wavelength

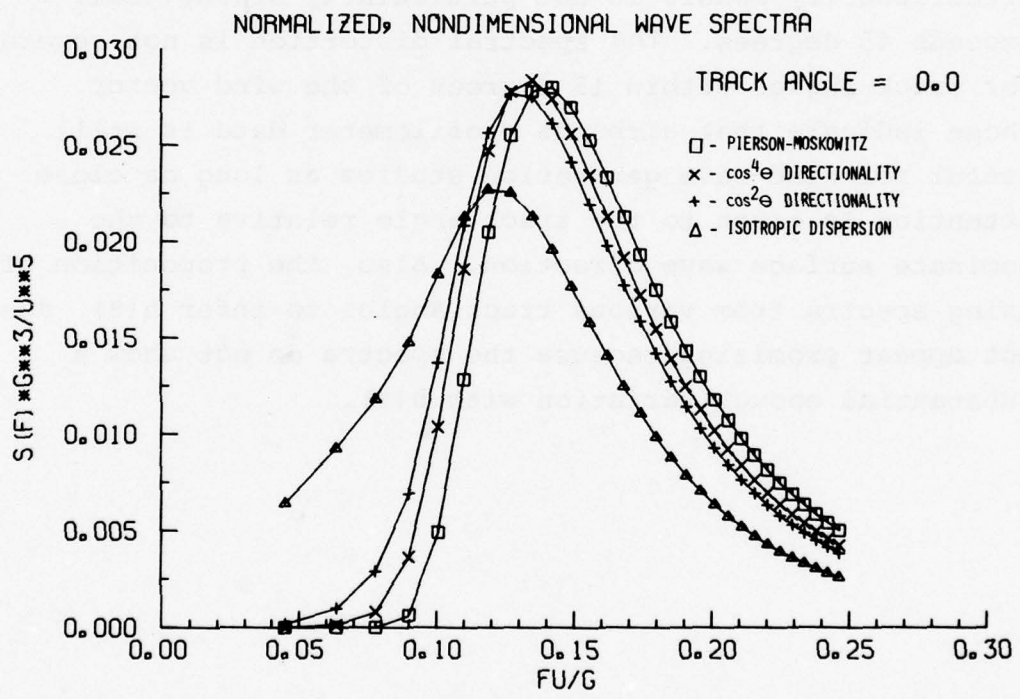


Fig. E-2 — Aliased spectrum for $\theta' = 0^\circ$

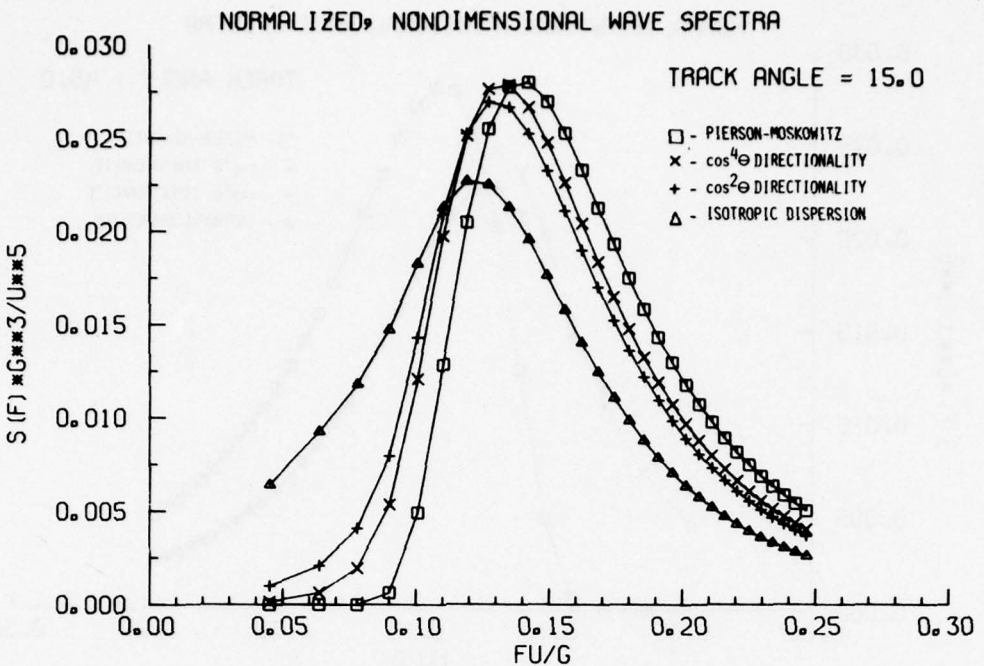


Fig. E-3 — Aliased spectrum for $\theta' = 15^\circ$

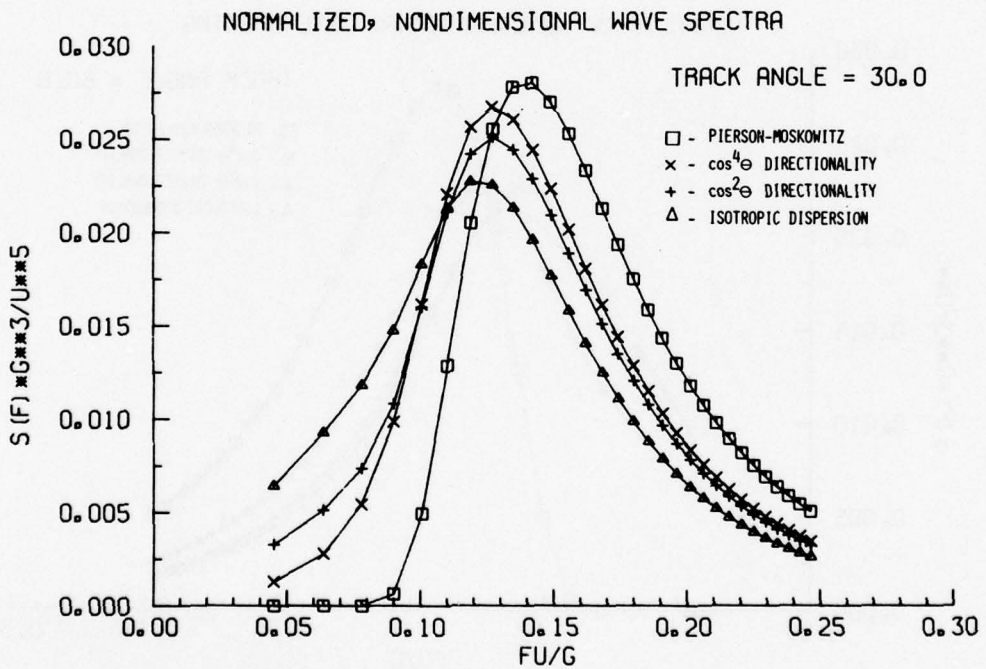


Fig. E-4 — Aliased spectrum for $\theta' = 30^\circ$

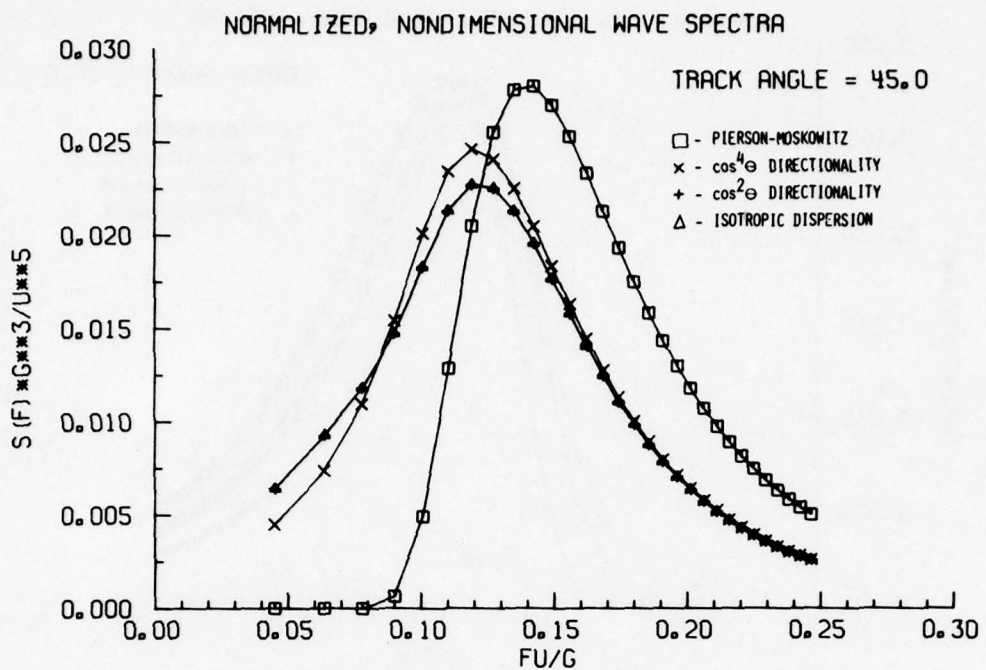


Fig. E-5 — Aliased spectrum for $\theta' = 45^\circ$

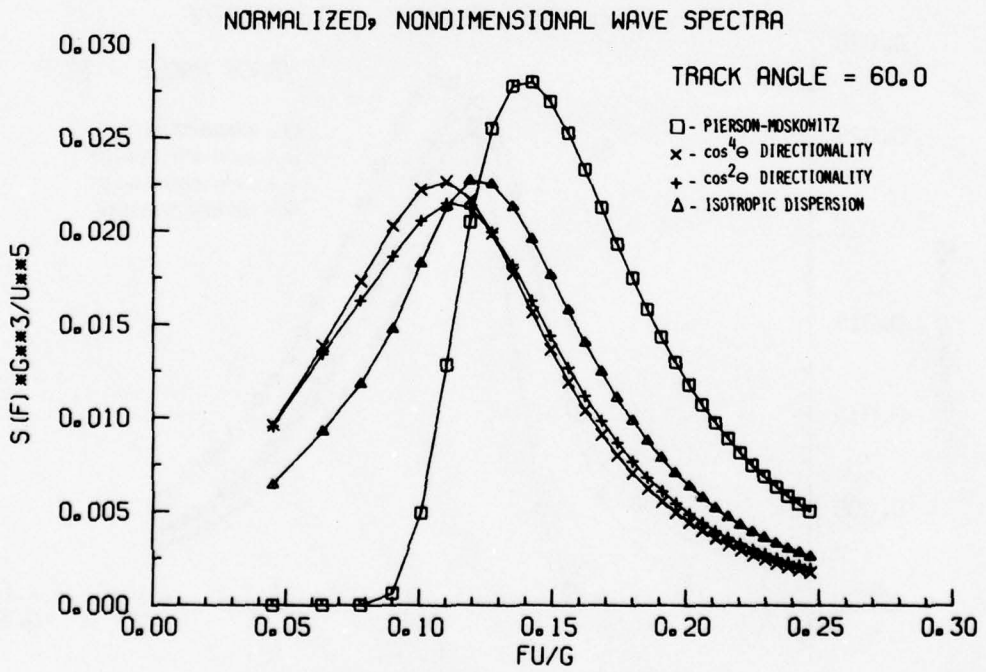


Fig. E-6 — Aliased spectrum for $\theta' = 60^\circ$

APPENDIX F

AIRSPEC 5

THIS PAGE IS BEST QUALITY PRACTICABLE
FROM COPY FURNISHED TO DDC

```

WS 00 PRINT, /110,MCC_AIN,S
WS 00 EQUIP,1***,HI,40
WS 00 EQUIP,5***,HY,R0
WS 00 EQUIP,10***,HI,RW
WS 00 *T*,X,L

PROGRAM AIRSPEC5
DIMENSION Y(4192),Z(8192),ASQ2NU(4097,2)
DIMENSION FORESF(5),FRFACTOR(5)
DIMENSION PLTARRAY(1024),IM(2),Q(8194)
DIMENSION FNUHT(4097,2)
DIMENSION FREQSPEC(4097,2), HBARF(2)
DIMENSION S(1025)
DIMENSION LPH1(10),IS1(2),IND(2),DFNC(301,2)
DIMENSION FILT(257),WEIGT(257),WFILT(5)
DIMENSION DEVN(301),LAbove(2),LBelow(2)
DIMENSION NGSPEC(15),EMAX(2),FBAR(2),SPECAVGN(2)
COMMON/A/Y,Z
COMMON/RDTAPEB/LFILE(7),KFILE,IFILE,MFILE
COMMON/UNDL/KR/RAD(160),CHAN(7),AINSS(8),INCODE(8),VFILE,
1NDAY,MONT4,NYR,NHR,MIN,ALT,DDOT,NHSCOPE,NVSCCPH,VSCALE,ISWEEP
COMMON/SF/NPEN,DELT,PLTSPACE
COMMON/3/DFNC
COMMON/B/J(5500,2),FNUH1F(4097,2)
EQUVALENCE (0,FNUHT),(FILT,WEIGT),(U,FNUHTF)
TYPE REAL KURTOSIS,LAbove,LBelow
TYPE INTEGER PRINT,PHAS,PLTON,THETA
DATA (IFILT = 8H LOW,BH HIGH,BH NU)
DATA((FRFACTOR(MP),MP = 1,5) = 1.,0.5,0.53,0.15,0,0.5)

C
C NOS = NUMBER OF SAMPLES
C IM(1) = NUMBER OF POINTS IN FAST FOURIER TRANSFORM
C IM(2) = POWER OF 2 FOR IM(1)
C IS1 = NUMBER OF DATA SAMPLES FROM WHICH ONE DATA POINT IS
C SELECTED FOR SPECTRAL ANALYSIS
C XMAXVL = MAXIMUM VALUE OF FREQUENCY FOR PLOTTING SPECTRA
C DELT = SAMPLE INTERVAL CALCULATED FROM THE SPEED OF THE TAPE
C RECORDED
C V = AIRCRAFT GROUND SPEED IN KNOTS. IF = 0, NO DOPPLER SHIFT. IT
C SHOULD BE NOTED THAT CONST CONTAINS A DIVISION BY V.
C W = WIND SPEED IN METERS/SEC
C IFILDATE=1, FILTERED DATA IS RECORDED ON OUTPUT TAPE
C CUT = CUT-OFF FREQUENCY/SAMPLING FREQUENCY
C H = FILTER SLOPE OF WEIGHTS
C NUMFT = NUMBER OF FILTER WEIGHTS. 2N+1=NUMBER OF PTS IN FILTER.
C LOWF = LOW PASS FILTER = 1, HIGH PASS FILTER = 2.
C NO PASS FILTER = 3
C NAVOL = SAME AS NOS
C LPH1 = TITLE OF THE RUN
C FREQSPEC=AVG SPECTRUM OF TOTAL NUMBER OF SPECTRA COMPUTED
C PLTONE = 0, SPECTRA ARE CALCULATED. LISTED IN OUTPUT AS PLOT.
C SWONLY=1,0, SWH IS THE ONLY QUANTITY DERIVED FROM FFT ESTIMATES
C WHDIST=0,0, PLOT WAVE HEIGHT DISTRIBUTION
C NOWAVPLT=1, NO HISTOGRAMS. LISTED IN OUTPUT AS WAVE PL.
C NUMHIST=1(LASER HISTOGRAM PLOTTED), =2(ACCELERATION PLOTTED ALSO)
C N1=1, PLOT FREQSPEC
C N2 = 1 INCORPORATES ANGULAR SPREADING INTO DOPPLER SHIFT
C NS=1, A/C DISPL SPECTRUM IS REMOVED FROM LASER SPECTRUM
C IPAUSE = 0 = NO MACHINE PAUSE, = ANY OTHER INTEGER = PAUSE, 6600
C PRINT = 10 PRINT = 0, NOT TO PRINT = 1

```

THIS PAGE IS BEST QUALITY PRACTICABLE
FROM COPY FURNISHED TO DDC

C PHAS = NOT TO REMOVE PHASE SHIFT = 0. TO REMOVE PHASE SHIFT = 1
C IFLOTSP= 0, SPECTRA (ASU2NU) ARE PLOTTED
C NRCSKP = NUMBER OF FILES TO SKIP ON OUTPUT TAPE FILES
C NPEN = CODED NUMBER FOR COLOR PENS OF THE PLCTTER
C NRREC = NUMBER OF RECORDS PER FILE ON INPUT TAPE
C LI = INPUT TAPE
C LO = OUTPTJT TAPE
C PLTSPACE=PARAMETER IN PLOT2, IT EQUALS INCHES PER DELT,
C MTRW = TO REWIND INPUT TAPE = 1, NOT TO REWIND INPUT TAPE = 0
C THETA = ANGLE IN DEGREE BETWEEN GROUND TRACK AND MEAN WIND
C DIRECTION
C QP = LASER RANGE SCALE
C DFLASER = CONVERSION COEFFICIENT FOR LASER CORRESPONDING TO QP .
C IT IS SET NEGATIVE TO INVERT THE LASER PROFILE,
C DF = CONVERSION COEFFICIENT FOR ACCELEROMETER
C NSPEC=CAVG = NUMBER OF SPECTRA TO BE AVERAGED TOGETHER PER FILE
C NSPEC = NUMBER OF SPECTRA IN SEQUENTIAL NUMBER WHICH ARE NOT TO
C BE AVERAGED
C TSPEC=CAVG=TOTAL NUMBER OF LASER SPECTRA DERIVED TO YIELD FREUSPEC.
C VSHIP = SHIP SPEED IN FEET/SEC
C NF = NUMBER OF FILES TO BE UNPACKED
C NLC = NUMBER OF THE LASER CHANNEL
C NAC = NUMBER OF THE ACCELERATION CHANNEL
C LFILE = PARAMETER DETERMINING WHICH FILES ARE UNPACKED
C KFILE = NUMBER OF FILE INPUT TAPE IS POSITIONED TO READ
C ISWEEP = NUMBER OF SWEEPS PER RECORD
C NFLAG = PARAMETER DETERMINING NO. DATA PTS./SWEEP TO BE UNPACKED
C NSETS=TOTAL NUMBER OF DATA SETS TO BE ANALYZED SEPARATELY,
C RSTART = 1.00 INDICATES THAT COMPUTATIONS ON A DATA SET
C (WHICH MAY BE COMPOSED OF SEVERAL FILES)ARE FINISHED AND
C THAT REINITIALIZATION OF PARAMETERS FOR NEXT DATA SET
C MUST BE DONE.
C
9001 FORMAT (3I5,F10.7,F9.0,2F10.5,4I5,F10.5)
9002 FORMAT (3I4B)
9003 FORMAT (15I5)
9004 FORMAT (//,2UX,*THE CONTROL CARDS FOR THE NEXT FILE ARE,,.,,1nX
*,*ON CONTROL CARD 1 -*,/,5X,*NUS*3X,*IM(1)*3X,*IM(2)*6X,*DELT*6X,
**V*5X,*CUT*8X,*H*4X,*NUMPT*3X,*LOWHI*6X,*NF*3X,*NAVGL*4X,*DF*/,.31
*8,F10.7,F9.2,2F10.5,4I8,F10.5,/,10X,*ON CONTROL CARD 2 * LABEL TN
* 80 COLUMNS//2X,10A8//10X*ON CONTROL CARD 3 -*//6X*N1*6X*N2*3X*PA
*USE*3X*PRINT*3X*PHASE*4X*PLOT NRCSKP WAVE PL*5X*PEN*2X*SP AVG*,1X
*,*IFLOTSP//11I8//1UX*ON CONTROL CARD 4 -*//3X*NUM REC*3X,
* 7HLU INPT,4X,*LU OUT*3X,12HPLUT2 PT INT,6X,4HMTHW,8X,2HUP,5X,
**1H-TA*, 3X,*DF LASER//, 1I0, 2I10,F15.8,I10,F10.0,I10,F10.
*3,/))
9006 FORMAT (* DATA FILE CONTAINED *15,* SAMPLES*)
9007 FORMAT (* *,5X,*MAX VALUE = *,F8,2,5X,*MIN VALUE = *,F8,2)
9008 FORMAT (1I4,59X,14HPOWER SPECTRUM//20X,12HTHIS RUN IS ,10A8,/,15X,
*16HNUMBER OF ODS =,10,50X,14HDATA FACTOR = ,F10.5,/,15X,16HNUMBER
* OF LAGS =16,50X,*CUT*9X,=* F9.4,/15X,*DELTA TIME*5X,=* F14.7,49X
**SLOPE*7X,=* F9.4,/15X*A/C VELOCITY*3X,=* F11.4,45X*WEIGHTS*5X,=*
* *14./15X*VARIANCE(1) *=F11.4,45X*H 1/3 (1) = *F9.4,/15X*VARI
*ANCE(2) *=F11.4,45X*STD DEV A/C = *F9.4,/49X,A8,* PASS FILTERED
/)
9009 FORMAT (* APPARENT VARIANCE APPARENT CIRC TRUE CIRC
* TRUE TRUE FREQ TRUE TRUE WAVE/*/* FREQ*19X,*FRE
*Q SPEC FREQ FREQ SPEC FREQ SPECTRUM WAVE
* NUMBER*/63X,*HZ*,20X,*NUMB SPECTRUM//)
9010 FORMAT(1H1,4X,*FREQ(HZ) VARIANCE FREQ SPEC CIRC FREQ CIRC

```

* FREQ SPEC //)
9011 FORMAT(4E12.4,E17.4)
9012 FORMAT(140.,//,5X,*1ST(*,I1,*)) = *,15,5X,*IND(*,I1,*) = *,15,/,5Y,
**CENTROID = *F10.4,/5X*STD DEV = *F10.4,/5X*SKEWNESS = *F10.4,/5X
**KURTOSIS = *F10.4)
9014 FORMAT(315, F10.8,15,F5.0,15,F6.0)
9015 F(RMAT(2513)
9016 FORMAT(*0*)
9018 FORMAT(*) SELECT EVERY *,I2,* SAMPLES//)
9019 FORMAT(* *,F7.2,2X,E12.4,2X,E12.4,2X,F6.2,2X,E12.4,2X,F0,3,2X,
1E14.4,2X,F6.3,2X,E14.4,4X,F10.4)
9020 FORMAT(F10.2,415,2F9.1,15)
9021 FORMAT(//,2X,*WIND SPEED*,3X,*NLC*,3X,*NAC*,3X,*NS*,3X,*NUMHIST*,
2 2X,*SWHOLY*,3X,*WHDIST*,3X,*IFILDAT*)
9022 FORMAT(F9.2,18,316,2F10.1,I10)
9023 FORMAT(10I8)
9024 FORMAT(//,3X,*KFILE*,2X,*LFILE1*,2X,*LF(LE2*,2X,*LF(LE3*,2X,
2*LF(LE4*,2X,*LFILE5*,2X,*LFILE6*,2X,*LFILE7*,2X,*ISWEEP*,3X,
3*NFLAG*)
9025 FORMAT(//,5X,*HBARF(1)=*,F7.3,5X,*HBARF(2)=*,F7.3,5X,*TSPCAVG=*,2F3.0,/)
9026 FORMAT(//,5X,*FILTERED DATA ON OUTPUT TAPE*)
9027 FORMAT(2X,*RESTART = *,F3.1)
9028 FORMAT(I5)
9029 FORMAT(1H1,2X,*NSETS = *,I3,5X,*NREPEAT = *,I3)
9030 FORMAT(//,5X,*APPARENT FREQU*,5X,*A/C SPEC*,5X,*TRUE FREQ*,5X,
2 *WAVE SPECT*)
9031 FORMAT(8X,F6.3,7X,E10.4,6X,F6.3,6X,E10.4)
1925 FORMAT(//,2X,*Y(IR) = *,15X,*Z(IH) = *)
1926 FORMAT(10K,F8.4,15X,F8.4)
1927 FORMAT(39X,*T1*,8X,*T2*,8X,*T3*,8X,*T4*,8X,*T5*)
1928 FORMAT(//,3X,*FREQUENCY RESPONSE FUNCTIONS = *,5F10.5,/)
1929 FORMAT(//,3X,*AVGY =*,F8.3,10X,*AVGZ =*,F8.3,/)
1930 FORMAT(//,3X,*SPECAVGN(1) =*,F5.2,5X,*SPECAVGN(2) =*,F5.2)
1933 FORMAT(3X,*YS=*,F10.6,5X,*ZS=*,F10.6)
1934 FORMAT(2X,*U(1,1) =*,F9.6)
1935 FORMAT(2X,*U(1,2) =*,F9.6)
1936 FORMAT(2X,*I =*,I4,5X,*U(I,1) =*,E10.3,5X,*U(I,2) =*,E10.3)
PAUSE 1
CALL PLOTS(PLTARRAY,1026,1)
CALL FACTDR(1.)
C ONLY ONE DATA CARD FOR NSETS IS NEEDED FOR EACH RUN.
READ 9028, NSETS
C IF ANY NEW TAPES ARE NEEDED WHEN NREPEAT CHANGES VALUE, SET
C IFAUSE = 1 IN PREVIOUS FILE'S DATA DECK.
DO 6900 NREPEAT = 1,NSETS
C
C INITIALIZE PARAMETERS
C
IM2FREV = 0
MPLGTF = 0
PI = 3.141592654
TWOPID = 6.283185308
G = 32.1725
GXPI = G*PI
TWOPIVG = 2.0/G
GUVTWO = 3/2.
VSHP = 0.
IABUVEF = 13FLWF = 0
SPECMAXF = TNUMSPEC = TSPCAVG = 0.

```

PSWAR-65

THIS PAGE IS BEST QUALITY PRACTICABLE
FROM COPY FURNISHED TO DDC

THIS PAGE IS BEST QUALITY PRACTICABLE
FROM COPY FURNISHED TO DDC

```
DO 50, N=1,2
  HHARF(N)=.
  DO 50, I=1,4097
    DO FREUSPEC(I,N)=0.
C
C      READ IN DATA
C
  100 READ 9001, NOS,IM(1),IM(2),DELT,V,CUT,H,NLMPT,LWHI,NF,NAVGL,UF
    IF (EOF,60) 9999,240
  200 II = 0
    READ 9002, LPH1
    READ 9003, N1,N2,IPAUSE,PRINT,PHAS,PLTON,NRECSKP,NOWAVPLT,NPEN
    * ,NSPECAV3,IPLOTSP
    READ 9014, NREC, LI,LO,PLTSPACE,MTREW,UP,THETA,DFLASER
    READ 9020, W,NLC,NAC,N3,NUMHIST,SWHONLY,WHDIST,IFILDAT
    READ 9023, KFILE,(LFILE(I),I=1,7),ISHEEP,NFLAG
    READ 9015, NGSPEC
    READ 9020, RESTART
    DFLASER=DFLASER
    II=NTO=NDS
    XMAXVL = 1.6266
    REXTS = 0,
    RAVG = 0.0
C
C      PRINT OUT CONTROL CARUS
C
  215 PRINT 9029, NSETS,NMEHEAT
  PRINT 9004, NOS,IM(1),IM(2),DELT,V,CUT,H,NLMPT,LWHI,NF,NAVGL,
  * ,UF,LPH1,N1,N2,IPAUSE,PRINT,PHAS,PLTON,NRECSKF,NOWAVPLT,NPEN,NSPECA
  * ,VG,IPLOTS>,NREC, LI,LO,PLTSPACE,MTREW,UP,THETA,DFLASER
  PRINT 9021
  PRINT 9022, W,NLC,NAC,N3,NUMHIST,SWHONLY,WHDIST,IFILDAT
  PRINT 9024
  PRINT 9023, KFILE,(LFILE(I),I=1,7),ISHEEP,NFLAG
  PRINT 9015, NGSPEC
  PRINT 9027, RESTART
  IF (IM(2) .NE. IM2PREV) 220,260
  220 IFS = -1
  IM2PREV = IM(2)
  260 IF (NPEN .EQ. 0) 270,275
  270 NPEN = 1
C
C      DOWNWIND TRACKS REQUIRE NEGATIVE (-) AIRCRAFT VELOCITIES
C      CONVERT AIRCRAFT VELOCITY FROM KNOTS TO FEET/SEC.
C      IF OMEGA = THETA, DOWNSIDE SHIFT SPECTRA AS IF WAVES MOVED PARALLEL
C      TO WIND.  IF OMEGA = U OR 180, IT IS ASSUMED THAT WAVES MOVED
C      PARALLEL TO FLIGHT TRACK.
  275 OMEGA = THETA
    IF (THETA.GT.90.AND,THETA.LT,270) 276,277
  276 OMEGA = 180.
    GU TO 278
  277 OMEGA = 0.
  278 V = V*1.69/8*COSF(P1+OMEGA/180.)
    IF (THETA.EQ.90.OR,THETA.EQ.270) 280,290
  280 V=0.
C
C      SKIP NRECSKP FILES ON OUTPUT TAPE OR ON INPUT TAPE IF LI = LO.
  290 DO 350 I = 1,NRECSKP
    CALL SKIPFILE (LO)
  350 CONTINUE
```

```

IF(VSHIP.EQ.0.) 523,520
C
C   CALCULATION WHICH ALLOWS SHIPBOARD RADAR AND AIRBORNE PROFILOMETER
C   TO ANALYZE DATA OVER TRACKS OF SIMILAR LENGTHS. IT DETERMINES
C   THE PROPER SAMPLE INTERVAL AND EVERY 1SEC-TH POINT WILL BE USED.
C
C   520 TOSHTR = 1024.*VSHIP*0.125
C     VABS = ABSF(V)
C     TIREF = TOSHTR/VABS
C     RIM1 = IM(1)
C     TIREDA = TIREF/RIM1
C     RISEC = TIREDA/DELT + 0.99
C     IF (RISEC .LT. 1.) 521,522
C
C   521 RIS=C = 1.
C   522 ISEC = RIS=C
C     DELT = ISEC*DELT
C     GO TO 524
C
C   IF A DESIRED SAMPLE INTERVAL IS LARGER THAN THAT OF THE ORIGINAL
C   DATA SET OR THAN THAT DETERMINED ABOVE, DEFINE THE DESIRED DELT
C   IN THE INPUT DECK AND THE BELOW EQUATION WILL PROPERLY DEFINE
C   ISEC PROVIDED THE DENOMINATOR IS CORRECT.
C   523 ISEC = DELT/0.0111333
C   524 PRINT 9013. ISEC
C     PSEC = ISEC
C     PLTSPACE = PSEC*PLTSPACE
C     DX = ABSF(V*DELT)
C     NUMPTP1 = NUMPT + 1
C
C   TEST IF FILTER IS TO BE COMPUTED. IF(NUMPT.GT. 0) = YES
C
C   525 IF(NUMPT.EQ.0) 1800,550
C
C   COMPUTE FILTER
C   NUMPT = NUMBER OF POINTS OVER WHICH THE AVERAGE IS TO BE TAKEN
C   CUT = CUT-OFF FREQUENCY/SAMPLING FREQUENCY
C   H = SLOPE OF WEIGHTS
C
C   550 KA = NUMPT + 1
C     CTH = CUT + H
C     FILT(KA) = 2.*CTH
C     SUMK = 0.
C     DO 700 I = 1,NUMPT
C       P = I
C       QO = 1. - (16.*H*H*H*P)
C       IF(QO .NE. 0.) 600,575
C       575 FILT(I) = 0.
C       GO TO 700
C   600 FILT(I) = (COSF(TWOMI*P*H)*SINF(TWOMI*P*CTH))/(PI*2.*QO)
C     SUMK = SUMK + FILT(I)
C   700 CONTINUE
C     FLJO = (1. - (FILT(KA) + 2.*SUMK))/(2.*NUMPT + 1.)
C     DO 800 I = 1,KA
C       WEIGHT(I) = FILT(I) + FLJO
C   800 CONTINUE
C     IF(LOWHI.EQ.2) 825,850
C   825 WEIGHT(KA) = 1. - WEIGHT(KA)
C     DO 840 I=1,NUMPT
C   840 WEIGHT(I) = -WEIGHT(I)
C
C   CALCULATE AND PRINT FREQUENCY RESPONSE FUNCTIONS OF THE FILTER
C   850 DO 900 M=1,5
C     BP2=FRFACTOR(MP)

```

THIS PAGE IS BEST QUALITY PRACTICABLE
FROM COPY FURNISHED TO DDC

THIS PAGE IS BEST QUALITY PRACTICABLE
FROM COPY FURNISHED TO DDC

```
FR=1./(IM(1)*BP2)
FOR I SF(MP)=WEIGT(KA)
DO 900 1<J=1,NUMPT
900 FOR I SF(MP)=FORRESF(MP) + 2.*WEIGT(IKJ)*CUSF(TKUPI*I(J*FR)
PRINT 1927
PRINT 1923,(FORRESF(MP), MP=1,5)
1800 CONTINUE
C
C      READ IN DATA
C
C      IF(LI,EQ,LO) 1810,1840
C      IF READING IN MORE THAN ONE FILE PER RUN, NO NEED TO REWIND LI,
C      MERELY ADJUST NHECSNP ACCORDINGLY IN DATA DECK OF FOLLOWING FILE.
1810 BUFFER IN(LI,1)(Y(1),Z(8192))
1815 IF(UNIT,LI) 1815,1820,1820,1820
1820 CALL SKIPFILE(LI)
GO TO 2190
C
C      UNPACK AND ASSIGN VALUES TO Y AND Z
C
C      FOR UNPACKING FILES IN SEQUENCE OFF A TAPE, DO NOT REWIND LI,
C      MERELY SET KFILE=1+NUMBER OF LAST FILE UNPACKED IN DATA DECK OF
C      NEXT FILE, BUT, IF LI IS REWOUND, KFILE MUST = 1 INSTEAD,
1840 I1 = 0
NP=1
DO 2155 FILE = 1,NF
DO 1870 JZ=NP,7
IF(LFILE(JZ),EQ,0) 1870,1860
1860 FILE=JZ
NP=JZ+1
GO TO 1880
1880 CONTINUE
1880 CALL RDTAPE
DO 2150 IREC= 1,NREC
DO 2150 ISWP = 1,ISWEEP
CALL UNPC((ISWP,IREC,NFLAG)
I1 = I1 + 1
Y(I1) = CHAN(NLC)*UFLASER
Z(I1) = CHAN(NAC)*DF
2150 CONTINUE
CALL SKIPFILE(LI)
2155 CONTINUE
C      OPTION TO PHASE SHIFT DATA
IF(PHAS,EQ,0) 2165,2160
2160 CALL PHASE(NTOT,OP)
C      OPTION TO RECORD DATA BEFORE OR AFTER FILTER
2165 IF(IFILDAT,EQ,1.AND,NUMPT,NE,0) 2190,2170
2170 BUFFER OUT (LO,1) (Y(1),Z(8192))
2175 IF(UNIT,LO) 2175,2180
2180 ENDFILE LO
IF(IFILDAT,EQ,1.AND,NUMPT,NE,0) 2185,2190
2185 PRINT 9025
GO TO 3440
2190 IF(MREW,GT,0) 2195,2200
2195 REWIND LI
2200 NTOT = NDS = I1
C
C      PRINT FIRST VALUE OF EACH RECORD OF Y AND Z.
C
PRINT 1925
```

```

DU 2205, IZ = 1,NREC
IR = (IZ + 1)*TSWEEP + 1
2205 PRINT 1925, Y(IR),Z(IR)
C
C      CALCULATE YMAX,YMIN,ZMAX, AND ZMIN.
C
2212 YMAX = ZMAX = -100,
YMIN = ZMIN = 100,
PRINT 9005, NTOT
DO 2300 I = 1,NTOT
IF(Y(I) .GT. YMAX) 2220,2230
2220 YMAX = Y(I)
GO TO 2250
2230 IF(Y(I) .LT. YMIN) 2240,2250
2240 YMIN = Y(I)
2250 IF(Z(I) .GT. ZMAX) 2260,2270
2260 ZMAX = Z(I)
GO TO 2300
2270 IF(Z(I) .LT. ZMIN) 2280,2300
2280 ZMIN = Z(I)
2300 CONTINUE
PRINT 9007, YMAX,YMIN
PRINT 9007, ZMAX,ZMIN
PRINT 9015
IF(NEXTS.EQ.0.) 2370,3400
2370 IF((ISEC.GT.1) 2380,3440
C
C      SELECT LASER AND ACCELEROMETER DATA
C
2380 I1=1
DO 2630 I = 1 ,NTOT ,ISEC
Y(I1) = Y(I)
Z(I1) = Z(I)
2600 I1 = I1 + 1
JISEC = I1 + 1
IF((ISEC.EQ.1) 2660,2610
2610 DO 2650 I = JISEC,NTOT
Y(I) = 0.
2650 Z(I) = 0.
2660 N101=N0S=I1
C      FIND AVERAGE VALUES BEFORE FILTERING
GO TO 3440
C
C      APPLY FILTER TO DATA (0 = NO)
C
2700 RAVG = 1.0
2800 N101 = NTOT - 2*NUMPT
MIN = 1
DO 3200 I = MIN,NTOT
KB = I + NUMPT
SUMCK = WEIGHT(KA)*Y(KB)
SUMDK = WEIGHT(KA)*Z(KB)
DO 2900 J = 1,NUMPT
IA = NUMPT + 1 - J
IB = IA + NUMPT + I
IC = J - 1 + I
SUMCK = SUMCK + WEIGHT(IA)*(Y(IC) + Y(IB))
SUMDK = SUMDK + WEIGHT(IA)*(Z(IC) + Z(IB))
2900 CONTINUE
3100 Y(I) = SUMCK

```

THIS PAGE IS BEST QUALITY PRACTICABLE
FROM COPY FURNISHED TO DDC

THIS PAGE IS BEST QUALITY PRACTICABLE
FROM COPY FURNISHED TO DDC

```
Z(I) = SUMPK
3200 CONTINUE
C      SET RESIDUAL DATA PTS TO 0.
N10(P1=NTOT + 1
DO 3250 I=NTOTP1,NOS
3250 Z(I)=Y(I)=0.
C      RECOMPUTE EXTREMES OF Y AND Z AFTER FILTERING
REXIS = 1,
GO TO 2212
3400 IF (IFILDAT.EQ.1) 2170,3440
C      FIND AVERAGE VALUE OF INPUT
C
3440 AVGY = AV37 = 0,
IF (NAVGL .GT. NTOT) 3450,3475
3450 NAVRL = NTOT
3475 DO 3500 I = 1,NAVGL
AVGY = AV3Y + Y(I)
AVGZ = AV3Z + Z(I)
3500 CONTINUE
AVGY = AV3Y/NAVGL
AVGZ = AV3Z/NAVGL
PRINT 1929, AVGY, AVGZ
IF (4AVG.GT.0.0) 3550,3575
3550 IF (NUMPT.EQ.0.0) 3575,2700
3575 DO 3600 I = 1,NTOT
Z(I) = Z(I) - AVGZ
3600 Y(I) = Y(I) - AVGY
YMAX=LABOVE(1)=YMAX - AVGY
YMIN=LBELOW(1)=YMIN - AVGY
ZMAX=LABOVE(2)=ZMAX - AVGZ
ZMIN=LBELOW(2)=ZMIN - AVGZ
NSPECTRA = NTOT/IM(1)
C
C      IF (PLTON .GT. 0) DO NOT COMPUTE SPECTRA
C
IF (PLTON .GT. 0) 3625,3650
3625 J10I=NTOT
NST=IST=NT=NTIMES=1
NSP=CAVG = 1
GO TO 4325
3650 I1 = 1
I2 = IM(1)
I4 = I2/2 + 1
I6 = I4 - 1
FREGRES = 1./(2.*DELT*IM(1))
FACTD = DE_T*IM(1)/TWOP1
NTIMES=NSPECTRA/NSPECAGV
C      FOR THE GULF STREAM EXPERIMENT, SET NTIMES = 1.
NTIMES = 1
IF (NTIMES .LT. 1) 3660,3675
3660 NTIMES = 1
C      IF NTIMES<1 IS CORRESPONDUS TO DATA WHICH SHOULD NOT BE ANALYZED AND
C      IF N1=1, SET NTIMES = 1.
3675 DO 3650 NT = 1,NTIMES
DO 4150 N = 1,2
SPECTAVG = 0.
IADE = 0
NTOT = 0
DO 3700, I=1,5500
```

```

      U(I,N) = 0.
      NSTHIST = (NT-1)*NSPECAVG*IM(1) + 1
      J1OT = NSTHIST
      NSTH = 0
      DO 4100 I = 1,NSPECAVG
C      TEST FOR GOOD DATA. NSTHIST=START OF DESIRABLE DATA AND LOCATION
C      WHERE HISTOGRAM BEGINS. FOLLOWING DO LOOP ALLOWS US TO KICK OUT
C      SEGMENTS OF LENGTH = IM(1) FROM THE ANALYSIS.
      DO 3730 J = 1,15
      IF((NT-1)*NSPECAVG + I,EQ.NGSPEC(J)) 3705,3730
      3705 NSTH =NSTH + 1
      IF(NSTH,EQ.1) 3710,3715
      3710 NSTHIST = I*IM(1) + NSTHIST
      3715 GO TO 4100
      3730 CONTINUE
      N1OT = NTOT + IM(1)
      L = 1
      IA = ((N1-1)*NSPECAVG + I - 1)*IM(1) + 1
      IB = ((NT-1)*NSPECAVG + I)*IM(1)
      IF((IB-IA).EQ.NAVGL) 3758,3751
C      FIND AVERAGE OF THE DATA SEGMENT (IA,IB)
      3751 YS = ZS = 0.
      IF(N,EQ.1) 3752,3754
      3752 DO 3753 JV=IA,IB
      3753 YS=YS + Y(JN + IADD)
      YS = YS/12
      GO TO 3755
      3754 DO 3755 JV=IA,IB
      3755 ZS=ZS + Z(JN + IADD)
      ZS = ZS/12
      3756 PRINT 1933, YS,ZS
      3758 DO 3800 J = IA,IB
      IF ( N .EQ. 1 ) 3760,3770
      3760 Q(L) = Y(J+IADD) - YS
      GO TO 3800
      3770 Q(L) = Z(J+IADD) - ZS
      3800 L = L + 1
      CALL FOURIER (Q,S,IM(2),IFS)
      3810 RQS = 2
C      CALCULATE POWER SPECTRA
      3895 DO 3900 J = 1,I4
      3900 Q(J) = Q(2+J-1)**2 + Q(2+J)**2
      DO 4000 J=1,I4
      4000 U(J,N)=U(J,N) + Q(J)
      SPECTAVG = SPECTAVG + 2.0
      IF(N,EQ.1) 4060,4070
      4060 PRINT 1934, Q(1)
      GO TO 4100
      4070 PRINT 1935, Q(1)
      4100 CONTINUE
      SPECAVGN(V) = SPECTAVG
      4150 CONTINUE
      TSPECAVG = TSPECAVG + SPECAVGN(1)/2.
C
C      TEST FOR END OF GOOD DATA SO AS TO AVOID PLOTTING UNDESIRABLE DATA
C      AT THE END OF DATA RECORD BEING ANALYZED IN ABOVE LOOPS.
C
      NFIN = NT*NSPECAVG
      JSTOP = 0
      IF(NGSPEC(NFIN),EQ.0) 4154,4151

```

THIS PAGE IS BEST QUALITY PRACTICABLE
FROM COPY FURNISHED TO DDG

```
4151 NSTA = (NT-1)*NSPEC AVG + 1
JSTOP = 1
DO 4153 IMP = NSTA,NFIN
JJP = NFIN - IMP + NSTA
JJPM1 = JJP - 1
IF(NGSPEC(JJP).EQ.NGSPEC(JJPM1) + 1) 4152,4154
4152 JSTOP = JSTOP + 1
4153 CONTINUE
4154 JT0T= JT0T - NSTHIST + (NSPEC AVG-JSTOP)*IM(1)
PRINT 1930, SPECAVGN(1),SPECAVGN(2)
IF(SPECTAVG.EQ.0.) 6400,4155
C
C      APPLY HAMMING TO THE TOTAL VARIANCE
C
4155 DO 4170 N=1,2
U(1,N)= 0.54*U(1,N) + 0.46*U(2,N)
DO 4160 I=2,16
4160 U(I,N)= 0.23*(U(I-1,N) + U(I+1,N)) + 0.54*U(I,N)
4170 U(I4,N)= 0.54*U(I4,N) + 0.46*U(16,N)
C
C      DO LOOP TO TRANSFORM ACCELERATION TO DISPLACEMENT SPECTRUM
C      TRANSFORMATION SHOULD ONLY BE INITIATED FOR ACCELERATION DATA
C
4171 U(1,1)=U(1,2)=0.
DO 4175 LW=2,14
R=2*(LW-1)
FTRU=R*FREORES
FIRU4 = (FTRU*TWOPI)**4
4175 U(LW,2)=U(LW,2)/FIRU4
C
C      AVERAGE THE VARIANCES AND CALCULATE SIGNIFICANT WAVE HEIGHT
C
EMAX(1) = FMAX(2) = 0.
4180 DU 4200  I = 1,14
U(I,2) = J(I,2)/SPECAVGN(2)
U(I,1) = J(I,1)/SPECAVGN(1)
C      N3=1, SUBTRACT A/C MOTION SPECTRUM FROM LASER SPECTRUM,
IF(N3.EQ.1) 4182,4190
C      TEST VALUES OF THE VARIANCES--DU NOT ALLOW NEGATIVE VALUES OF U(1)
4182 IF(U(I,1).LT.U(I,2)) 4184,4185
4184 PRINT 1935, I,U(I,1),U(I,2)
U(I,1)=0.0
GO TO 4190
4185 U(I,1) = J(I,1) - U(I,2)
4190 EMAX(1) = EMAX(1) + U(I,1)
EMAX(2) = EMAX(2) + U(I,2)
4200 CONTINUE
4203 HHAR(1) = 4.0*SQRTF(EMAX(1))
HHAR(2) = SQRTF(EMAX(2))
C
C      WRITE HEADINGS
4210 PRINT 9003, LPH1,NTUT,DFLASER,IM(1),CUT,DELT,H,V,NJMPT,EMAX(1),
* HHAR(1),EMAX(2),HHAR(2),IF1LT(LOWHI)
4215 HHARF(1)=HHARF(1) + HHAR(1)
HHARF(2) = HHARF(2) + HHAR(2)
TNUMSPEC = TNUMSPEC + 1.0
IF(N1.EQ.1.AND.NT.EQ.NTIMES) 4216,4217
4216 HHARF(1)=HHARF(1)/TNUMSPEC
HHARF(2)=HHARF(2)/TNUMSPEC
4217 IF(SWHONLY.EQ.1.0) 4325,4219
```

```

C
C DO LOOP FOR CALCULATION OF POWER SPECTRA AND RELATED QUANTITIES
C A DOPPLER SHIFT ALGORITHM IS INCLUDED TO REMOVE THE FREQUENCY SHIFT
C DUE TO THE HORIZONTAL AIRCRAFT MOTION. IF N2 EQUALS 1, AN ADDITIONAL
C CORRECTION IS APPLIED TO ACCOUNT FOR ANGULAR SPREADING AS PREDICTED BY PHILLIPS' RESONANCE THEORY AND IS APPLICABLE FOR FLIGHTS
C THAT PARALLEL THE WIND DIRECTION.
C
4219 DO 4300 N = 1,2
   IF (N.EQ.2) 4280,4220
4220 PRINT 9009
4221 MSAT = 1
C WANT TO PRINT EVERY NZ-TH PI PLUS FIRST 50 PT.
NZ = 14/64
ANZ = NZ
DO 4265 I = 1,14
R = 2*(I-1)
FTRU = R*FRDRES
IF (V.EQ.0.) 4222,4223
4222 FMUHT=2.*PI.*FTRU
GO TO 4223
4223 CONST = G/(2.*V)
CUNSQ = CONST*CONST
FMUHT = SQRT(CUNSQ + GXPI*K/(IM(1)*DX)) - CCNST
4224 IF (I.EQ.1, AND. CONST. GT. 0.) 4225,4226
4225 FMUHT = 0,
4226 ASQ1 = U(I,N)*DELT*IM(1)
IF (V.EQ.0.) 4228,4230
4228 ASQMU1 = ASQ1/TWOP1
GO TO 4231
4230 ASQMU1 = ASQ1*(TWODVG*(FMUHT + CONST)*ASQ1*V)/TWOP1
4231 ASQKT1 = 0.
IF (N2.EQ.1) 4232,4242
C STATEMENTS 4232 TO 4242 PERFORM THE RESONANCE THEORY DOPPLER SHIFT
4232 IF (FMUHT.EQ.0.) 4234,4236
4234 FKT = ASQMU1 = ASQ2NU(I,N) = FNUHT(I,N) = 0.
GO TO 4245
4236 FMUHT = W*FMUHT**2/G
4240 ASQMU1 = ASQMU1*SQRT(G/(FMUHT*W))/2.
4242 FNUHT(I,N) = FMUHT/TWOP1
FKT = (FMJHT**2)/G
ASQ2NU(I,V) = TWOP1*ASQMU1
FREUSPEC(I,N) = FREUSPEC(I,N) + ASQ2NU(I,N)
IF (FMUHT.VE.0.) 4244,4246
4244 ASQKT1 = ASQMU1*GDVTW0/FMUHT
4246 IF (PRINT.EQ.0.) 4247,4265
4247 IF (I4.GT.128) 4248,4249
4248 PRNUM1 = I
PRNUM2 = PRNUM1/ANZ
IPR1 = PRNUM2
PRNUM3 = IPR1
PRNUM4 = PRNUM2 - PRNUM3
IF (I.LE.50.OR.PRNUM4.EQ.0.) 4249,4265
4249 IF (I.LE.NJMPT+1) 4250,4255
4250 PRINT 9019,FTRU,U(I,N),ASQ1,FMUHT,ASQMU1,FNUHT(I,N),ASQ2NU(I,N),
*FKT,ASQKT1,WEIGT(I)
GO TO 4265
4255 PRINT 9019,FTRU,U(I,N),ASQ1,FMUHT,ASQMU1,FNUHT(I,N),ASQ2NU(I,N),
*FKT,ASQKT1
4265 CONTINUE

```

THIS PAGE IS BEST QUALITY PRACTICABLE
FROM COPY FURNISHED TO DDC

THIS PAGE IS BEST QUALITY PRACTICABLE
FROM COPY FURNISHED TO DDC

```
GO TO 4300
4280 PRINT 9011
DO 4290 I = 1,14
R = 2*(I-1)
FTRU = R*FREORES
FNUHT(I,N) = FTRU
FMUHT = FTRU*TWOPI
ASQ2 = U(I,N)*DELT*IM(1)
ASQ2NU2 = ASQ2
ASQMU2 = ASQ2/TWOPI
IF(PRINT.EQ.0.) 4285,4289
4285 IF(I4.GT.128) 4286,4288
4286 PRNUM1 = I
PRNUM2 = PRNUM1/ANZ
IPR1 = PRNUM2
PRNUM3 = IPR1
PRNUM4 = PRNUM2 - PRNUM3
IF(I.LE.5).OR.PRNUM4.EQ.0.) 4288,4289
4288 PRIAT 9011, FTRU,U(I,N),ASQ2,FMUHT,ASQMU2
4289 ASQ2NU(I,V) = ASQ2NU2
FREOSPEC(I,N) = FREUSPEC(I,N) + ASQ2NU(I,N)
4290 CONTINUE
4300 CONTINUE
C
C      CALCULATE WAVE HEIGHT DISTRIBUTION FUNCTION
C      IF SPECTRA (IPLOTP SP NE 0) ARE NOT PLOTTED, THEN PLOT FOR
C      THE WAVE HEIGHT DISTRIBUTION MAY BE POSITIONED WRONG, ALSO,
C      THERE IS NO EQUIVALENT TO FREUSPEC FOR THIS PARAMETER.
C
4325 DO 6000 N = 1,2
IADD = 0
4345 DO 4400 M = 1,301
4400 DFNC(M,N) = 0.
DO 4500 M = 1,NSPECAVG
MA = ((NT-1)*NSPECAVG + M - 1)*IM(1) + 1
MB = ((NT+1)*NSPECAVG + M)*IM(1)
DO 4415 MM = 1.25
IF((NT-1)*NSPECAVG + M .EQ. NGSPEC(MM)) 4500,4415
4415 CONTINUE
DO 4500 MM = MA,MB
IF(N .EQ. 1) 4416,4417
4416 INDEX = Y(MM+IADD)*4.0 + 151.5
GO TO 4419
4417 INDEX = Z(MM+IADD)*4.0 + 151.5
4418 IF(INDEX ,LT. 1) 4425,4450
4425 INDEX = 1
GO TO 4485
4450 IF(INDEX ,GT. 301) 4475,4485
4475 INDEX = 301
4485 DFNC(INDEX,N) = DFNC(INDEX,N) + 1
4500 CONTINUE
DO 4600 M = 5,301
IF(DFNC(M,N) .GT. 0.) 4700,4600
4600 CONTINUE
4700 IST(N) = 4-XMODF(M,4) + 1
IF(IST(N) .LT. 1) 4725,4750
4725 IST(N) = 1
4750 DO 4800 MM = 4,302
M = 301 - MM
IF(DFNC(M,N) .GT. 0) 4900,4800
```

```

4800 CONTINUE
4900 IND(N) = 4 + 1-XMOUF(M,4)
IF(IND(N) .GT. 301) 4925,4950
4925 IND(N) = 301
4950 CENTROID = STANDDEV = SKEWNESS = KURTOSIS = 0.
DEV = (IST(N) - 151)/4,
I = IST(N)
J = IND(N)
FNTOT = NTOT
DO 5000 M = I,J
CENTROID=CENTROID+DFNC(M,N)*DEV
STANDDEV = STANDDEV + DFNC(M,N)*DEV**2
SKEWNESS = SKEWNESS + DFNC(M,N)*DEV**3
KURTOSIS = KURTOSIS + DFNC(M,N)*DEV**4
5000 DEV = DEV + 0.25
CENTROID = CENTROID/FNTOT
STANDDEV = STANDDEV/FNTOT
SKEWNESS = SKEWNESS/FNTOT
KURTOSIS = KURTOSIS/FNTOT
KURTOSIS = KURTOSIS - 4.*CENTROID*SKEWNESS + 6.*CEVTROID*CENTROID*
* STANDDEV - 3.*CENTROID**4
SKEWNESS = SKEWNESS - 3.*CENTROID*STANDDEV + 2.*CEVTROID**3
VARIANCE = STANDDEV - CENTROID*CENTROID
STANDDEV = SORTF(VARIANCE)
SKEWNESS = SKEWNESS/(STANDDEV*VARIANCE)
KURTOSIS = KURTOSIS/(VARIANCE*VARIANCE)
PRINT 9012, N,I,N,J,CENTROID,STANDDEV,SKEWNESS,KURTOSIS
6000 CONTINUE
MIN = XM1VOF(IST(1),IST(2))
MAX = XMAXOF(IND(1),IND(2))
IBELOW = (154 - MIN)/4
IABOVE = (MAX - 148)/4
IBELOW = IBELOW - 4*MOD(IBELOW,2)
IABOVE = IABOVE + 4*MOD(IABOVE,2)
MIN = 151 - 4*IBELOW
MAX = 151 + 4*IABOVE
IF(MIN .LE. 3 .AND. MAX .GE. 299) 6025,6030
6025 IBELOW = IABOVE = 50
6030 IF(HBAR(1).LT.0.) 6070,6050
6050 IF(IBELOW.LT.IBELOW) 6055,6060
6055 IBELOWF = IBELOW
6060 IF(IABOVE.LT.IABOVE) 6065,6070
6065 IABOVEF = IABOVE
C
C PLOT DESIRED RESULTS.
C
6070 IF(NOWAVP_.T.EQ.1) 6150,6100
6100 CALL PLOT2(JTOT,NUMPT,IM(1),IPLOTSP,L BELOW,L ABOVE,YUMHIST,N1,
2 NSTHIST,NT,NTIMES,MOS,SMONLY)
6150 IF(PLTON.NE.0.OR.SMONLY.EQ.1.0) 6500,6160
6160 FSPECMAX = FDMAX = U.
DO 6400 N = 1,2
6164 DO 6200 I=1,14
IF(N1.EQ.1.AND.NT.EQ.NTIMES) 6165,6170
6165 FREQSPEC(I,N)=FREQSPEC(1,N)/TNUMSPEC
6170 IF(ASQ2NU(I,N).GT.FSPECMAX) 6175,6200
6175 FSPECMAX = ASQ2NU(I,N)
6200 CONTINUE
IF(SPECMAXF.LT.FSPECMAX) 6215,6225
6215 SPECMAXF=FSPECMAX

```

THIS PAGE IS BEST QUALITY PRACTICABLE
FROM COPY FURNISHED TO DDC

```
6225 DO 6300, I=MIN,MAX
      IF(DFNC(I,N) .GT. FUMAX) 6250,6300
6250 FUMAX = DFNC(I,N)
6300 CONTINUE
6400 CONTINUE
      IF(N1.EQ.1.AND.NT.EQ.NTIMES) 6403,6406
C     ASSIGN VAUES TO FNUHTF
6403 DO 6405 N3=1,2
      DO 6405 ID=1,4097
6405 FNUHTF(ID,NB)= FNUHT(ID,NB)
6406 IF(HBAR(1).LT.0.) 6409,6407
6407 IF(|PLOTS|,EQ.0) 6408,6409
6408 CALL PLTSPEC (ASQ2NU,FNUHT,LPH1,HBAR,I4,1,FSPECHAX,NOHAPLT,
*XMMAXV,ISEC,IBELOW,IABOVE,MSAT,N2,THETA,N1,NCS,PLTSPACE)
6409 IF(N1.EQ.1.AND.NT.EQ.NTIMES) 6410,6415
6410 PRINT 9023, HBARF(1),HBARF(2),TSPEC AVG
      PRINT 9033
      DD 6412  (M=1,75
6412 PRINT 9031, FNUHTF(KM,2),FREQSPEC(KM,2),FNUHTF(KM,1),
2  FREQSPEC(KM,1)
      CALL PLTSPEC(FREQSPEC,FNUHTF,LPH1,HBARF,I4,1,SPECHAXF,NOHAPLT,
2 XMMAXV,ISEC,IBELOWF,IABOVEF,MSAT,N2,THETA,N1,NOS,PLTSPACE)
6415 IF(|SEC|,E).1.AND.|WHIST|,EQ.0,U) 6425,6450
6425 CALL PLOTDF (FDMAX,IBELOW,IABOVE,MIN,MAX,LPH1,MPLUTDF)
6450 CONTINUE
6500 IF(|PAUSE|,NE, 0) 6600,6720
6600 PAUSE
6720 IF(RESTART,EQ.1,) 6700,100
6900 CONTINUE
9999 CALL STOPPLOT
      END
      SUBROUTINE PLOT2 (NPS,NUMPT,IM,PLTONLY,LBELOW,IABOVE,NUMHIST,N1,
2 NST,NT,NTIMES,NSAMP,SHONLY)
      DIMENSION LBELOW(2),IABOVE(2)
      COMMON/SF/NPEN,PLTSPACE,DELT
      COMMON/A/Y(8192),Z(8192)
      TYPE REAL  IAbove,LBelow
      TYPE INTEGER  PLTONLY,IDEc
C     NOTE THAT DELT AND PLTSPACE HAVE SWITCHED LOCATIONS AND VALUES.
210 FORMAT(/,3X,*NSAMP = *,15)
      PRINT 210, NSAMP
C     FOR GUL STREAM EXPERIMENT, NUMPT = 512,
      NUMPT = 512
      NFFINAL = NST + NPS + 1
      XXFMAX = VSAMP*DELT
      NPTS = IM
      CALL NEWPEN(NPEN)
      IF(NSAMP = 2*NUMPT, EQ,NPS) 3,1
      RECALCULATE IAbove,LBelow
      1 LBELOW(1)=LBELOW(2)=0,
      IAbove(1)=IAbove(2)=0.
      DO 200 I=NST,NFINAL
      IF(IAbove(1).LT.Y(I)) 180,184
180 IAbove(1)=Y(I)
      GO TO 188
184 IF(LBELOW(1).GT.Y(I)) 186,188
186 LBELOW(1)=Y(I)
188 IF(IAbove(2).LT.Z(I)) 190,192
190 IAbove(2)=Z(I)
      GO TO 200
```

```

192 IF(LBELOW(2).GT.Z(I))194,200
194 LBELOW(2)=Z(I)
200 CONTINUE
3 IF(PLTONLY.GT.0.OR.SWHONLY.EQ.1.0) 8,4
4 CALL PLOT(0.0, 15.0,-3)
8 CALL SYMBOL (-1.0,1.70,0.35,14HMEASUREMENTS IN MKS, 90,0,20)
CALL PLOT(0.0,5.0,-3)
C
C      SET UP VERTICAL AXIS OF LASER PLOT
C
IMARK = 4
XM = IMARK/2.
RABOVE = _ABOVE(1)
ABOVE = RABOVE*0.3048
RBELOW = _BELOW(1)
BELOW = RBELOW*0.3048
ABELOW = ABSF(BELOW)
SCALAR = MAX1F(ABOVE,ABELOW)
XMID = 2.0
CALL PLOT(-0.1,0.0,3)
CALL PLOT(0.0,0.0,2)
DO 10 I = 1,4
YY = I
CALL PLOT ( 0.0,YY,1)
CALL PLOT (-0.1,YY,1)
CALL PLOT ( 0.0,YY,1)
10 CONTINUE
CALL NUMBER (-0.6, 3.95, 0.105, SCALAR,0.0,4FF6.2)
SCALAR = -SCALAR
CALL SYMBOL (-0.6, 1.95, 0.105, 4H 0.0.0,4)
CALL SYMBOL (-0.6, 1.58, 0.210,5HLASER,90,0,5)
CALL NUMBER (-0.6,-0.05, 0.105, SCALAR,0.0,4FF6.2)
SCALAR = -SCALAR/2.
C
C      PLOT LASER RECORD
C
XX = DELT*(NUMPT + NST)
LL = 3
DO 20 I = NST,NFINAL
YAMP = Y(I)*0.3048/SCALAR+XMID
IF(YAMP .LT. 4.0) 12,14
12 YAMP = 4.0
GO TO 17
14 IF(YAMP .LT. 0.0) 16,17
16 YAMP = 0,
17 CALL PLOT (XX,YAMP,LL)
IF(LL = 2) 175,170,170
170 LL = LL - 1
175 IF(PLTONLY .EQ. 0) 20,18
18 IF(MOD(I,NPTS) .EQ. 0) 19,20
19 CALL PLOT (XX,4.5,3)
CALL PLOT (XX,4.0,2)
CALL PLOT (XX,YAMP,3)
CALL PLOT (XX,YAMP,2)
20 XX = XX + DELT
C
C      SET UP HORIZONTAL AXIS
C      IMARK SHOULD BE AN EVEN INTEGER
C
DELTAX = KXFMAX/IMARK

```

THIS PAGE IS BEST QUALITY PRACTICABLE
FROM COPY FURNISHED TO DDC

```
CALL PLOT (XXFMAX,-0.5,3)
JMARK = IMARK + 1
DO 30 I=1,JMARK
XA = XXFMAX - (I-1)*DELTAX
XB = XA+P_TSPACE/DELT
CALL PLOT (XA,-0.5,2)
CALL PLOT (XA,-0.55,1)
CALL PLOT (XA,-0.49,1)
CALL NUMBER (XA-0.255,-0.40,0.105,XB,0.0,4HF4.0)
IF(I.EQ.IMARK/2 + 1) 25.27
25 CALL SYMBOL (XA - 0.66,-0.85,0.14,15HTIME IN SECUNDS,0.0,15)
27 CALL PLOT (XA,-0.5,3)
30 CONTINUE
IF(NJMMIST.EQ.2) 32,55
C
C      SET UP VERTICAL AXIS OF ACCELERATION PLOT
C
32 CALL PLOT (0.,-5.0,-3)
CALL PLOT (-0.1,0.0,-3)
CALL PLOT ( 0.0,0.0,-2)
DO 40   I = 1,4
YY = I
CALL PLOT ( 0.0,YY,1)
CALL PLOT (-0.1,YY,1)
CALL PLOT ( 0.0,YY,1)
40 CONTINUE
RABOVE = ABOVE(2)
ABOVE = RABOVE*0.3048
R BELOW = BELOW(2)
BELOW = R BELOW*0.3048
ABBELOW = ABSF(BELOW)
SCALAR = MAX1F(ABOVE,ABBELOW)
CALL NUMBER (-0.6, 3.95, 0.105, SCALAR,0.0,4HF6.2)
SCALAR = -SCALAR
CALL SYMBOL (-0.6, 1.95, 0.105, 4H 0.0.0,4)
CALL SYMBOL (-0.6, 1.58, 0.210,5HACCEL,90.0,5)
CALL NUMBER (-0.6,-0.05, 0.105, SCALAR,0.0,4HF6.2)
SCALAR = -SCALAR/2,
XX = DELT*(NUMPT + NST)
LL = 3
C
C      PLOT ACCELERATION RECORD
C
DO 50 I = NST,NFINAL
YAMP = Z(I)*0.3048/SCALAR + XMID
IF(YAMP .GT. 4.5) 42,44
42 YAMP = 4.5
GO TO 48
44 IF(YAMP .LT. -0.5) 46,48
46 YAMP = -0.5
48 CALL PLOT (XX,YAMP,LL)
IF(LL-2) 50.49,49
49 LL = LL - 1
50 XX = XX + DELT
CALL PLOT(0.0,5.0,-3)
C
C      POSITION PEN FOR NEXT PLOT
C
55 IF(SWHONLY.EQ.1.0) 56,58
56 CALL PLOT(0.0,4.5,-3)
```

```

      GO TO 66
58 IF(PLT ONLY.EQ.0) 60,62
60 CALL PLOT(0.0,-19.0,-3)
GO TO 66
62 IF(N1.EQ.1.AND.NT.EU.NTIMES) 64,56
64 XF=XXFMAX + 4.0
CALL PLOT(XF,-8.0,-3)
66 RETURN
END
SUBROUTINE PLTSPEU (YP,XP,LPH1,HBAR,NUP,NP,YMAX,NOHAWPLT,
*XMAXVL,ISEC,IBELOW,IABOVE,MSAT,N2,THETA,N1,NCS,PLTSPACE)
DIMENSION YP(4097,2),XP(4097,2),LPH1(10)
DIMENSION HBAR(2),ISTART(2)
TYPE INTEGER THETA
C
C LPH1 CONTAINS PLOTTING LABEL TO BE PLOTTED ON TOP OF PLUT
C MAXIMUM OF 72 CHARACTERS PLOTTED OUT
C
C YP(I,N) = ARRAY OF Y VALUES OF THE N-TH VARIABLE TO BE PLOTTED
C XP(I,N) = ARRAY OF X VALUES OF THE N-TH VARIABLE TO BE PLOTTED
C NOP = TOTAL NUMBER OF POINTS
C NP = STARTING POINT IN ARRAY FROM WHICH TO START PLOTTING
C FMAX = PHYSICAL LENGTH OF ABSISSA
C XLEFT = LOG OF MINIMUM VALUE ON ABSISSA
C XMAXVL = LOG OF MAXIMUM VALUE ON ABSISSA
200 FORMAT(/,2X,*1START(1) =*,13,5X,*NOP =*,15,5X,*1START(2) =*,13,
2 5X,*NP =*,15,/)
300 FORMAT(3X,*LASTPLT= *,15)
C
C CONVTM = 0.3048
CONVETM = CONVTM**2
CONV = 1./LOGF(10.)
ATHETA = THETA
IF(THETA.GT.180) 529,550
525 THETA = 360 - THETA
550 DO 3, N=1,2
2 ISTART(N) = 1
3 CONTINUE
CALL NEWPEN(1)
6 FMAX = 12
C
C CONVERT DATA TO METRIC SYSTEM
C
HBAR(1) = CONVTM*HBAR(1)
HBAR(2) = CONVTM*HBAR(2)
DO 10 I = 1,NOP
YP(I,1) = CONVETM*YP(I,1)
10 YP(I,2) = CONVETM*YP(I,2)
YMAX = CONVETM*YMAX
C
C DETERMINE INITIAL Y AND Z VALUES FOR PLUTS, CALCULATE LOG VALUES
C
XMAXVL = 0.5
XLEFT = -2.5
XLEFT10 = 10.*XLEFT
SCALE = 5.
DO 103 N = 1,2
DO 100 I=1,NOP
IF(XP(I,N) .LT. XLEFT10) 50,60
50 ISTART(N)= I+1

```

THIS PAGE IS BEST QUALITY PRACTICABLE
FROM COPY FURNISHED TO DDC

```
GO TO 100
60 XPL = XP(I,N)
XPL = LOG*XPL
XP(I,N)=CONV*XPL
100 CONTINUE
105 CONTINUE
IF(N2.EQ.1) 104,106
104 IF(MSAT.GT.ISTART(1)) 105,106
105 ISTART(1) = MSAT
106 ISTART1 = ISTART(1)

C      SET UP BOTH AXES, PLOT AND LABEL VERTICAL AXIS
C
DO 108 I = ISTART1,NOP
IF (XP(I,1) .GT. XMAXVL) 107,108
107 NOPP = -1
GO TO 109
108 CONTINUE
NOPP = NOPP
XMAXLVL = XMAXVL-XLEFT
XMIN = FM4X/XMAXLVL
GO TO 110
109 XMAXLVL = XP(NOPP,1) - XLEFT
XMIN = FM4X/XMAXLVL
110 YMAX = LOGF(YMAX)
YMAX = CONV*YMAX
YMAX = YMAX+1.
YMAX = YMAX
YTOP = YMAX
YBOTTOM = YTOP-SCALE
YBOTTONR = 10.*-YBOTTOM
CALL PLOT ( 0.0, -0,1.3)
CALL PLOT ( 0.0, 1,0.2)
DO 111 I = 1,9
Y = I
CALL PLOT (-0,1, Y,1)
CALL PLOT ( 0.0, Y,1)
CALL PLOT ( 0.0,Y+1,,1)
111 CONTINUE
CALL PLOT (-0,1 , Y+1. , 1 )
CALL SYMBOL (0.5,10,1,0.14,LPH1,0,0,72)
CALL SYMBOL (9.08,9.5/,0.14,0,0.0,-1)
CALL SYMBOL (9.15,9.50,0.14,26H = LASER (SWH =      M, ),0.0,26)
CALL NUMBER (11.07, 9.50,0.14,HBAR(1),0.0,4HF5.2)
CALL SYMBOL (9.08,9.32,0.14,4,0.0,-1)
CALL SYMBOL (9.15,9.25,0.14,30H = A/C DISP. (STD =      M, ),0.0,
*30)
CALL NUMBER (11.60, 9.25,0.14,HBAR(2),0.0,4HF5.2)
CALL SYMBOL (9.15,9.00,0.14,BHTHETA = ,0.0,8)
CALL NUMBER (10.15,9.00,0.14,ATHETA,0.0,4HF5.1)
YY = 9.95
FLABEL = YTOP
DO 116 I = 1,6
CALL NUMBER (-0,8,YY,0,105,FLABEL,0.0,4HF6.2)
FLABEL = FLABEL - SCALE/5.
YY = YY - 2.0
IF(I .EQ. 4) 115,116
115 CALL SYMBOL (-0,8,3,6,0.175,22HLOG(SPECTRA) M**2-SEC.9U,0,22)
116 CONTINUE
```

C

```

C      TRANSFORM DEPENDENT VARIABLE TO LOG BASE 10, CONVERT COORDINATES
C      TO INCHES.
C
C      JJ = NOPP
DO 121 N = 1,2
IF(N,EQ,2) 117,119
117 JJ = NOP
119 ISTART1 = ISTART(N)
DO 120 I = ISTART1, JJ
YPL = YP(I,N)
IF(YPL,LE,YBOTTOMR) 1002,1000
1000 YPL = LOGF(YPL)
YP(I,N) = CONV*YPL + YBOTTOM
YP(I,N) = YP(I,N)/SCALE*10.
GO TO 1004
1002 YP(I,N) = 0.
1004 XP(I,N) = XP(I,N) - XLEFT
120 XP(I,N) = XP(I,N)*XMIN
121 CONTINUE
FMID = FMAX/2,
J1 = 0
NEND = NOPP - NP + 1
JJ = NEND
IF( THETA,LE,90.AND.ISTART(1),EQ,1) 122,210
122 ISTART(1) = 2
210 PRINT 200, ISTART(1), NOPP, ISTART(2), NOP
C      PLOT SPECTRA (LOG-LUG)
C
C      INZ=NOP/256
ANZ=INZ
DO 140 N = 1,2
L = -1
IF(N,EQ,2) 123,125
123 J1 = 4
JJ = NOP
125 ISTART1 = ISTART(N)
DO 135 I = ISTART1 ,JJ
NN = I
IF(N,EQ,2) 127,129
127 NN = JJ - I + ISTART(2)
129 IF(YP(NN,V) .LE. 0.) 131,133
131 L = 0
GO TO 135
133 IF(N,EQ,2) 134,500
C      LIMIT THE NUMBER OF HIGH FREQ PTS PLOTTED (LASER)
500 PRNUM1=NN
PRNUM2=PRNUM1/ANZ
IPR1=PRNUM12
PRNUM3=IPR1
PRNUM4=PRNUM2-PRNUM3
IF(NN,LE,125.OR.PRNUM4,EQ,0,) 134,135
134 CALL SYMBOL (XP(NN,N),YP(NN,N),U,U7,JI,U,0,L)
LASPI,T = NN
135 L = L - 1
140 CONTINUE
C      PLOT AND LABEL HORIZONTAL AXIS, POSITION PEN FOR NEXT PLOT
C      IF XLEFT OR XMAXVL IS CHANGED, LIMITS FOR DO LOOPS MAY CHANGE
C

```

THIS PAGE IS BEST QUALITY PRACTICABLE
FROM COPY FURNISHED TO DDG

THIS PAGE IS BEST QUALITY PRACTICABLE
FROM COPY FURNISHED TO DDC

```
XINC = FMAX*0.5/XMAXLVL
CALL PLOT(-0.1, 0, , 3)
CALL PLOT (XINC,0.,2)
X = 0.
DO 141 I = 1,5
X = X + XINC
CALL PLOT ( X, -0.1, 1 )
CALL PLDT ( X, 0, , 1 )
CALL PLOT (X + XINC, 0.,1)
141 CONTINUE
CALL PLOT (X + XINC, -0.1, 1)
X = -0.3
XX = 0,
DO 150 I = 1,7
FREQ = XX/XMIN+XLEFT
CALL NUMBER (X,-0.25,0.105,FREQ,0.0,4HF6.3)
IF(XX .GT. FMID-1.5 .AND. XX .LE. FMID) 145,149
145 CALL SYMBOL (FMID-1.47,-0.5,0.175,20HLOG(FREQUENCY) HZ ,0.0,20)
149 XX = XX + XINC
150 X = X + XINC
IF(NDWAEP_T.EQ.1) 155,157
155 CALL PLOT(FMAX + 4.,0.0,-3)
GO TO 180
157 IF ( ISEC .EQ. 1 ) 160,170
160 IF(N1.EQ.1) 162,165
162 CALL PLDT (FMAX + 5.0,0.0,-3)
GO TO 180
165 XFIN = NOS*PLTSPACE + 5.0
CALL PLOT (XFIN,0.0,-3)
GO TO 180
170 NPOINTS = (IABOVE+IBELOW)*4
INCHES = NPOINTS/4
IISTAN = INCHES*9
DISIAN = IISTAN
CALL PLOT (FMAX+DISTAN,0.0,-3)
180 RETURN
END
SUBROUTINE PLOTDF(DM,IBELOW,IABOVE,MIN,MAX,LPH1,4PLOTDF)
RETURN
END
SUBROUTINE RDTAPE
COMMON/RDTAPEB/LFILE(7),KFILE,IFILE,MFILE
IF(MFILE-LFILE.EQ.0) 30,10
10 K1=MFILE-LFILE
DO 20 I=1,K1
20 CALL SKIPFILE(5)
KFILE=MFILE+1
30 CALL UNPC((0,0,0))
RETURN
END
SUBROUTINE UNPCK(ISWP,IREC,NFLAG)
DIMENSION INS1(8,8),INS(264),VSUOPE(9),INS2(8),NRA(1100),
1NRAD(167)
COMMON/UNPCKB/RAD(100),CHAN(7),AINSS(8),INCODE(8),VFILE,
1NDAY,MONT4,NYR,NHR,MIN,ALT,DDUT,NHSCOPE,NVSCCP,E,VSCALE,ISWEEP
COMMON/B/J(5500,2),NUHTF(4097,2)
EQUIVALENCE (NRA,U,NUHTF)
DATA (M1=17B),(M2=7778),(M3=18),(M4=3700B),(M5=1000B),
DATA (M6=7777777777776000B),(MSK1=77774000006),
C(MSK2=777740000B),(MSK3=377B),(MSK4=1400000000B),
```

```

C(MSK5=7777700000000000)
DATA (MC=3/H),((VSCUPE(1),I=1,9)=1.,2.,5.,10.,20.,50.,100.,200.,
C500.)
1K(IREC,E3.0)2000,1020
2000 CONTINUE
BUFFER IN(5,1)(NRA(1),NRA(2))
110 IF(UNIT,5)10,30,30,40
40 PRINT 50
50 FORMAT(* PARITY ERROR IN FIRST RECORD*)
50 DO 1 J=1,2
DO 1 I=1,3
MTS=NRA(J)/2**((I-1)*6)
INS1(I,J)=MTS.AND.M2
1 CONTINUE
NFILE=INS1(4,1) $NDAY=INS1(8,1)+10+INS1(7,1)
MONTH=INS1(6,1)*10+INS1(5,1) $NYR=70+INS1(3,1)
NHR=INS1(2,1)*10+INS1(1,1)
MIN=INS1(3,2)*10+INS1(7,2)
ALT=INS1(5,2)*10+INS1(5,2)
DDOT=INS1(4,2)*10.+INS1(3,2)
NHSCOPE=INS1(2,2)
NVSCOPE=INS1(1,2)
VSCALE=VSCOPE(NVSCOPE)
PRINT 100,NFILE,NDAY,MONTH,NYR
100 FORMAT(1X,5HFILE ,I2,2X,I2.1H/,I2.1H/,I2,/)
PRINT 101,NHR,MIN
101 FORMAT(1X,7HTIME= ,I2,3HHR ,2X,I2,4HMIN ,I2,/)
PRINT 102,DDOT,NVSCOPE,NHSCOPE,ALT
102 FORMAT(2X,10HDFLAY DOT=F4.1,2X,11HVERT SCALE=,
01X,I2,2X,10HHOR SCALE=,1X,I2,2X,4HALTz,F5.1,/)
IRC=0
RETURN
1020 CONTINUE----- IF(IRC.EQ.IREC) 75,52
IRC=IREC----- 52 IRC2 = IREC - IRC
DO /7 IBUF=1,IRC2
55 BUFFER IN(5,1)(NRA(1),NRA(11000))
60 IF(UNIT,5)60,70,65,80
60 PRINT 90
90 FORMAT(* PARITY ERROR IN SWEEP DATA*)
GO TO 70
65 CONTINUE
/0 CONTINUE
/7 CONTINUE
75 CONTINUE
MM=(IREC-1)*ISWEEP+ISWP
JJ=MOD(MM,256)
DO 301 J=1,NFLAG
NUM=(ISWP+1)*167+J
IWORD=(NUM+3)/4
NSHIFT=(4*IWORD-NUM)*12
NRAD(J)=NRA(IWORD)/2**NSHIFT
MTS=NRAD(J)
NRA(J)=MTS.AND.M2
301 CONTINUE
IF(JJ.EQ.1)302,109
302 I=0
DO 3 J=1,132
I=I+1
MTS=NRAD(J)/2**11
INS(I)=MTS.AND.M3

```

THIS PAGE IS BEST QUALITY PRACTICABLE
FROM COPY FURNISHED TO DDC

```

I=I+1
M1S=NRAD(J)/2**5
INS(I)=MTS.AND.M3
3 CONTINUE
I1=7
DO 11 K=1,8
INS2(K)=0
DO 10 I=1,8
I1=I1+1
INS2(K)=INS(I1)*2**8-I)+INS2(K)
10 CONTINUE
DO 210 I=9,32
I1=I1+1
INS2(K)=INS(I1)*2**8-I)+INS2(K)
210 CONTINUE
11 CONTINUE
DO 20 K=1,8
INC0DE(K)=MTS.AND.MSK3
M1S=INS2(K)
IF(K.EQ.2,OR.K.EQ.5)133,14
133 INS2(K)=MTS.AND.MSK2
GO TO 15
14 INS2(K)=MTS.AND.MSK1
15 NSIGN=MTS.AND.MSK4
IF(NSIGN.NE.0)16,17
16 M1S=INS2(K)-1
INS2(K)=MTS.OR.MSK5
17 CONTINUE
IF(X.EQ.2,OR.X.EQ.5)18,19
18 AINSS(K)=INS2(K)/2**29*3276,7
GO TO 20
19 AINSS(K)=INS2(K)/2**29*180,
20 CONTINUE
AINSS(5)=AINSS(5)*2,
IF(AINSS(3).LT.0.)22,24
22 AINSS(3)=AINSS(3)+360.
24 IF(AINSS(4).LT.0.)26,28
26 AINSS(4)=AINSS(4)+360.
28 IF(AINSS(1).LT.0.)29,31
29 AINSS(1)=AINSS(1)+360.
31 IF(AINSS(3).LT.0.)32,33
32 AINSS(8)=AINSS(8)+360.
33 CONTINUE
PRINT 103,(AINSS(I),I=1,8)
103 FORMAT(2X,4HINS=,8(2X,F8.1))
109 DO 114 I1=1,167
M1S=NRAD(I1)
M1S1=MTS.AND.M4
M1S2=MTS.AND.MC
NRA1(I1)=4TS1/2+MTS2
M1S=NRAD(I1)
NSIGN=MTS.AND.M5
IF(NSIGN.NE.0)12,13
12 M1S1=MTS-1
NRA1(I1)=4TS1.OR.M6
13 CONTINUE
114 CONTINUE
DO 115 J6=1,7
CHAN(J6)=NRAD(J6)*1.953125
115 CONTINUE

```

THIS PAGE IS BEST QUALITY PRACTICABLE
FROM COPY FURNISHED TO DDC

```

DO 107 I=1,160
RAU(I)=NRAD(I+7)*VSUALE/51.2
107 CONTINUE
RETURN
END
SUBROUTINE PHASE(NTOT,QP)
COMMON/A/Y,Z
DIMENSION Y(8192),Z(8192),ITYPE(2)
DATA (ITYPE)=5HLASER,5HACCEL
900 FORMAT (*1 ATEST =F6.1,* RTEST =F6.1,* STEST =F6.1,//)
901 FORMAT (*1 NUMBER OF PHASE SHIFTS FOR *A5,* DATA = *,14,/
* 6X,*MAX PHASE SHIFT = *,F6.2,5X,*MIN PHASE SHIFT = *,F6.2,/
* 6X,*DIFFERENCES GREATER THAN RTEST = *,14/)
IF (QP = 10.) 20,14,30
10 ATEST = 4.0
RTEST = 2.4
STEST = 0.0
UTEST = 32.2
TTEST = 64.4
BTEST = 32.2
GO TO 40
20 ATEST = 3.5
RTEST = 2.0
STEST = 0.0
UTEST = 32.2
TTEST = 64.4
BTEST = 32.2
GO TO 40
30 ATEST = 5.0
RTEST = 3.2
STEST = 0.0
UTEST = 32.2
TTEST = 64.4
BTEST = 32.2
40 PRINT 900, ATEST,RTEST,STEST
ICOUNT = 1
MTOT = NTOT - 1
NLASPS = NRADPS = NLASDIF = NRAUDIF = 0
RYMAX = RZMAX = 0.
RYMIN = RZMIN = 1000.
60 DCY = DCZ = 0.
DO 160 I = 1,MTOT
V = Y(I)
W = Z(I)
Y(I) = Y(I) + DCY
C
C IF Z = ACCELERATION, NO PHASE SHIFT IS NEEDED AND DCZ = 0.
DCZ = 0.
C
Z(I) = Z(I) + DCZ
AY = Y(I)
AZ = Z(I)
BY = Y(I+1) + DCY
BZ = Z(I+1) + DCZ
RY = ABSF(AY - BY)
RZ = ABSF(AZ - BZ)
SY = AY - RY
SZ = AZ - RZ
IF(ICOUNT .EQ. 2) 120,70
110 IF(RY .LT. ATEST) 80,75

```

THIS PAGE IS BEST QUALITY PRACTICABLE
 FROM COPY FURNISHED TO DDG

AD-A057 420 NAVAL RESEARCH LAB WASHINGTON D C
GULF STREAM GROUND TRUTH PROJECT: RESULTS OF NRL AIRBORNE SENSO--ETC(U)
JUN 78 C R MCCLAIN, D T CHEN, D L HAMMOND

F/G 8/3

NRL-MR-3779

NL

UNCLASSIFIED

2 of 2
AD
A057420



```
15 DCY = DCY + QP*(RY/SY)
NLASPS = NLASPS + 1
IF(RY .GT. RYMAX) 70,77
70 RYMAX = RY
GU TO 80
71 IF(RY .LT. RYMIN) 73,80
73 RYMIN = RY
80 IF(RZ .LT. RTEST) 100,90
90 DCZ = DCZ + RZ*(RZ/SZ)
NRADPS = NRADPS + 1
IF(RZ .GT. RZMAX) 95,100
95 RZMAX = RZ
GU TO 160
100 IF(RZ .LT. RZMIN) 105,160
105 RZMIN = RZ
GU TO 160
120 IF(RY .GT. RTEST ,ANJ, RY .LT. STEST) 130,140
130 DCY = DCY + RY*RY/SY
NLASDIF = NLASDIF + 1
140 IF(RZ .GT. UTEST ,ANJ, RZ .LT. TTEST) 150,160
150 DCZ = DCZ + RZ*RZ/SZ
NRADDIF = NRADDIF + 1
160 CONTINUE
Y(NTOT) = Y(NTOT) + DCY
C Z(NTOT) = Z(NTOT) + DCZ
IF(ICOUNT .EQ. 2) 200,180
180 ICOUNT = ICOUNT + 1
GO TO 60
200 PRINT 901, ITYPE(1),NLASPS,RYMAX,RYMIN,NLASDIF
PRINT 901, ITYPE(2),NRADPS,RZMAX,RZMIN,NRADDIF
RETURN
END
SUBROUTINE FOURIER (A,S,M,IFS)

C THIS ROUTINE PERFORMS AN ANALYSIS OF 2**M POINTS BY FIRST DOING
C AN ANALYSIS OF 2**M/2 COMPLEX POINTS AND THEN ARRANGING THE RESULTS
C
C ARGUMENTS
C 1. A - REAL DATA ARRAY - OF DIMENSION 2**M + 2
C 2: S - SIN/COS TABLE - DIMENSION 2**((M-3))
C 3. M - EXPONENT OF 2 - SIZE OF REAL ARRAY
C 4. IFS - -1 FOR FIRST TIME, -2 THEREAFTER
C
C DIMENSION A(1),S(1)
N = 2**((M-1))
CALL HARMON(A,S,M-1,IFS,IFEHR)
C MERGE 2 N-POINT ANALYSIS INTO 1 2N-POINT ANALYSIS
NHALF = N/2
NTWO = N/2 + 4
X = XU = COSF(3.1415926536/FLUATF(N))
Y = YO = SINF(3.1415926536/FLUATF(N))
DO 1000 K2 = 4,N,2
K1 = K2 - 1
N2 = NTWO - K2
N1 = N2 - 1
BK1 = A(K1) + A(N1)
BK2 = A(K2) - A(N2)
BN1 = A(K2) + A(N2)
BN2 = A(K1) - A(N1)
XBN1 = X*BK1
```

THIS PAGE IS BEST QUALITY PRACTICALLY
FROM COPY FURNISHED TO DDC

```

XBN2 = X*3N2
YBN1 = Y*3N1
YBN2 = Y*3N2
A(K1) = .5*(BK1 + XBN1 - YBN2)
A(K2) = .5*(-BK2 + XBN2 + YBN1)
A(N1) = .5*(BK1 - XBN1 + YBN2)
A(N2) = .5*(BK2 + XBN2 + YBN1)
Q = X*X0 - Y*Y0
Y = Y*X0 + X*Y0
1000 X = 0
C COMPLEX ELEMENT A(N)
A(2*N+1) = (A(1) - A(2))*.5
A(2*N+2) = 0.0
C COMPLEX ELEMENT A(0)
A(1) = .5*(A(1)+A(2))
A(2) = 0.0
C COMPLEX ELEMENT A(N/2)
C A(N+1) = A(N+1)
C A(N+2) = A(N+2)
RETURN
END
SUBROUTINE HARMON(A,S,M,IFS,IFERR)
DIMENSION A(1),S(1)
      HARM, ONE-DIMENSIONAL BASIC FORTRAN VERSION. J.W.COOLEY      HARM 001
      MODIFIED TO RUN ON CDC 3100.                                HARM 002
C
C
C DUES EITHER FOURIER SYNTHESIS, I.E., COMPUTES COMPLEX FOURIER SERIES HARM 009
C GIVEN A VECTOR OF N COMPLEX FOURIER AMPLITUDES, OR, GIVEN A VECTOR HARM 010
C OF COMPLEX DATA X DUES FOURIER ANALYSIS, COMPUTING AMPLITUDES. HARM 011
C A IS A COMPLEX VECTOR OF LENGTH N=2**M COMPLEX NOS, OR 2*N REAL HARM 012
C NUMBERS. A IS TO BE SET BY USER.                                HARM 013
C M IS AN INTEGER 0.LT.M.LE.13, SET BY USER.                  HARM 014
C S IS A VECTOR S(J)= SIN(2*PI*j/NP), J=1,2,...,NP/4=1,          HARM 015
C COMPUTED BY PROGRAM.                                         HARM 016
C IFS IS A PARAMETER TO BE SET BY USER AS FOLLOWS-
IFS=0 TO SET NP=2**M AND SET UP SINE TABLE S.          HARM 017
IFS=1 TO SET N=NP=2**M, SET UP SIN TABLE, AND DO FOURIER    HARM 018
SYNTHESIS, REPLACING THE VECTOR A BY                      HARM 019
HARM 020
HARM 021
X(J)= SUM OVER K=0,N-1 OF A(K)*EXP(2*PI*I/N)**(J*K).      HARM 022
J=0,N-1, WHERE I=SQRT(-1)                                     HARM 023
THE X'S ARE STORED WITH RE X(J) IN CELL 2*j+1             HARM 024
AND IM X(j) IN CELL 2*j+2 FOR J=0,1,2,...,N-1.           HARM 025
THE A'S ARE STORED IN THE SAME MANNER.                      HARM 026
HARM 027
IFS=-1 TO SET N=NP=2**M,SET UP SIN TABLE, AND DO FOURIER   HARM 028
ANALYSIS, TAKING THE INPUT VECTOR A AS X AND               HARM 029
REPLACING IT BY THE A SATISFYING THE ABOVE FOURIER SERIES. HARM 030
IFS=-2 TO DO FOURIER SYNTHESIS ONLY, WITH A PRE-COMPUTED S. HARM 031
IFS=-3 TO DO FOURIER ANALYSIS ONLY, WITH A PRE-COMPUTED S. HARM 032
IFERR IS SET BY PHROGRAM TO-
=0 IF NO ERROR DETECTED.                                    HARM 033
=1 IF M IS OUT OF RANGE., OR, WHEN IFS=-2,-3, THE        HARM 034
PRE-COMPUTED S TABLE IS NOT LARGE ENOUGH.                 HARM 035
=-1 WHEN IFS =-1,-2, MEANS ONE IS RECOMPUTING S TABLE    HARM 036
UNNECESSARILY.                                              HARM 037
HARM 038
HARM 039
HARM 040
HARM 041

C NOTE- AS STATED ABOVE, THE MAXIMUM VALUE OF M FOR THIS PROGRAM
ON THE IBM 7094 IS 13. ON 360 MACHINES HAVING GREATER STORAGE

```

THIS PAGE IS BEST QUALITY PRACTICABLE
 FROM COPY FURNISHED TO DDC

```

C   CAPACITY. ONE SHOULD CHANGE THIS LIMIT BY REPLACING 13 IN          HARM 042
C   STATEMENT 3 BELOW BY LOG2 N, WHERE N IS THE MAX. NO. OF          HARM 043
C   COMPLEX NUMBERS ONE CAN STORE IN HIGH-SPEED CORE.          HARM 044
C   IF THE CAPACITY OF HARM IS TO BE INCREASED, ONE MUST          HARM 045
C   ALSO ADD MORE DO STATEMENTS TO THE BINARY SORT ROUTINE          HARM 046
C   FOLLOWING STATEMENT 24 AND CHANGE THE EQUIVALENCE STATEMENTS          HARM 047
C   FOR THE K'S.          HARM 048
C   HARM 049

C   DIMENSION K(12)
C   EQUIVALENCE (K(11),K1),(K(10),K2),(K(9),K3),(K(8),K4),(K(7),K5)          HARM 055
C   EQUIVALENCE (K(6),K6),(K(5),K7),(K(4),K8),(K(3),K9),(K(2),K10)
C   EQUIVALENCE (K(1),K11),(K(1),N2)
C   IF (M)2,2,3.
C   3 IF (M-11) 3,5,2          HARM 057
C   2 IF ERR=1          HARM 058
C   1 RETURN          HARM 059
C   5 IF ERR=0          HARM 060
C   N=2+*M
C   IF (XABSF(IFS) - 1 ) 200,200,10          HARM 062
C   WE ARE DOING TRANSFORM ONLY, SEE IF PRE-COMPLETED          HARM 063
C   S TABLE IS SUFFICIENTLY LARGE
C   10 IF ( N-VP )20,20,12          HARM 064
C   12 IF ERR=1          HARM 065
C   GO TO 200          HARM 066
C   SCRAMBLE A, BY SANDERS METHOD          HARM 067
C   20 K(1)=2*N          HARM 068
C   DO 22 L=2,M          HARM 069
C   22 K(L)=K(L-1)/2          HARM 070
C   DO 24 L=M,10
C   24 K(L+1)=2
C   NOTE EQUIVALENCE OF KL AND K(14-L)          HARM 072
C   BINARY SORT-
C   IJ=2          HARM 073
C   J1=2          HARM 074
C   25 DO 30 J2=J1,K2,K1          HARM 075
C   DO 30 J3=J2,K3,K2          HARM 078
C   DO 30 J4=J3,K4,K3          HARM 079
C   DO 30 J5=J4,K5,K4          HARM 080
C   DO 30 J6=J5,K6,K5          HARM 081
C   DO 30 J7=J6,K7,K6          HARM 082
C   DO 30 J8=J7,K8,K7          HARM 083
C   DO 30 J9=J8,K9,K8          HARM 084
C   DO 30 J10=J9,K10,K9          HARM 085
C   DO 30 J1=J10,K11,K10
C   IF (IJ-J1)28,30,30          HARM 089
C   28 T=A(IJ-1)
C   A(IJ-1)=A(JI-1)          HARM 090
C   A(JI-1)=T          HARM 091
C   T=A(IJ)
C   A(IJ)=A(JI)          HARM 093
C   A(JI)=T          HARM 094
C   30 IJ=IJ+2          HARM 095
C   J1=J1+2
C   IF (K1-J1)31,25,25
C   31 IF (IFS)32,2,36          HARM 097
C   DOING FOURIER ANALYSIS, SO DIV. BY N AND CONJUGATE.          HARM 098
C   32 FN = FLOATE(N)
C   DO 34 I=1,N          HARM 100
C   A(2*I-1) = A(2*I-1)/FN          HARM 101
C   34 A(2*I)=-A(2*I)/FN          HARM 102

```

```

C      SPECIAL CASE- L=1          HARM 103
36 DO 40 I=1,N,2          HARM 104
T = A(2*I+1)          HARM 105
A(2*I-1) = T + A(2*I+1)          HARM 106
A(2*I+1) = T-A(2*I+1)          HARM 107
T=A(2*I)
A(2*I) = T + A(2*I+2)          HARM 108
40 A(2*I+2) = T - A(2*I+2)          HARM 109
IF(M-1) 2,1 ,50          HARM 110
C      SET FOR L=2          HARM 111
50 DO LEXP1=2          HARM 112
C      LEXP1=2*(L-1)          HARM 113
LEXP=8          HARM 114
C      LEXP=2**(-1)          HARM 115
NPL= 2**M1          HARM 116
C      NPL = NP* 2**-L          HARM 117
DO 130 L=2,M          HARM 118
C      SPECIAL CASE- J=0          HARM 120
DO 60 I=2,N2,LEXP          HARM 121
I1=I + LEXP1          HARM 122
I2=I1+ LEXP1          HARM 123
I3 =I2+LEXP1          HARM 124
T=A(I-1)          HARM 125
A(I-1) = T +A(I2-1)          HARM 126
A(I2-1) = T-A(I2-1)          HARM 127
T =A(I)
A(I) = T+A(I2)          HARM 128
A(I2) = T-A(I2)          HARM 129
T= -A(I3)          HARM 130
T1 = A(I3+1)          HARM 131
A(I3-1) = A(I1-1) - T          HARM 132
A(I3 ) = A(I1 ) - T1          HARM 133
A(I1-1) = A(I1-1) +T          HARM 134
80 A(I1) = A(I1 ) +T1          HARM 135
IF(L=2) 120,120,90          HARM 136
90 KLAST=N2-LEXP          HARM 137
JJ=NPL          HARM 138
DO 110 J=4,LEXP1,2          HARM 139
NPJJ=NT-JJ          HARM 140
UR=S(NPJJ)          HARM 141
UI=S(JJ)          HARM 142
ILAST=J+K_AST          HARM 143
DO 100 I= J,ILAST,LEXP          HARM 144
I1=I+LEXP1          HARM 145
I2=I1+LEXP1          HARM 146
I3 =I2+LEXP1          HARM 147
T=A(I2-1)*UR-A(I2)*UI          HARM 148
T1=A(I2-1)*UI+A(I2)*UR          HARM 149
A(I2-1)=A(I-1)-T          HARM 150
A(I2 )=A(I ) - T1          HARM 151
A(I-1) =A(I-1)+T          HARM 152
A(I) =A(I)+T1          HARM 153
T=-A(I3-1)*UI-A(I3)*UR          HARM 154
T1=A(I3-1)*UR-A(I3)*UI          HARM 155
A(I3-1)=A(I1-1)-T          HARM 156
A(I3 )=A(I1 )-T1          HARM 157
A(I1-1)=A(I1-1)+T          HARM 158
A(I1) =A(I1 ) +T1          HARM 159
100 END OF I -DO P          HARM 160
110 JJ=JJ+NPL          HARM 161
                                HARM 162

```

THIS PAGE IS BEST QUALITY PRACTICABLE
FROM COPY FURNISHED TO DDC

THIS PAGE IS BEST QUALITY PRACTICABLE
FROM COPY FURNISHED TO DDC

C	END OF J_DOP	HARM 163
120	LEXP1=2*LEXP1	HARM 164
	LEXP = 2*.EXP	HARM 165
130	NPL=VPL/2	HARM 166
C	END OF L_DOP	HARM 167
	IF((IFS)145,2,1)	
CC	DOING FOURIER ANALYSIS. REPLACE A BY CONJUGATE.	HARM 169
145	DO 150 I=1,N	HARM 170
150	A(2*I) =-A(2*I)	
	GO TO 1	
C	RETURN	HARM 173
C	MAKE TABLE OF S(J)=SIN(2*PI*j/NP), J=1,2,...,NT-1, NT=NP/4	HARM 174
200	NP=N	HARM 175
	MP=M	HARM 176
	NT=N/4	HARM 177
	M1=M-2	HARM 178
	IF (MT) 260,260,205	HARM 179
205	THETA=7833981634	HARM 180
C	THE1A=PI/2*(L+1) FOR L=1	HARM 181
	JSTEP = NT	
C	JSTEP = 2*(MT-L+1) FOR L=1	HARM 183
	JDIF = NT/2	HARM 184
C	JDIF = 2*(MT-L) FOR L=1	HARM 185
	S(JDIF) = SINF(THETA)	
	IF (MT-2) 260,220,220	HARM 187
220	DO 250 L=2,MT	HARM 188
	THETA = THETA/2,	HARM 189
	JSTEP2 = JSTEP	HARM 190
	JSTEP = JDIF	HARM 191
	JDIF = JDIF/2	HARM 192
	S(JDIF)=SINF(THETA)	
	JC1=NT-JDIF	HARM 194
	S(JC1) =CJSF(THETA)	
	JLAST=NT-JSTEP2	HARM 196
	IF (JLAST-JSTEP) 250,230,230	HARM 197
230	DO 240 J=JSTEP,JLAST,JSTEP	HARM 198
	JC=NT-J	HARM 199
	JD=J+JDIF	HARM 200
240	S(JL)=S(J)*S(JC1)*S(JDIF)*S(JC)	HARM 201
250	CONTINUE	HARM 202
260	IF ((IFS)20,1,20	
	END	HARM 203
	SCOPE	
W# 00	LOAD	
W# 00	RUN,200,60000	